



**Use of a Field Portable Photometer for Rapid  
Geochemical Analysis of Stream and Spring  
Waters: A Case History from Poison Mountain,  
British Columbia (NTS 0920/02)**



## Use of a Field Portable Photometer for Rapid Geochemical Analysis of Stream and Spring Waters: A Case History from Poison Mountain, British Columbia (NTS 0920/02)

Geoscience BC Report 2015-17



Ron Yehia<sup>1</sup> and David R. Heberlein<sup>2</sup>

<sup>1</sup>MYAR Consulting, Vancouver BC, [myar@telus.net](mailto:myar@telus.net)

<sup>2</sup>Heberlein Geoconsulting, North Vancouver BC

## Executive Summary

Hydrogeochemistry, or aqueous geochemistry, is used extensively in the exploration for geothermal resources, but has not seen widespread use in mineral exploration. Leybourne and Cameron (2010) and other workers, have demonstrated it to be an effective technique for identifying commodity and pathfinder element dispersion patterns from both outcropping and concealed mineralization. Furthermore, it is a potentially useful technique for exploring areas with difficult access, such as the coastal mountain ranges of British Columbia. A range of analytical instruments called portable spectrophotometers, or photometers, is available for field-based water testing providing potentially significant time advantage over stream sediments. They provide low cost near-real time field analysis for a diverse suite of anions and cations to relatively low detection limits.

This proof of concept study was carried out around the Poison Mountain copper-gold porphyry prospect, in order to test the effectiveness Palintest® Photometer 8000 by comparing results from water samples analyzed in the field with laboratory analyses of the same samples. The study also compared the water results with conventional stream sediment geochemistry from the same sample locations. Sampling was carried out in August and, again, in October 2014.

Results demonstrate that the photometer can be an effective tool for performing rapid and low cost hydrogeochemical surveys. The instrument was found to have good accuracy and precision, and results for most analytes compared well with laboratory water analyses. Stream sediment results provided complementary information to further validate element distribution patterns obtained from the photometer analyses results collected from the same localities. Water analyses yielded much lower absolute concentrations than the stream sediments particularly in the October results compared to those measured in August. This study shows that the photometer can provide good quality water analyses, at a lower cost and with shorter turnaround time than by analyzing the same parameters at a local laboratory. However, in order to obtain a comprehensive suite of analytical determinations, the use of high-sensitivity analytical equipment in a commercial laboratory is still required. The big advantage of using the field portable photometer is that it provides same-day indications of areas that might be worthy of follow up.

## Table of Contents

Executive Summary.....	ii
List of Tables .....	v
List of Figures .....	v
Introduction .....	1
Background .....	2
Study Objectives .....	2
Location and Access.....	2
Geology .....	4
Sample Collection .....	6
Quality Control Measures .....	7
Analysis .....	7
Photometer.....	7
Health and Safety.....	10
Laboratory Analysis.....	11
Quality Control Results .....	12
Accuracy.....	12
Precision.....	14
Analytical Precision .....	14
Field Duplicate Precision.....	15
Stream Sediment Precision .....	16
Field Blank Results .....	17
Results.....	19
Laboratory Comparison .....	19
Metals and Anions .....	19

Turbidity, TDS, Conductivity and pH results ..... 29

Inconsistent Results ..... 32

    Photometer ..... 32

    Laboratory ..... 32

Field Test and Photometer Results ..... 35

    Field Tests ..... 35

    Photometer Results ..... 42

        Commodity Elements..... 42

        Halogens and other analytes ..... 47

        Other Elements and Anions ..... 51

Stream Sediment Results ..... 63

    Commodity Elements..... 63

    Pathfinder Elements ..... 66

    Other Elements ..... 72

    Downstream Dispersion..... 79

Discussion..... 85

    Comparison of Photometer and Stream Sediment Results ..... 86

    Cost per sample ..... 87

        Turnaround Time ..... 87

        All in Cost per Analysis ..... 88

Conclusions ..... 89

Recommendations ..... 89

Acknowledgments..... 89

References ..... 90

Appendix A – Dispersion Analysis Continued ..... 91

Digital Appendix ..... 103

## List of Tables

Table 1. List of analytes with detection ranges measured (published by Palintest.) ..... 8

Table 2. Analytical methods employed by ALS Environmental<sup>1</sup> ..... 11

Table 3. %RSD results from replicate analyses. .... 15

Table 4. Average %RSD values for photometer field duplicate analyses. .... 16

Table 5. Average % RSD values for selected elements from the stream sediment field duplicate results 17

Table 6. Field blank results..... 18

Table 7. Inconsistent Analyses..... 34

Table 8. Percentiles distribution. .... 36

Table 9. Summary of cost per sample..... 88

## List of Figures

Figure 1. Location of study area, southern British Columbia..... 3

Figure 2. Project area and sample collection points around Poison Mountain..... 3

Figure 3. Local geology of study area (Massey et al, 2005). .... 5

Figure 4. Photo showing a typical set-up for photometer analysis. Reagents are in silver packaging aligned atop. Coloured sample solutions ready for analyses are shown in the 10 ml tubes in rack. The Photometer is in the lower right of the photo. .... 9

Figure 5. Close-up of rack showing a collection of tubes with reagents ready for photometer testing. ... 10

Figure 6. Control chart for standard solution 38271/B..... 12

Figure 7. Control chart for standard solution 38271/C..... 13

Figure 8. Control chart for standard solution 38271/D. .... 13

Figure 9. Laboratory samples locations. .... 19

Figure 10. Boron laboratory comparison. Single high point corresponds to spring at GPS location #10... 20

Figure 11. Fluoride laboratory comparison. Single high point corresponds to spring at GPS location #10. .... 21

Figure 12. Molybdenum laboratory comparison. Photometer Mo values are converted from Molybdate readings. Single high point corresponds to spring at GPS location #10. .... 22

Figure 13. Aluminum laboratory comparison. Single high point corresponds to spring at GPS location #16. .... 23

Figure 14. Iron laboratory comparison. Single high point corresponds to spring at GPS location #16. .... 23

Figure 15. Manganese laboratory comparison. Single high point corresponds to spring at GPS location #10. .... 24

Figure 16. Hardness (Hardicol) laboratory comparison. Single high point corresponds to spring at GPS location #10. .... 25

Figure 17. Alkalinity (Calcicol) laboratory comparison. Single high point corresponds to spring at GPS location #35. .... 26

Figure 18. Calcium laboratory comparison. Photometer values are converted from Calcicol test. Single high point corresponds to spring at GPS location #10. .... 26

Figure 19. Copper (Total) laboratory comparison. Single high point corresponds to spring at GPS location #14. .... 27

Figure 20. Magnesium laboratory comparison. Single high point corresponds to spring at GPS location #10. .... 27

Figure 21. Sulphate laboratory comparison. Single high point corresponds to spring at GPS location #10. .... 28

Figure 22. Silica laboratory comparison..... 28

Figure 23. Potassium laboratory comparison. Single high point corresponds to spring at GPS location #10. .... 29

Figure 24. A Comparison of field and laboratory turbidity measurements..... 30

Figure 25. A Comparison of field and laboratory conductivity measurements..... 30

Figure 26. A Comparison of field and laboratory TDS measurements. .... 31

Figure 27. A Comparison of field and laboratory pH measurements. .... 31

Figure 28. Field pH results August (top) and October (bottom)..... 37

Figure 29. Field TDS Oakton PCS Testr 35 August (top) and October (bottom). ..... 38

Figure 30. Field conductivity Oakton PCS Testr 35 August (top) and October (bottom)..... 39

Figure 31. Field temperature Oakton PCS Testr 35 August (top) and October (bottom)..... 40

Figure 32. Turbidity photometer analysis August (top) and October (bottom). ..... 41

Figure 33. Copper photometer analysis August (top) and October (bottom)..... 43

Figure 34. Iron photometer analysis August (top) and October (bottom). ..... 44

Figure 35. Molybdate photometer analysis August (top) and October (bottom). ..... 45

Figure 36. Zinc EDTA photometer analysis August (top) and October (bottom)..... 46

Figure 37. Bromine photometer analysis August (top) and October (bottom)..... 48

Figure 38. Chloride photometer analysis August (top) and October (bottom). ..... 49

Figure 39. Fluoride photometer analysis August (top) and October (bottom). ..... 50

Figure 40. Potassium photometer analysis August (top) and October (bottom). ..... 52

Figure 41. Sulphate photometer analysis August (top) and October (bottom)..... 53

Figure 42. Silica photometer analysis August (top) and October (bottom)..... 54

Figure 43. Aluminum photometer analysis August (top) and October (bottom)..... 55

Figure 44. Boron photometer analysis August (top) and October (bottom)..... 56

Figure 45. Calcium photometer analysis August (top) and October (bottom)..... 57

Figure 46. Hardicol photometer analysis August (top) and October (bottom). ..... 58

Figure 47. Magnesium photometer analysis August (top) and October (bottom)..... 60

Figure 48. Manganese photometer analysis August (top) and October (bottom)..... 61

Figure 49. Nickel photometer analysis August (top) and October (bottom)..... 62

Figure 50. Copper stream sediment August (top) and October (bottom)..... 64

Figure 51. Molybdenum stream sediment August (top) and October (bottom)..... 65

Figure 52. Iron stream sediment August (top) and October (bottom)..... 68

Figure 53. Manganese stream sediment August (top) and October (bottom)..... 69

Figure 54. Nickel stream sediment August (top) and October (bottom)..... 70

Figure 55. Zinc stream sediment August (top) and October (bottom)..... 71

Figure 56. Aluminum stream sediment August (top) and October (bottom)..... 74

Figure 57. Boron stream sediment August (top) and October (bottom)..... 75

Figure 58. Calcium stream sediment August (top) and October (bottom)..... 76

Figure 59. Potassium stream sediment August (top) and October (bottom)..... 77

Figure 60. Magnesium stream sediment August (top) and October (bottom)..... 78

Figure 61. Copper 'Copper Creek' dispersion August (top) and October (bottom). Coloured bar on this and subsequent diagrams indicates the position of the mineralized zone. .... 81

Figure 62. Molybdenum 'Copper Creek' dispersion August (top) and October (bottom)..... 82

Figure 63. Nickel 'Copper Creek' dispersion August (top) and October (bottom)..... 83

Figure 64. Calcium 'Copper Creek' dispersion August (top) and October (bottom)..... 84

Figure 65. Sample analysis turnaround times. Photometer analysis was performed by single operator in August and two in October ..... 88

Figure 66. Aluminum 'Copper Creek' dispersion August (top) and October (bottom)..... 91

Figure 67. Boron 'Copper Creek' dispersion August (top) and October (bottom)..... 92

Figure 68. Bromine 'Copper Creek' dispersion August (top) and October (bottom)..... 93

Figure 69. Chloride 'Copper Creek' dispersion August (top) and October (bottom)..... 94

Figure 70. Fluoride 'Copper Creek' dispersion August (top) and October (bottom). .... 95

Figure 71. Iron 'Copper Creek' dispersion August (top) and October (bottom)..... 96

Figure 72. Potassium 'Copper Creek' dispersion August (top) and October (bottom)..... 97

Figure 73. Magnesium 'Copper Creek' dispersion August (top) and October (bottom)..... 98

Figure 74. Manganese 'Copper Creek' dispersion August (top) and October (bottom).....	99
Figure 75. Silica 'Copper Creek' dispersion August (top) and October (bottom). ....	100
Figure 76. Sulphate 'Copper Creek' dispersion August (top) and October (bottom). ....	101
Figure 77. Zinc 'Copper Creek' dispersion August (top) and October (bottom). ....	102

## Introduction

Mineral exploration traditionally focuses on the analysis of rock, soil and stream sediment sampling for the detection of primary and secondary dispersion anomalies derived from outcropping mineralization. In the past, the analysis of surficial water samples for this purpose has been underutilized by the mineral exploration community because of the perceived difficulty of sampling and the high cost of water analysis at commercial laboratories. Now, alternative techniques are available that can provide rapid field analysis of waters at a relatively low cost. These techniques can significantly improve the ability to make exploration and environmental decisions by providing near real-time results.

Hydrogeochemistry is used extensively in the exploration for geothermal resources (Zehner et al., 2006). The application of hydrogeochemistry to mineral exploration is well documented by Taufen (1997); Lett et al. (1998) and Leybourne and Cameron (2010). It has been shown to be a useful technique for identifying commodity and pathfinder element dispersion patterns from both outcropping and concealed mineralization. It is a useful technique for exploring areas with difficult access, such as the coastal mountain ranges of British Columbia. Large areas can be sampled at a low sample density to identify hydrological basins containing anomalous metal sources. When water sampling is used in conjunction with stream sediment geochemistry and water pH, it can be an effective tool for both regional and local scale exploration and providing the impetus for immediate follow-up without waiting for lab results.

Portable spectrophotometers, or photometers, are available for field-based water testing. They can determine ion concentrations by measuring the colour and light transmittance of a solution after the addition of metal-sensitive colour dyes; a technique called visible light reflectance photometry. These devices can measure concentrations of a diverse suite of dissolved anions and cations to relatively low detection limits (DL). The tests can be completed on location; providing almost real-time (i.e., within 48 hours) results. Cost of analysis, including photometer reagents, is a fraction of the cost of analysis at a commercial laboratory. For example, photometer analysis is \$6 to \$13 per sample suite (depending on reagent selection) compared to up to approximately \$200-\$300 for commercial water analysis that includes using ICP-MS for cations, as well as ion chromatography test for anions, and more (Table 2). Analytical costs for photometer analysis for this study were \$31.25/sample. Additional savings are realized by other aspects of real-time exploration, such as faster target identification, reduced field and overall exploration time, and a smaller environmental impact than some other sampling methods. This technique could have many benefits for mineral exploration and environmental testing and monitoring.

This proof of concept study was carried out at the previously drilled porphyry copper-gold-molybdenum deposit at Poison Mountain, near Lillooet, southwestern BC (NTS 0920/02) (Seraphim and Rainboth, 1976; Raven, 1994; Brown, 1995). The study aims to test the reliability of the Palintest® Photometer 8000 by comparing the results from water samples analyzed using this instrument with the results of identical samples analyzed using collision cell mass spectrometry (CCMS) and inductively coupled plasma optical emission spectrometry (ICP-OES) at ALS Environmental laboratory (Burnaby, BC) (Table 2). The study also tests for repeatability over time by comparing analyses of samples collected in late

summer and early fall. It also includes a comparison of water sample analyses with stream sediment samples from the same localities (where applicable), analyzed at ALS Minerals laboratory in North Vancouver.

Assessment of the results includes an examination of the accuracy and precision of the photometer readings based on replicate analyses, the analysis of the manufacturers' standard colour solutions and analysis of field duplicate samples. The interpretation also addresses the dispersion distances of key anions and cations from the exposed porphyry mineralization and discusses the advantages of using this technique over other methods for mineral exploration in BC and elsewhere.

## Background

The photometer field survey technique was conceived by the lead author and field tested on a geothermal exploration program carried out by Alterra Power Corp in 2012 (Yehia et al., 2013). The geothermal industry relies heavily on water analysis for early stage exploration. To accelerate exploration at reduced cost, a new types of devices (photometers and spectrophotometers), designed for rapid water testing were investigated. After comparing devices different manufactures available at the time, it was decided that the Palintest Photometer 8000 was the most suitable and cost-effective. It was chosen mainly for its portability, ease of use, reagent selection (Table 1) and cost. Early results from the geothermal project at three main locations in the Coast Mountains of southwestern BC demonstrated the photometer's reliability and showed that meaningful results could be achieved rapidly in the field (Yehia et al., 2013). MYAR Consulting subsequently received cost-sharing funding from Canada's National Research Council (NRC), under the Industrial Research Assistance Program (IRAP), to test the technique's potential for mineral exploration. Results of that study demonstrated that the photometer can produce rapid meaningful field data analyses at relatively low cost (Yehia, 2014).

## Study Objectives

This proof of concept study was conceived to:

1. Assess the practicality of using the photometer in the field.
2. Compare the photometer results with stream sediment geochemistry.
3. Compare photometer results with laboratory water analyses.
4. Determine the cost effectiveness of field based photometer geochemistry compared with conventional laboratory methods.

## Location and Access

The project is located in southwestern BC approximately 95 km northwest of Lillooet. It is accessible via the Yalakom River Forest Service road (FSR; Figure 1). It is bounded by the headwaters of the Yalakom River to the east, and Churn Creek and Buck Mountain to the west (Figure 2). Elevations range from 1600 m in the Yalakom River valley to 2250 m at Poison Mountain peak. Tree line is at approximately 2070 m. Alpine vegetation is present above this elevation. Below tree line, vegetation consists of natural

and replanted stands of lodgepole pine. The latter occurs mainly on the eastern slopes of Poison Mountain. The creek flowing over the mineral zone is informally named 'Copper Creek' based on exploration reports.

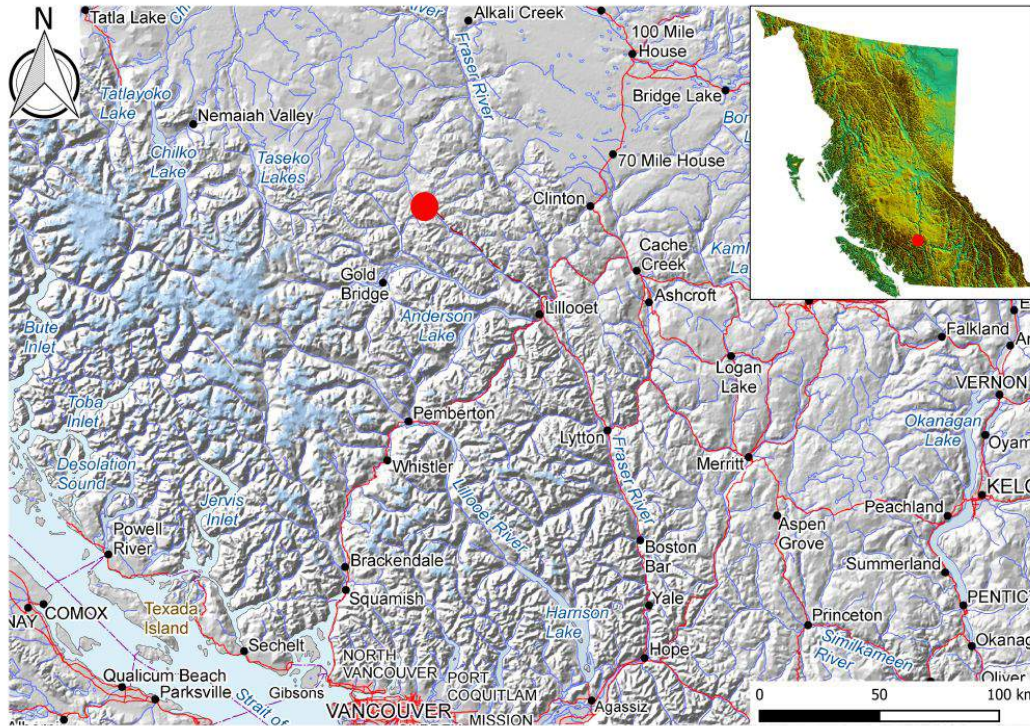


Figure 1. Location of study area, southern British Columbia.

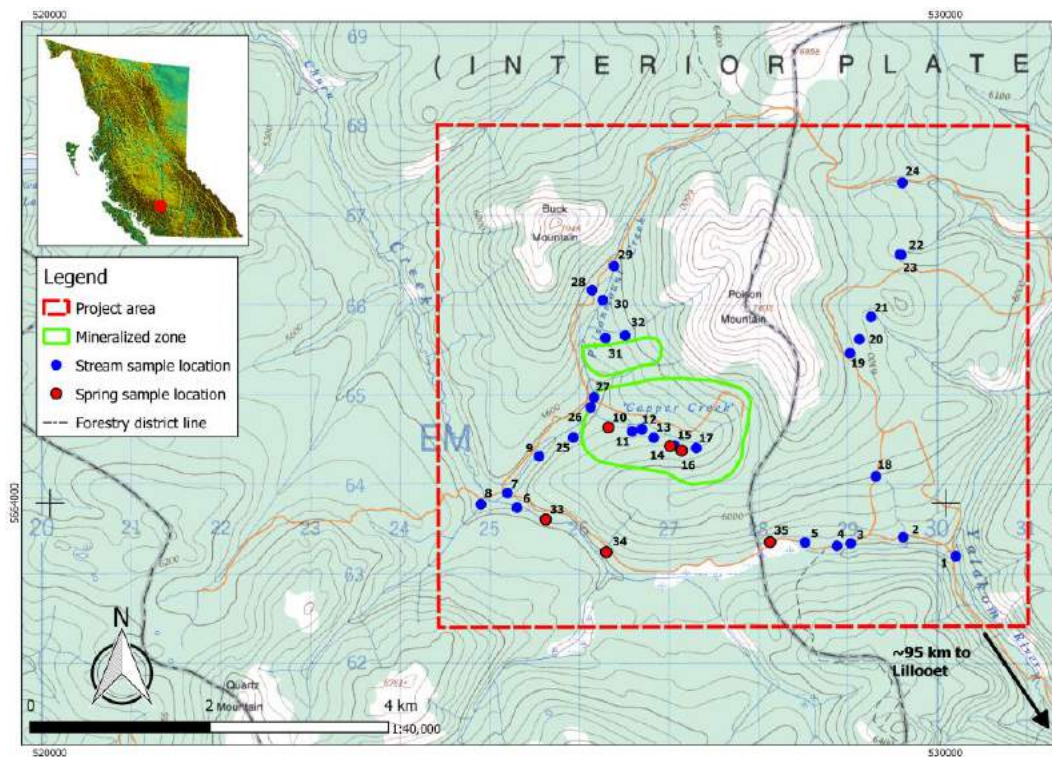


Figure 2. Project area and sample collection points around Poison Mountain.

## Geology

The Poison Mountain porphyry copper-gold-molybdenum prospect consists of disseminated and stockwork-style mineralization associated with small Paleocene-age stocks that intrude sandstone, shale and conglomerate of the Lower Cretaceous Jackass Mountain Group (Seraphim and Rainboth, 1976; Raven, 1994; Brown, 1995). The three main porphyry intrusions are biotite diorite, hornblende diorite and granodiorite. Primary sulphide mineralization consists of pyrite, chalcopyrite, molybdenite and bornite. Weathering of bedrock extends to about 5 m below the surface in the sedimentary units but is poorly developed over the intrusions. Supergene oxidation is intense along fractures and joints to a depth of about 80 m in both intrusive and sedimentary units. Secondary copper minerals (malachite, azurite, cuprite and native copper) occur to depths of up to 10 m from the surface. Supergene sulphide minerals (chalcocite and covellite) occur as overgrowths on chalcopyrite below the supergene oxide zone (Brown, 1995).

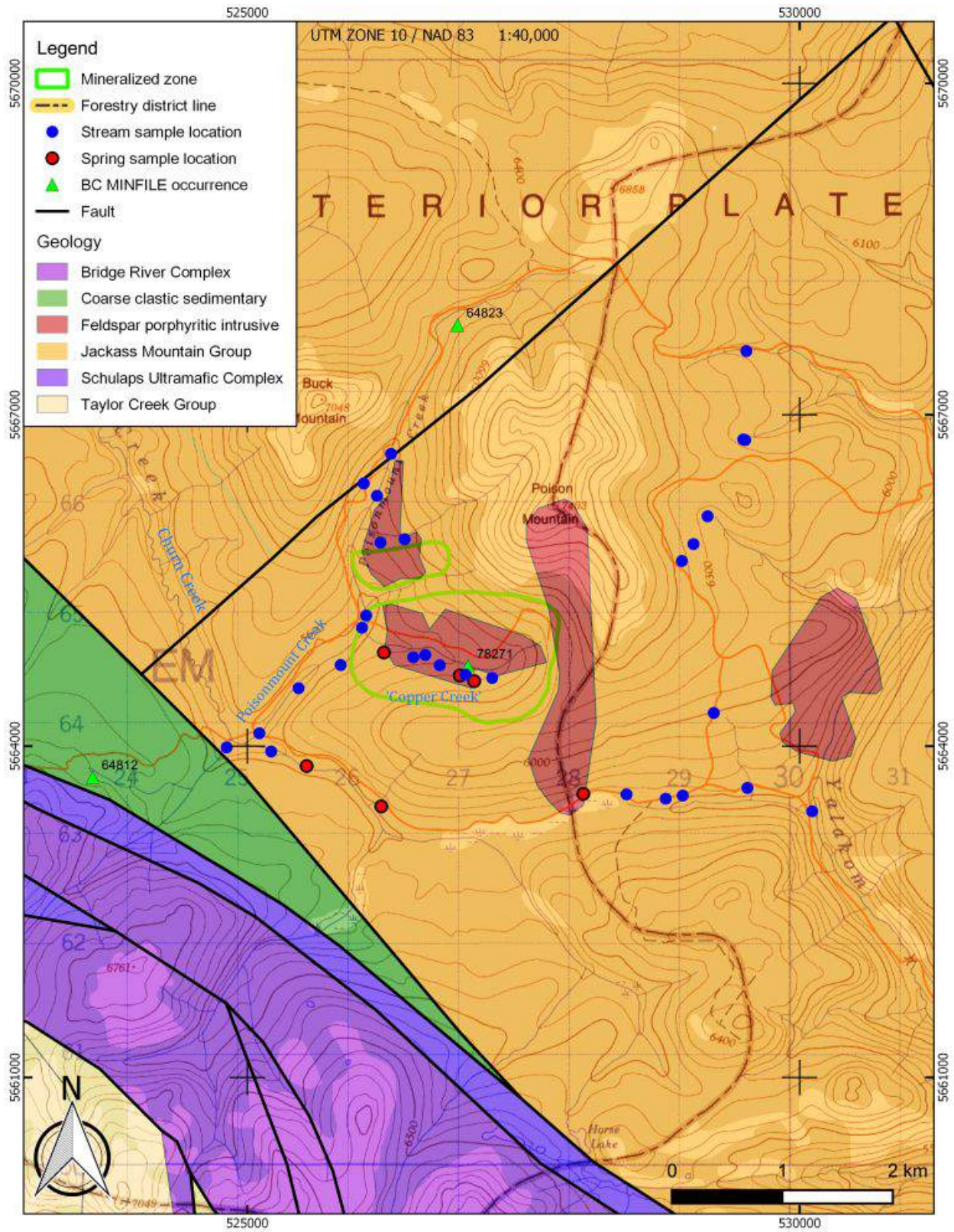


Figure 3. Local geology of study area (Massey et al, 2005).

## Sample Collection

Sample collection was performed in late August and early October 2014. This was done to document variations in the water and sediment chemistry over time. Samples were collected from the same locations in both campaigns (Figure 2). The sampling campaigns were too close together to be a meaningful test of a maximum seasonal variation.

Water collection sites were located a few metres up-stream from the stream sediment sample locations. They were selected from mid-stream and based on flow clearance, sediment load, organic contamination, and ease of access, to provide the best contaminant free sample as possible. Springs were sampled as close as possible to their sources.

Photometer samples were stored in 1 L high density polyethylene (HDPE) bottles, and laboratory samples in one 1 L and one 250 ml HDPE bottles. Water in the 250 mL bottles for cation analysis was acidified with 3 ml of ultrapure nitric acid in the field. The 1 L bottles submitted to the laboratory were used for pH, total dissolved solids (TDS), conductivity, turbidity and anion analysis. In addition, at each location, temperature, pH, conductivity, TDS and salinity were measured using an Oakton Instruments PCS Testr 35 meter. The pH meter was calibrated using standard buffer solutions at pH 4.01 and 7.01, as well as conductivity solution at 1413  $\mu\text{S}/\text{cm}$ .

Photometer sample bottles were reused throughout the study, and rinsed thoroughly at least twice with the waters at each sample site with the cap on before sample collection. If a sample bottle displayed any type of discoloration, it was discarded.

Filtration and acid preservation were not carried out on the photometer samples for the following reasons:

1. Analysis was carried out within 48 hours of collection.
2. The majority of samples were clear with very little suspended fines.
3. In most tests analysis was focused on total concentrations.
4. To expedite sampling and processing.

Stream sediment samples were wet sieved to –20 mesh and the fine fraction collected in HUBCO Inc.'s New Sentry II 5 by 8 in. (13 by 20 cm) sample bags. The bags were allowed to stand to drain excess water and then stored in sealed Ziploc® freezer bags to prevent cross-contamination between samples. All sampling equipment was rinsed thoroughly before and after each sample.

The following samples were collected during the study:

- 79 samples for photometer analysis: 40 in August and 39 in October.<sup>1</sup> This total included 8 field duplicates and 2 deionized water blanks added for QC purposes.

---

<sup>1</sup> One spring sample (GPS point #33) could not be collected in October because the spring was dry.

- 40 laboratory water samples including 8 duplicates and deionized water field blanks and were submitted to ALS Environmental laboratory in Burnaby, BC.
- 66 stream sediment samples including 8 field duplicates were submitted to ALS Minerals laboratory in North Vancouver, BC. Field samples were screened to -20 mesh (0.85 mm) and then sieved to -80 mesh after drying at the laboratory.

Complete sampling details and field observations are presented in the Digital Appendix.

All samples for photometer analysis were tested within 48 hours of collection. The reagents listed in Table 1 were used for each sample. During the survey, all of the samples were stored in coolers.

Weather conditions were comparable for both sampling campaigns, with mild temperatures, partial cloud cover and occasional showers. Due to the elevation and terrain, conditions at times could change rapidly and also be localized to small areas. For example, early morning showers to the east of Poison Mountain, while clear conditions to the west. These conditions are important to observe and record, as dilution from increased stream flow during rain events could affect the analytical results. Stream flows were fairly consistent during both field campaigns and increased dilution is unlikely.

## Quality Control Measures

Quality control measures used for the project include:

- 1) Collection of field duplicates for each sample type (approximately 10% for photometer and stream sediment samples and 17% for laboratory water samples).
- 2) Photometer calibration and drift tests after every eight samples using manufacturer's standard solutions.
- 3) Triplicate readings for each test to measure instrument precision; and
- 4) The use of deionized water blanks to monitor contamination and instrument drift.

## Analysis

### Photometer

A Palintest® Photometer 8000 was used for the field analyses. The tests included all of the available cations and anions of interest to mineral exploration. A full list of analytes and reagents with their corresponding detection limits is presented in Table 1.

**Table 1. List of analytes with detection ranges measured (published by Palintest.)**

Type	Palintest published detection range (mg/l)
Aluminum	0–0.5
Boron	0–2.5
Bromine	0–10.0
Calcium hardness (Calcicol <sup>1</sup> )	0–500
Chloride (Chloridol, NaCl)	0–50 000
Copper (Coppercol, free and total <sup>2</sup> )	0–5.0
Fluoride	0–1.5
Hardness (Hardicol, total)	0–500
Iron	0–10
Magnesium	0–100
Manganese	0–5.0
Molybdate (MoO <sub>4</sub> )	0–100
Nickel	0–10
Potassium	0–12
Silica (SiO <sub>2</sub> )	0–150
Sulphate (SO <sub>4</sub> )	0–200
Zinc	0–4.0

<sup>1</sup> Calcicol, Chloridol, Coppercol and Hardicol are reagents used for specific analyses.

<sup>2</sup> Chelation copper = total copper – free copper

After each sampling day, sample bottles were transported in coolers to a Motel in Lillooet, which provided a controlled testing environment. Sample bottles were left overnight to allow any suspended particles to settle. Depending on field work pace and weather conditions, analysis was usually carried out the next day. Prior to analysis, sampling tubes and accessories were rinsed thoroughly twice with sample waters, including tubes and caps. Reagents were laid out according to the order of testing to minimize interferences, errors, and to maximize testing efficiency (Figure 4). For example, if the Zn test needed to be checked for Cu interference, then the Cu test was performed first. A typical setup is shown in Figure 4.



Figure 4. Photo showing a typical set-up for photometer analysis. Reagents are in silver packaging aligned atop. Coloured sample solutions ready for analyses are shown in the 10 ml tubes in rack. The Photometer is in the lower right of the photo.

Results, including any interference warnings, were recorded on paper forms (Figure 4) specifically designed for the project. Stored results from the photometer were downloaded to a laptop computer and backed up digitally at the end of each testing day.

Tests were conducted by stirring crushed reagents in tubes containing the sample waters and waiting the appropriate time as indicated by the Palintest instructions. Figure 5 shows a suite of solutions from a sample ready for analysis.



Figure 5. Close-up of rack showing a collection of tubes with reagents ready for photometer testing.

At the end each day, tubes and accessories were rinsed well in tap water and left to dry overnight.

### Health and Safety

Each reagent is accompanied by a Material Safety Data Sheet (MSDS), which for Canada includes recommended only safety measures. For this study MYAR decided to use the more stringent European Union requirements. This was done not only for superior environmental and safety controls, but also to assess any issues and costs that may arise from the stricter measures.

Each member of the analysis team was required to wear nitrile disposable gloves and safety goggles. All solid waste associated with acids or reagents were disposed of in industrial-strength plastic garbage bags. Liquid waste, including used reagents and post-test rinse water were stored in a 22.7 L plastic pail with special no-spill lid. All waste was taken to Newalta's hazardous materials site in Delta, BC, for disposal.

## Laboratory Analysis

Table 2 lists the analytical methods and protocols used by ALS Environmental. Samples were not filtered prior to analysis.

**Table 2. Analytical methods employed by ALS Environmental<sup>1</sup>**

Type	Test	Test Description	ALS Test Code	Method Reference
Alkalinity	Colourimetric	Total Alkalinity is determined using the methyl orange colourimetric method	ALK-COL-VA <sup>2</sup>	EPA 310.2
Br, Cl <sup>-</sup> , F <sup>-</sup> and SO <sub>4</sub>	Ion Chromatography		ANIONS-IC-VA	APHA 4110 B
Conductivity	[Automated]	Determined using a conductivity electrode	EC-PCT-VA	APHA 2510
Hardness		Calculated from the sum of Ca and Mg concentrations, expressed in CaCO <sub>3</sub> equivalents.	HARDNESS-CALC-VA	APHA 2340B
Total Metals	CCMS & ICPOES	Procedures may involve preliminary sample treatment by acid digestion, using hot block or filtration. Instrumental analysis is by collision cell inductively coupled plasma – optical emission spectrophotometry.	MET-TOT-ICP-VA	APHA SW-846 3005A/6010B
pH	Meter [Automated]	Determined in the laboratory using a pH electrode.	PH-PCT-VA	APHA 4500-H
SiO <sub>2</sub>	Colourimetric analysis		SILICATE-COL-VA	APHA 4500-SiO <sub>2</sub> E.
Total Dissolved Solids	Gravimetric	Determined by filtering a sample through a glass fibre filter. TDS is determined by evaporating to dryness at 180 degrees Celsius.	TDS-VA	APHA 2540 C
Turbidity	Meter	Determined by the nephelometric method.	TURBIDITY-VA	APHA 2130

<sup>1</sup> Cited from ALS reference information included with Certificate of Analysis

<sup>2</sup> VA - Laboratory Definition Code: ALS Environmental, Burnaby, British Columbia, Canada

## Quality Control Results

### Accuracy

To examine photometer drift, calibration tests using manufactures' standard dye solutions were performed after every eighth analysis. The standard colour solutions are traceable to standards BS 6376 and ISO 6353, and are supplied in sealed 10 ml tubes with expiry dates. The tubes are designated 38271/B (yellow), 38271/C (red) and 38271/D (green). Solution 38271/A is a clear solution that is used to reset the photometer before each test. Test values are in transmittance % (mg/l Pt) units. Results are charted in order of date of analysis in Figure 6 to Figure 8. Results are available in the Digital Appendix.

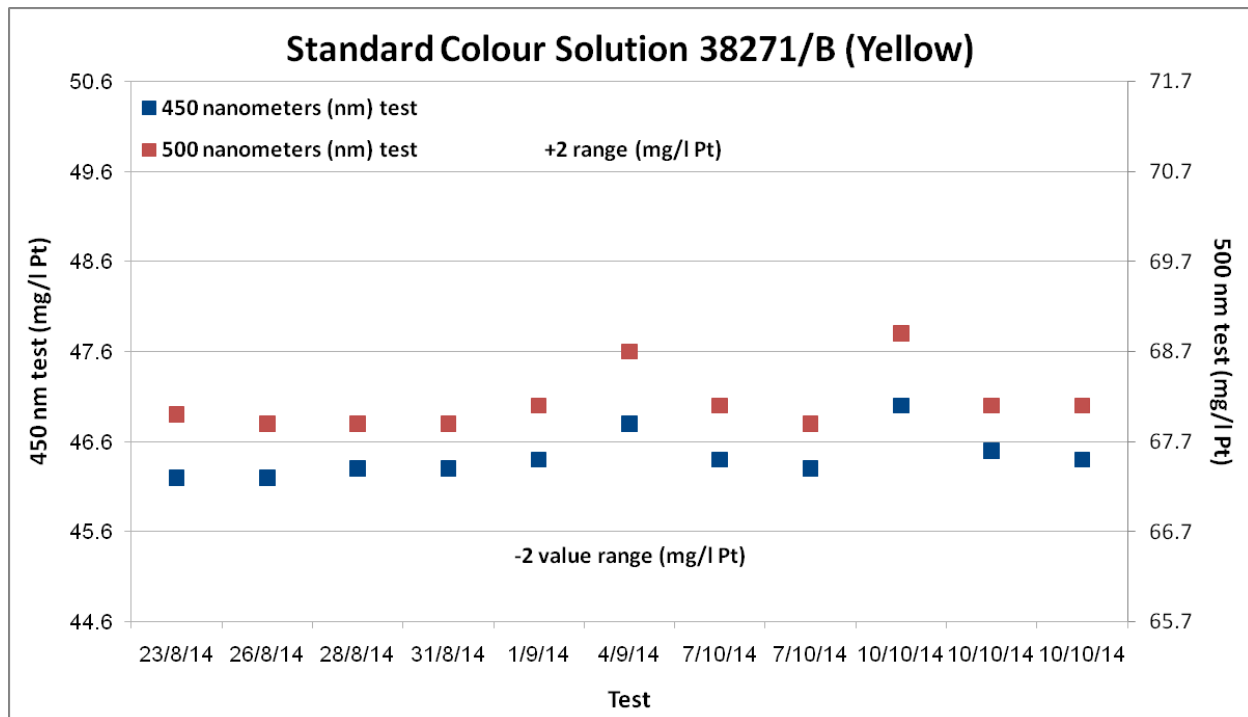


Figure 6. Control chart for standard solution 38271/B.

Blank results demonstrate excellent device stability. Results fall well within the manufacturer's recommended margin of error. Values range from 0.00% to 2.94% for assigned  $\pm 2$  test unit values (best accuracy at lowest percentage) for a total average accuracy of  $\pm 0.89\%$ . The wavelengths cover the expected range of the various reagents. These are pre-programmed into the photometer for each assigned reagent. The charts show that for each assigned colour, the photometer reading is highly accurate for each wavelength test.

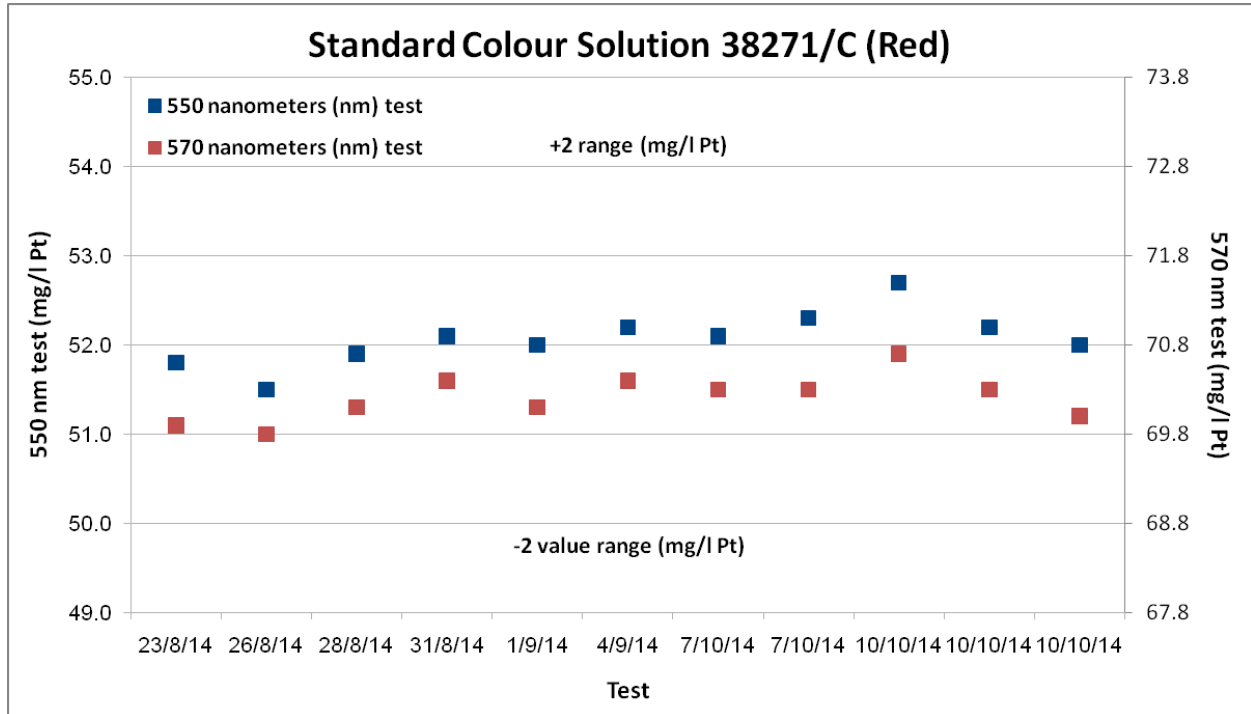


Figure 7. Control chart for standard solution 38271/C.

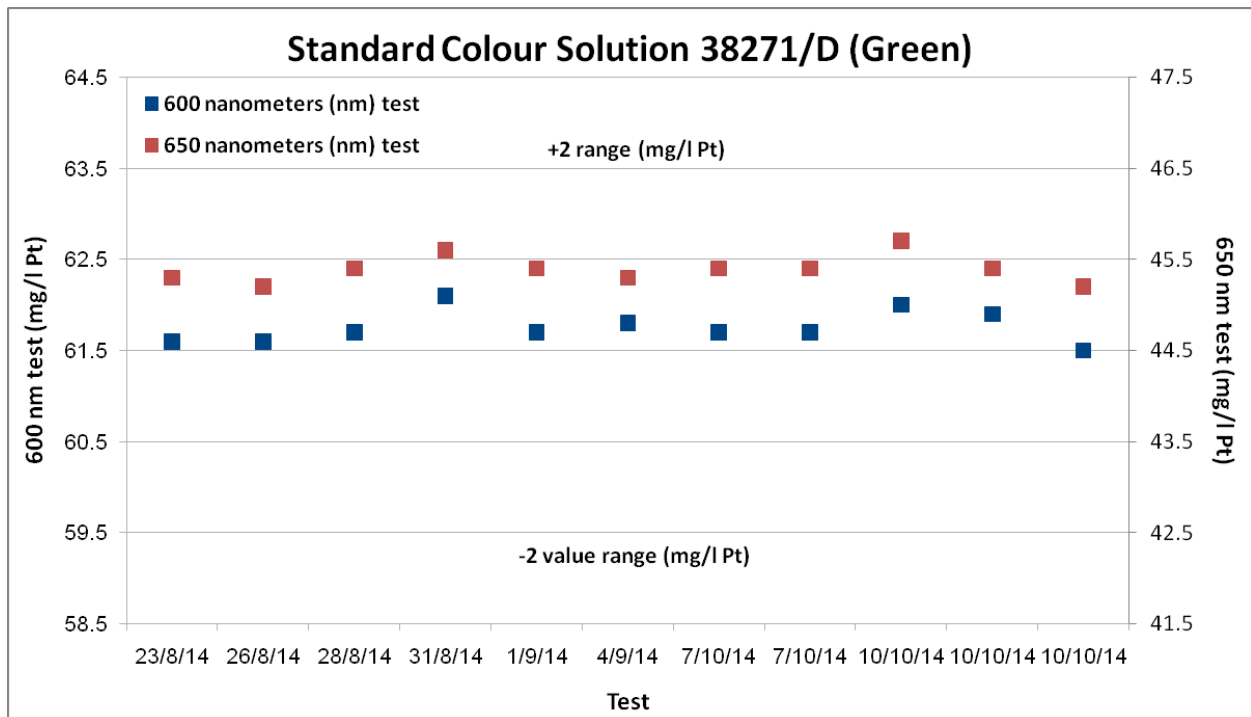


Figure 8. Control chart for standard solution 38271/D.

## Precision

In order to assess the quality of the photometer readings, precision, or measurement error was assessed in two different ways:

- a) From triplicate analysis of the photometer test solutions; and
- b) Through analysis of field duplicate samples.

Triplicate analyses provide an estimate of the precision of the analytical process while the field duplicate results provide important information about the representivity of a sample of the medium being sampled as well as an estimate for the combined sampling and measurement error.

For the purposes of this study precision is expressed as the average percent relative standard deviation or %RSD. It is calculated from the replicate and field duplicate results in an Excel spreadsheet by first determining the mean and standard deviation of each duplicate pair or set of replicate analyses and then calculating the %RSD value using the formula:

$$\%RSD = (\text{standard deviation}/\text{mean}) \times 100$$

Percent RSD results were then averaged for each analyte. Results for the photometer triplicate analyses are presented in Table 3 and the field duplicates in Table 4.

### Analytical Precision

Prior to each reagent test, the photometer was reset (blinking – Palintest terminology) using a distilled water-filled tube (blank). For each testing day, a new blank tube was created with a turbidity test performed to verify solution clarity.

Each reagent was read three times. If at least two consistent values were not achieved in the first set of three readings, the test was repeated on the same sample until consistent results were obtained. Below detection limit values indicated by '<<' or zero(s) were excluded from the precision calculation as were triplicate readings with only a single value above the instrument detection limit or zero results. Zero values occur when transmittance was too low to register a meaningful value.

Table 3 shows that the majority of the average %RSD values for the triplicate analyses fall below 3%, indicating a high level of precision, or low measurement error for the analyses. Only Br (5.32%), MoO<sub>4</sub> (3.24%), Ni (PR – 6.58%) and Zn (EDTA – 5.70%) have higher values but these are also considered to be acceptable error levels. The higher average % RSD values for these elements are caused by concentrations for some tests falling at or close to the instrument detection limit. This results in elevated average %RSD results. For example, Br test L140841520003 produced values of 0.01, 0.02 and 0.02 mg/l resulting in a %RSD of 34.6% (with a detection limit of 0.01 mg/l).

**Table 3. %RSD results from replicate analyses.**

Type	Average %RSD	# of samples
Al (mg/l)	0.88%	14
B (mg/l)	1.35%	79
Br (mg/l)	5.32%	64
CaCO <sub>3</sub> (Calcicol, mg/l)	0.24%	77
CaCO <sub>3</sub> (Hardicol, mg/l)	0.39%	77
Cl <sup>-</sup> (mg/l)	2.35%	79
Cu (Free, mg/l)	2.47%	29
Cu (Total, mg/l)	1.73%	34
F <sup>-</sup> (mg/l)	1.79%	78
Fe (mg/l)	1.03%	36
K (mg/l)	1.77%	78
Mg (mg/l)	1.65%	74
Mn (mg/l)	0.23%	53
MoO <sub>4</sub> (mg/l)	3.24%	62
Ni (mg/l)	0.96%	4
Ni (PR <sup>1</sup> , mg/l)	6.58%	13
SiO <sub>2</sub> (mg/l)	0.33%	79
SO <sub>4</sub> (mg/l)	0.33%	54
Zn (mg/l)	0.73%	30
Zn (EDTA <sup>2</sup> , mg/l)	5.70%	6
Turbidity (FTU <sup>3</sup> )	1.55%	28

<sup>1</sup>Powder Reagent

<sup>2</sup>Ethylenediaminetetraacetic tablets

<sup>3</sup>Formazin Turbidity Unit

### Field Duplicate Precision

The field duplicates were analysed immediately after the original samples and the triplicate values were averaged to produce final values, which after removing the '<<' and zero values, were used for the average % RSD calculations. Table 4 shows the results for the analyte suite.

A wide range of % RSD values are observed for the different analytes. Those displaying the lowest %RSD values, or best reproducibility, are CaCO<sub>3</sub> (Calcicol and Hardicol), Cu (Free), Cu (Total), Mg, SiO<sub>2</sub> and turbidity, which all have values of <10%. The majority of analytes display values in the 10% to 30% range, which is a reasonable range for field duplicates. Only Zn (EDTA) with a %RSD of 47.14% is considered to be of marginal quality and caution should be used when interpreting patterns for this

analyte. This higher value is caused by slight differences in concentration at the detection limit, which produce a large standard deviation.

The %RSD calculations are not always based on uniform numbers of duplicate pairs as some duplicates were below the detection limit. For some analytes for instance Fe, Ni and Ni PR the %RSD values are supported by only a single duplicate pair. This is because the results for the other seven field duplicates are below the instrument detection limit and were thus excluded from the calculations. The value for Ni (PR) in particular may not be realistic because there is no difference between the values of the original and duplicate sample. Therefore the standard deviation used for the %RSD calculation is zero.

**Table 4. Average %RSD values for photometer field duplicate analyses.**

<b>Type</b>	<b>%RSD Average</b>	<b># of duplicates</b>
B (mg/l)	30.02%	8
Br (mg/l)	23.07%	6
CaCO <sub>3</sub> (Calcicol, mg/l)	4.24%	8
CaCO <sub>3</sub> (Hardicol, mg/l)	6.34%	8
Cl <sup>-</sup> (mg/l)	27.48%	8
Cu (Free, mg/l)	3.72%	2
Cu (Total, mg/l)	7.59%	2
F <sup>-</sup> (mg/l)	25.25%	8
Fe (mg/l)	18.97%	1
K (mg/l)	30.72%	8
Mg (mg/l)	7.15%	7
Mn (mg/l)	12.33%	4
MoO <sub>4</sub> (mg/l)	28.34%	5
Ni (mg/l)	20.75%	1
Ni (PR, mg/l)	0.00%	1
SiO <sub>2</sub> (mg/l)	1.67%	8
SO <sub>4</sub> (mg/l)	22.29%	4
Zn (mg/l)	13.51%	2
Zn (EDTA, mg/l)	47.14%	1
Turbidity (FTU)	1.37%	1

In conclusion the field duplicate sample results and replicate analyses on the instrument indicate that the photometer results are of sufficiently good quality to produce meaningful interpretations.

### Stream Sediment Precision

Table 5 shows the %RSD values for selected elements calculated from the stream sediment field duplicate results. The subset of elements conforms to those reported by the photometer. Values for Al, Ca, Fe, K, Mg, Ni and Zn are below 10%, which are very low for stream sediment results. Measurement errors for Cu, Mn, and Mo are slightly higher but also indicate that the results are highly reproducible. A

%RSD value could not be calculated for B because results for both the original and duplicate samples are below the method detection limit.

**Table 5. Average % RSD values for selected elements from the stream sediment field duplicate results**

Type	%RSD	
	Total Average	# of samples
Al (%)	3.38%	8
B (ppm)	NA	8
Ca (%)	9.45%	8
Cu (ppm)	12.18%	8
Fe (%)	3.60%	8
K (%)	0.90%	8
Mg (%)	2.29%	8
Mn (ppm)	20.29%	8
Mo (ppm)	11.46%	8
Ni (ppm)	7.67%	8
Zn (ppm)	5.73%	8

## Field Blank Results

Photometer and laboratory field blank results and the detection limits for analytes are presented in Table 6. Most of the photometer results display values at or close to the detection limit but several results have somewhat higher concentrations (bold text). Results greater than ten times the detection limit (underlined) are of concern as indications of either potential cross over contamination or of a contaminated blank solution. Potential contamination is observed to B (one blank), Cl<sup>-</sup>, F<sup>-</sup> and K. The laboratory results also show slightly elevated concentrations for B, Cl<sup>-</sup>, K as well as Ni (one blank) but at much lower levels than the photometer. The fact that the same elements are elevated for both methods suggests that the source of the contamination is the blank solution itself, which was store bought deionized water. The field blank results do not show any indications of cross over contamination or contamination from external sources.

Table 6. Field blank results.

Analyte (mg/l)	Photometer			Laboratory		
	Observed DL <sup>2</sup>	L140841100040	L141041100079	DL	LB141041100040	LB14084110019
Al	0.005	0.005	0.005	0.003	0.003	0.003
B	0.02	<b>0.07</b>	<b><u>0.23</u></b>	0.010	<b>0.022</b>	<b>0.018</b>
Br	0.005	0.005	0.005	0.05	0.05	0.05
CaCO <sub>3</sub> <sup>1</sup>	3.0	3.0	3.0	2.0	<b>7.0</b>	<b>4.6</b>
CaCO <sub>3</sub> <sup>2</sup>	12.0	12.0	12.0	0.5	0.5	0.5
Cl <sup>-</sup>	0.01	<b><u>1.20</u></b>	<b><u>1.60</u></b>	0.50	<b>0.95</b>	<b>1.23</b>
Cu (Total)	0.005	0.005	0.005	0.0005	0.0005	0.0005
F <sup>-</sup>	0.01	<b><u>0.317</u></b>	<b><u>0.380</u></b>	0.02	0.02	0.02
Fe	0.005	0.005	0.005	0.01	0.01	0.01
K	0.05	<b><u>4.00</u></b>	<b><u>6.60</u></b>	0.05	<b>0.09</b>	<b>0.097</b>
Mg	0.5	0.5	0.5	0.1	0.1	0.1
Mn	0.0005	0.0005	0.0005	0.00005	0.00005	0.00005
Mo				0.00005	0.00005	0.00005
MoO <sub>4</sub>	0.005	<b><u>1.0000</u></b>	0.005			
Ni	0.005	0.005	0.005	0.0005	0.0005	<b>0.00073</b>
SO <sub>4</sub>	0.5	0.5	0.5	0.5	0.5	0.5
Zn	0.005	0.005	0.005	0.003	0.003	0.003

<sup>1</sup>Photometer Calcicol, Laboratory Alkalinity. <sup>2</sup>Photometer (Hardicol), Laboratory Hardness

<sup>2</sup>Certified DL from manufacture if zero. The observed DL is the actual DL measured by the instrument. Bold indicates values above detection limit and underline values greater than 10 times detection limit.

## Results

In this section we examine the photometer results and compare them to the laboratory analyses. Similarities and differences between the two datasets are examined and irregular or unpredictable results discussed.

### Laboratory Comparison

#### Metals and Anions

An objective of this study was to compare the photometer results to water analyses carried out at a commercial laboratory. A total of 40 samples, including their field duplicates and blanks, were sent for laboratory analysis: this constitutes 50% of the samples analysed by the photometer. Samples were selected to cover the widest possible range of photometer concentrations and included samples with elevated electrical conductivity and TDS readings: most of the spring samples matched this latter criterion. The rest of the samples were selected from every third site.

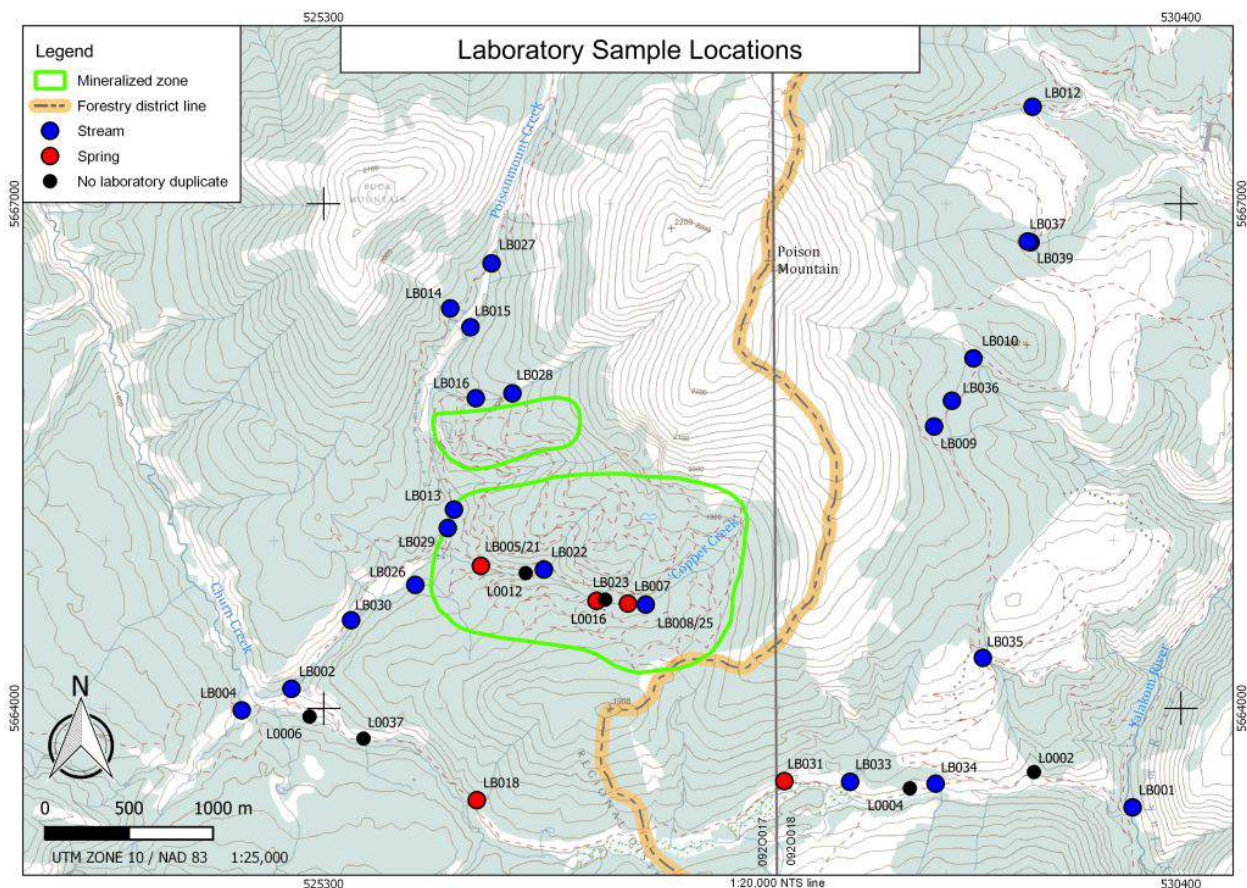


Figure 9. Laboratory samples locations.

Comparison of the laboratory and photometer results reveals some interesting differences for a number of analytes. For instance, B and F<sup>-</sup> (Figure 10 and Figure 11) show that the photometer appears to be much more sensitive than the laboratory at lower concentrations. In the case of B Figure 10), the laboratory analyses appear to resolve concentration differences only above 0.3 mg/l. At these concentrations there is still a positive bias in favour of the photometer. Fluoride (Figure 11) shows a similar pattern with a strong bias in the photometer results up to a concentration of 0.5 mg/l and thereafter a reasonable correlation in values but with the photometer values still being consistently higher.

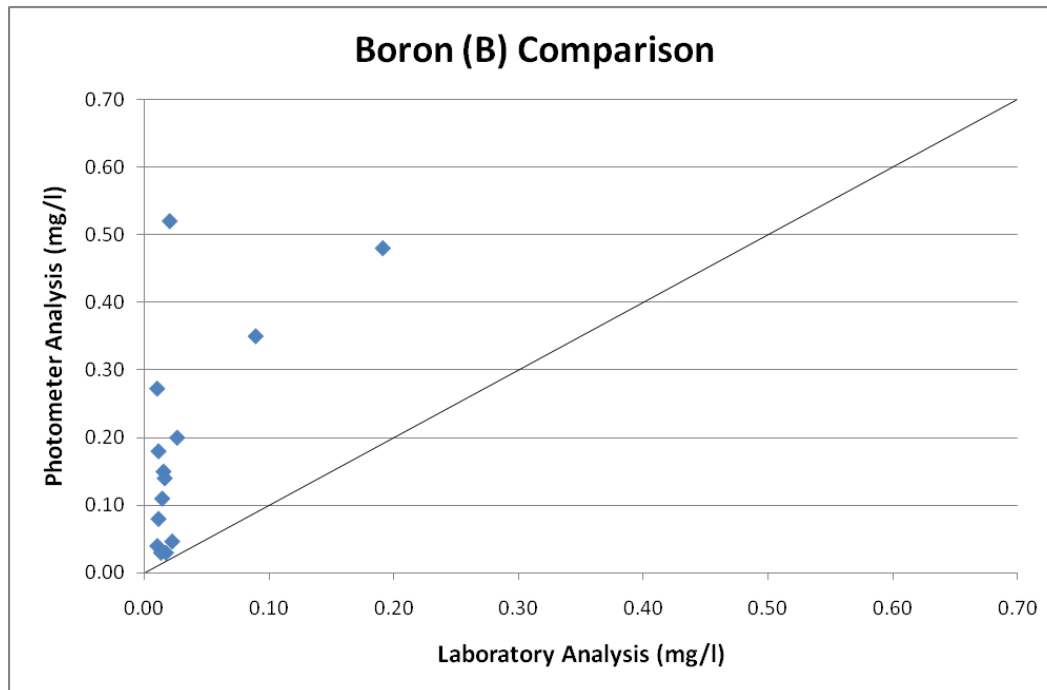
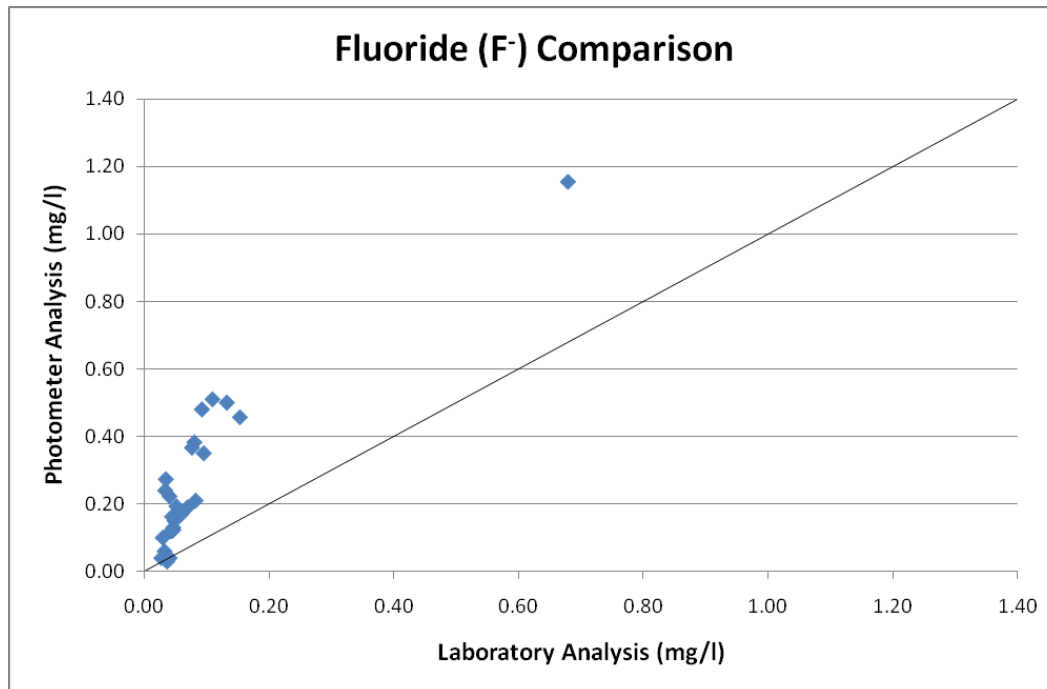


Figure 10. Boron laboratory comparison. Single high point corresponds to spring at GPS location #10.



**Figure 11. Fluoride laboratory comparison. Single high point corresponds to spring at GPS location #10.**

Extreme biases are illustrated by Mo, Al, Fe and Mn (Figure 12 to Figure 15). Molybdenum (calculated from  $\text{MoO}_4$  for the photometer results - Figure 12) shows almost no variation in the laboratory results with most values occurring at or slightly above the method detection limit (0.00005 mg/l). The photometer readings, on the other hand, display a wide range in concentrations between detection limit and 0.824 mg/l. This discrepancy at first glance suggests that the photometer is the more sensitive of the two analyses. However, it is also possible that Mo concentrations in the laboratory samples may have been affected by precipitation and/or adsorption onto the container walls or particulates in the water. This is despite the use of nitric acid preservation.

Aluminum, Fe and Mn (Figure 13 to Figure 15) show the opposite bias where the photometer readings are at or slightly above the detection limit and the laboratory results display a range of concentrations. For Al (Figure 13), it appears that the photometer did not detect the low concentrations in the samples, suggesting that the practical detection limit for this test is higher than the observed concentrations in the laboratory analyses (up to 3.09 mg/l). Alternatively Al has been lost from solution from the photometer samples as a result of hydroxide precipitation. Iron (Figure 14) does show a positive correlation between the two methods, but the laboratory results are approximately 8 times higher than the photometer readings.

A similar trend is present in the Mn results (Figure 15) where the photometer only appears to detect measurable concentrations above 0.07 mg/l. A possible explanation for these differences is the use of nitric acid preservative on the laboratory samples. Acidification prevents Fe and Mn hydroxide precipitation (and adsorption of other elements) and in addition serves to dissolve hydroxide precipitates that may otherwise form. The much lower values in the photometer indicate that Fe and

Mn may have been lost from solution even during the relatively short time period between sample collection and analysis. Hydroxide precipitation could potentially remove other analytes from solution, resulting in suppressed photometer readings. This observation is counter to the above mentioned Mo results, which would also be expected to be systematically lower in the photometer results. The fact that they are systematically higher points to the possibility of another unidentified issue.

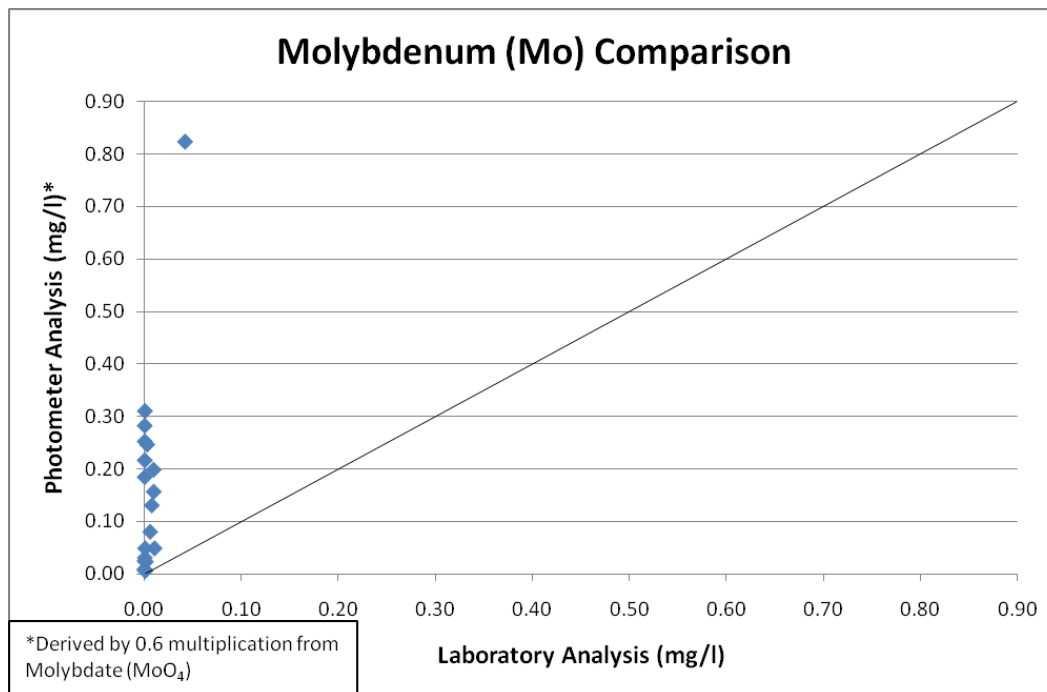


**Figure 12. Molybdenum laboratory comparison. Photometer Mo values are converted from Molybdate readings. Single high point corresponds to spring at GPS location #10.**

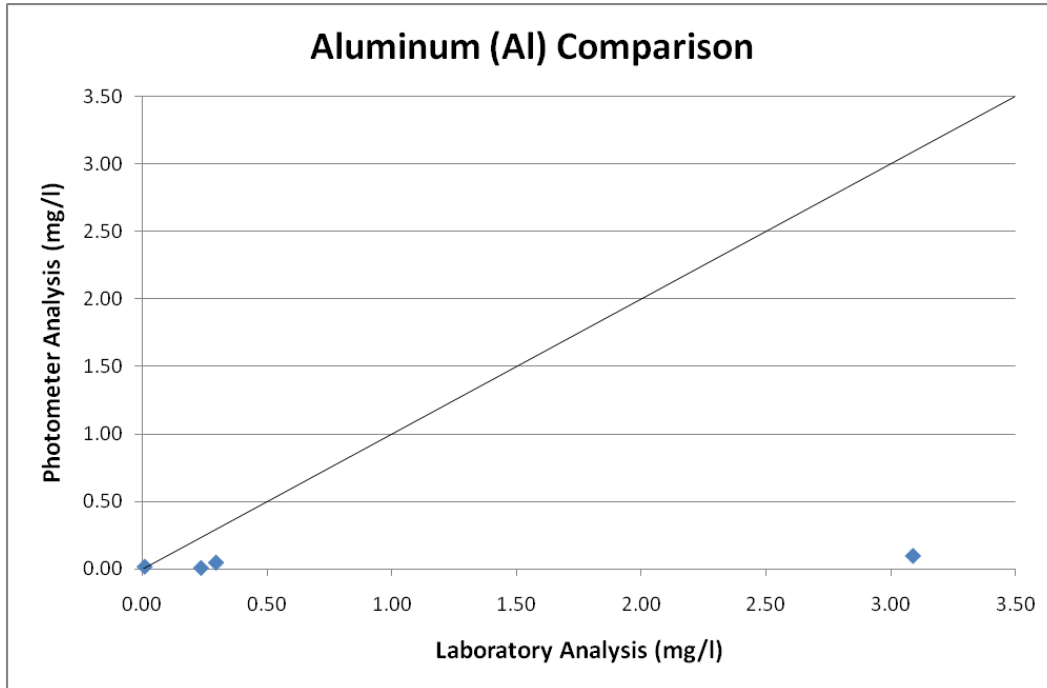


Figure 13. Aluminum laboratory comparison. Single high point corresponds to spring at GPS location #16.

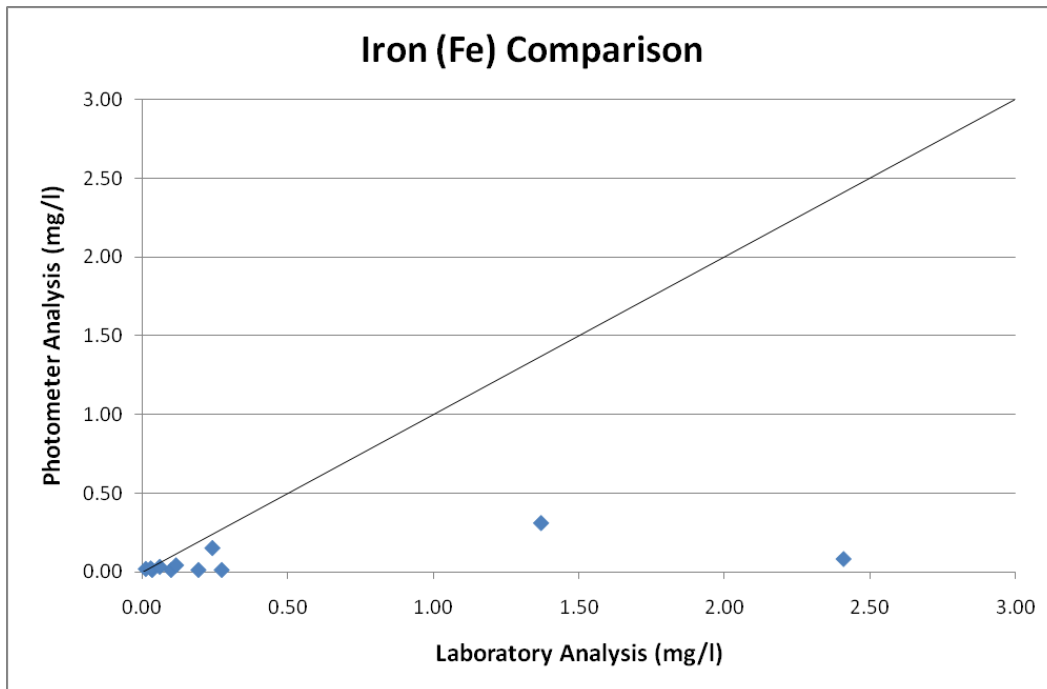


Figure 14. Iron laboratory comparison. Single high point corresponds to spring at GPS location #16.

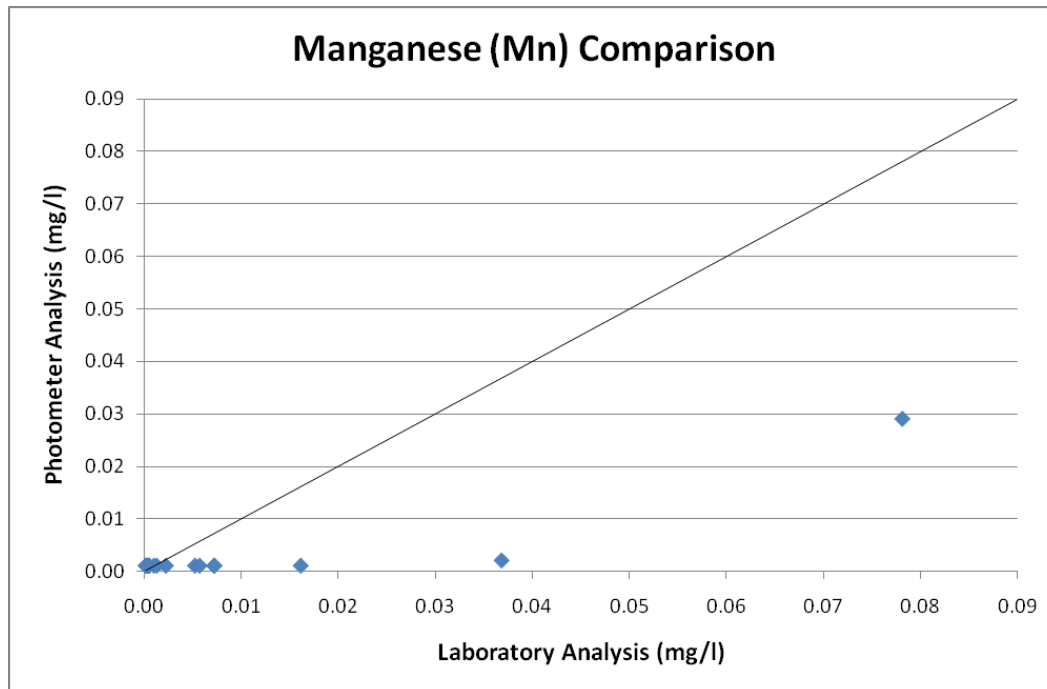


Figure 15. Manganese laboratory comparison. Single high point corresponds to spring at GPS location #10.

Reasonable correlations are shown by the  $\text{CaCO}_3$ , alkalinity, Ca,  $\text{Cl}^-$ , Mg, Cu (total),  $\text{SO}_4$  and Si (expressed as mg/l  $\text{SiO}_2$  equivalent) results (Figure 16 to Figure 22). For  $\text{CaCO}_3$  (Hardicol; Figure 16), the photometer results are consistently about 15% lower than the laboratory concentrations. Calcium carbonate by Calcicol (alkalinity; Figure 17) shows two populations. Below 100 mg/l in the laboratory results, the photometer readings display little variation and most values range between 25 and 100 mg/l. For values above 100mg/l, the photometer readings display a wide concentration range between 90 and 300 mg/l but the laboratory results show little variation. There appears to be an upper concentration limit at about 130 mg/l in the laboratory results.

Calcium (Figure 18) displays a good correlation at concentrations of <70 mg/l but at higher levels, values are biased with the photometer concentrations being about one third lower than the laboratory values.

Total Cu (Figure 19) shows a good correlation between the two methods but exhibits about a 20% low bias in the photometer readings. The trend is somewhat skewed by one sample that has a 50% low bias in the photometer results. This sample is considered to be an outlier, which is not representative of the rest of the sample population. Similar outliers are also observed in the Mg results (Figure 20) where most of the data points define a linear trend with no obvious bias. Two samples however, lie well outside the trend defined by the other points: one has a much higher concentration in the photometer results; and the other, a higher concentration for the laboratory analysis. The cause of these extraneous values is not readily apparent.

Strong correlations are seen in the  $\text{SO}_4$  and  $\text{SiO}_2$  results. Sulphate (Figure 21) shows a high degree of correlation with no bias for concentrations below 100 mg/l. An isolated population of samples with

much higher concentrations (about 500 mg/l) show a 40% low bias in the photometer results. Silica on the other hand, displays a good correlation between the two methods with the photometer results showing a slight high bias in the mid-concentration range (20 mg/l). There is no measureable bias at higher or lower concentrations.

Potassium (Figure 23) appears to show two populations: a scatter of points along the Y-axis and a linear trend. The linear trend indicates a good correlation between the two methods with no obvious bias. The points along the Y axis are difficult to explain. They represent samples with measureable K concentrations in the photometer determinations, but close to detection limit values in the laboratory analyses. Investigation of these populations to determine whether they represent batch effects caused by sampling campaign, reagents or laboratory sequence etc. has not revealed an obvious explanation for this division. One possibility is the difference between the field and laboratory analyses. The unfiltered samples analyzed by photometer reflect the overall system chemistry including colloids and ion forms whereas the acidified laboratory analyses detect predominantly ionic forms.

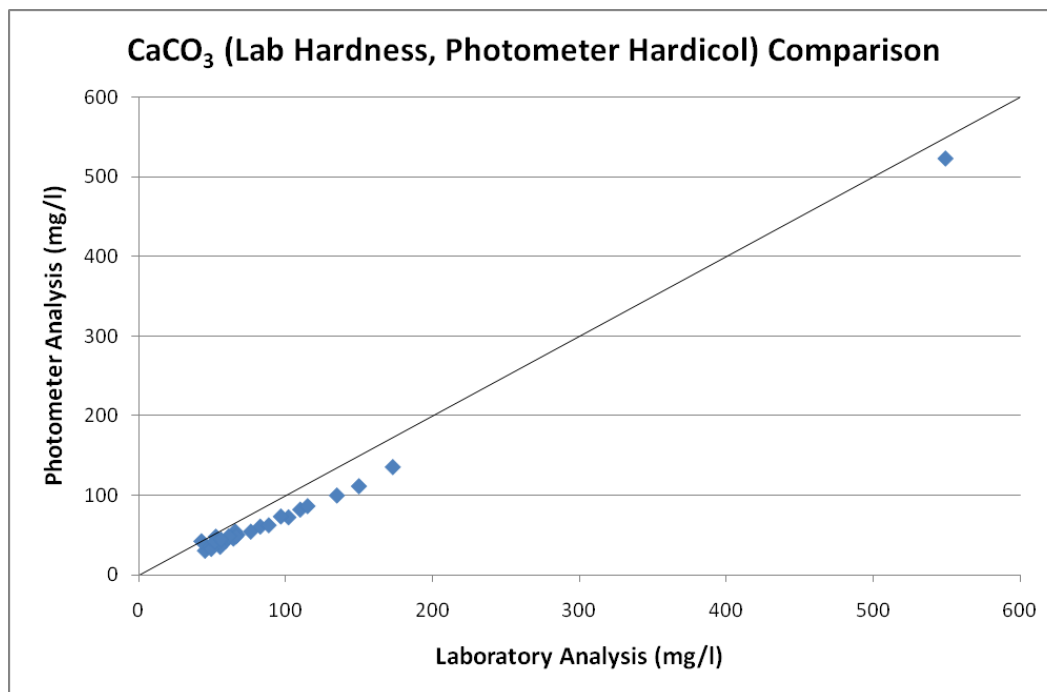


Figure 16. Hardness (Hardicol) laboratory comparison. Single high point corresponds to spring at GPS location #10.

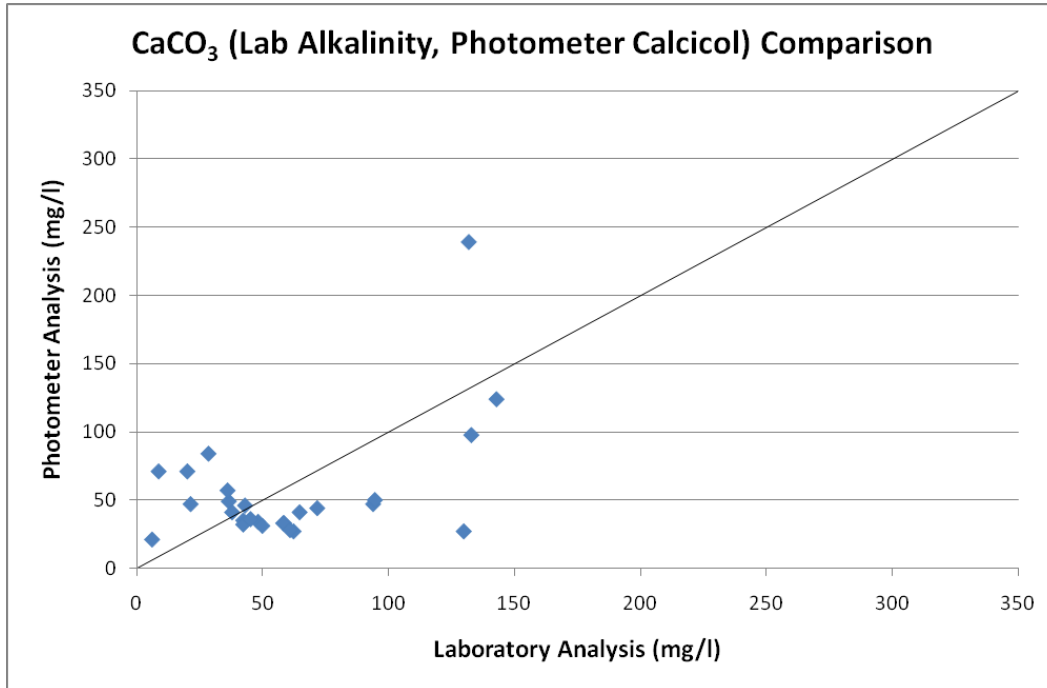


Figure 17. Alkalinity (Calcicol) laboratory comparison. Single high point corresponds to spring at GPS location #35.

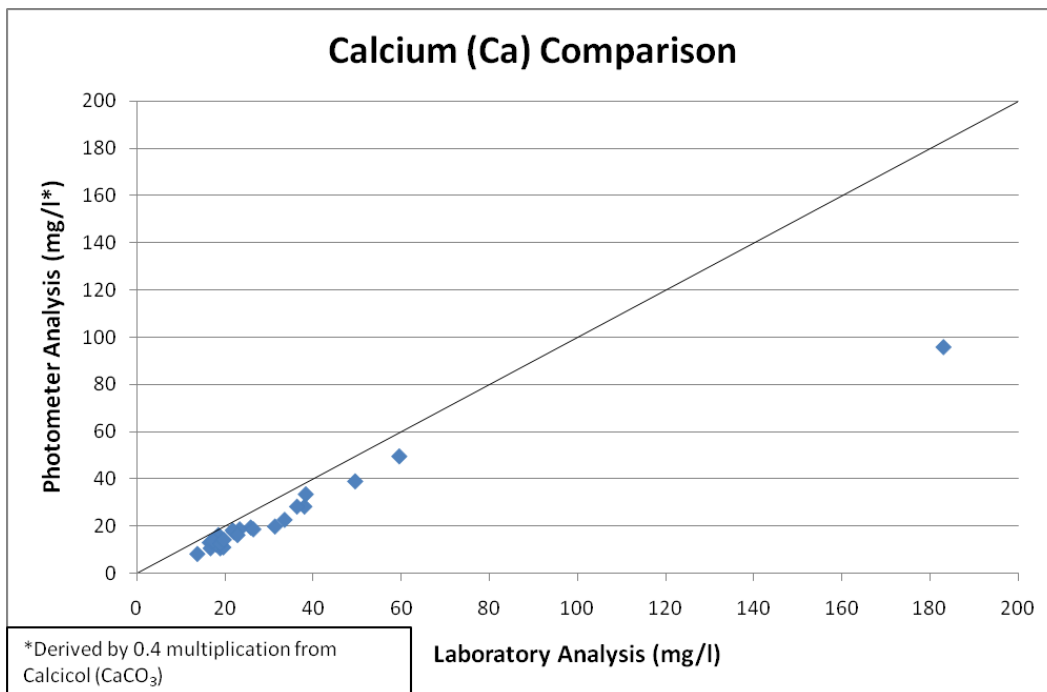


Figure 18. Calcium laboratory comparison. Photometer values are converted from Calcicol test. Single high point corresponds to spring at GPS location #10.

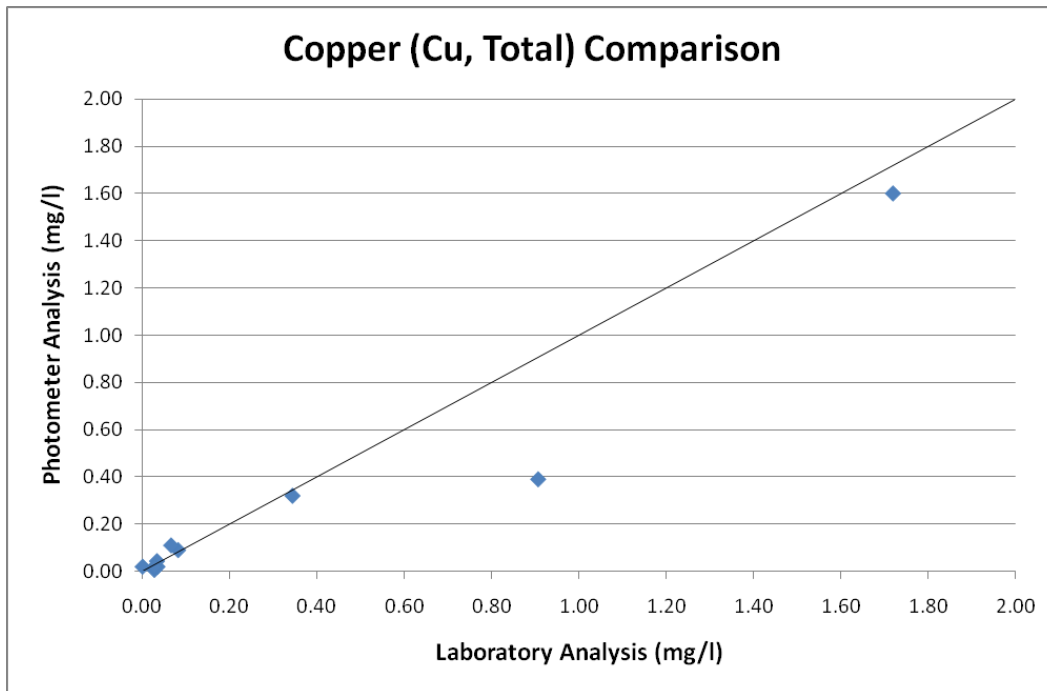


Figure 19. Copper (Total) laboratory comparison. Single high point corresponds to spring at GPS location #14.

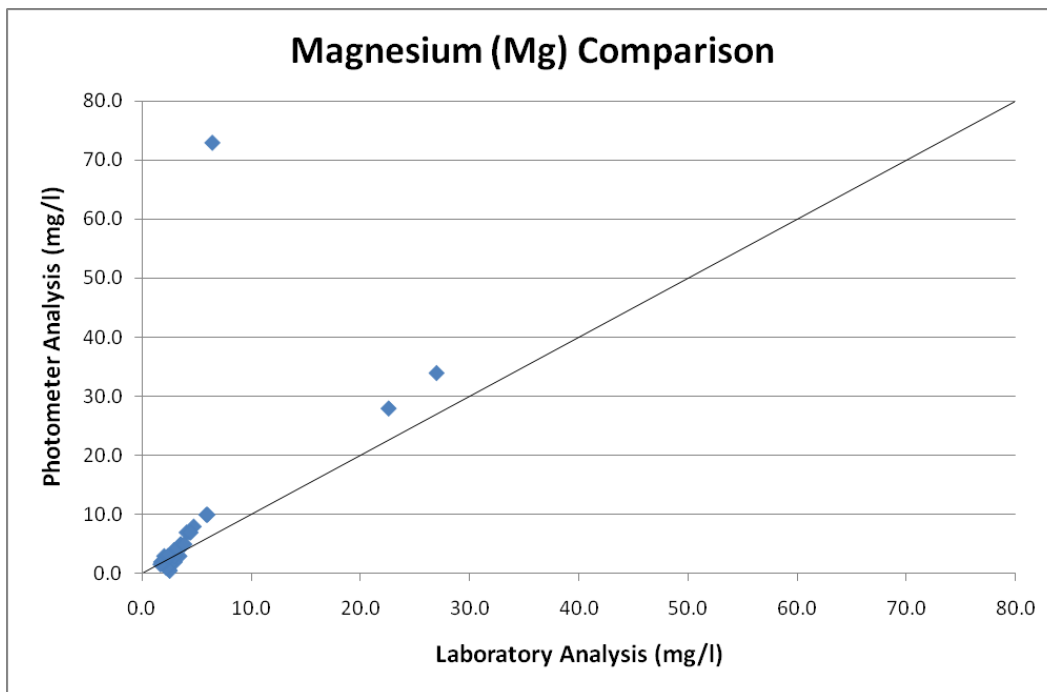


Figure 20. Magnesium laboratory comparison. Single high point corresponds to spring at GPS location #10.

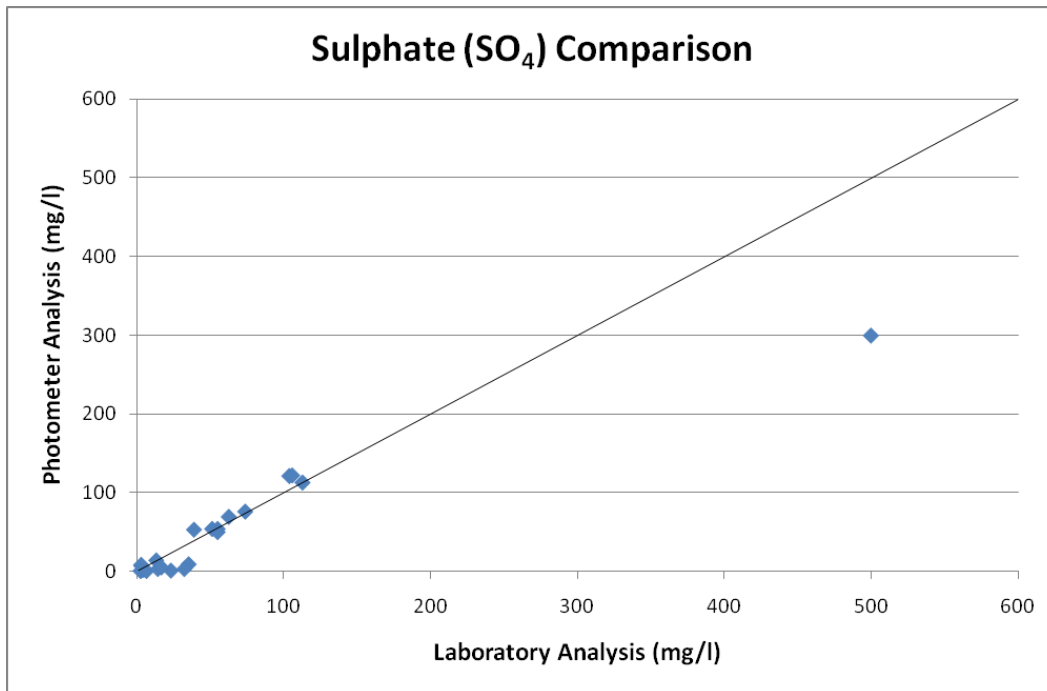


Figure 21. Sulphate laboratory comparison. Single high point corresponds to spring at GPS location #10.

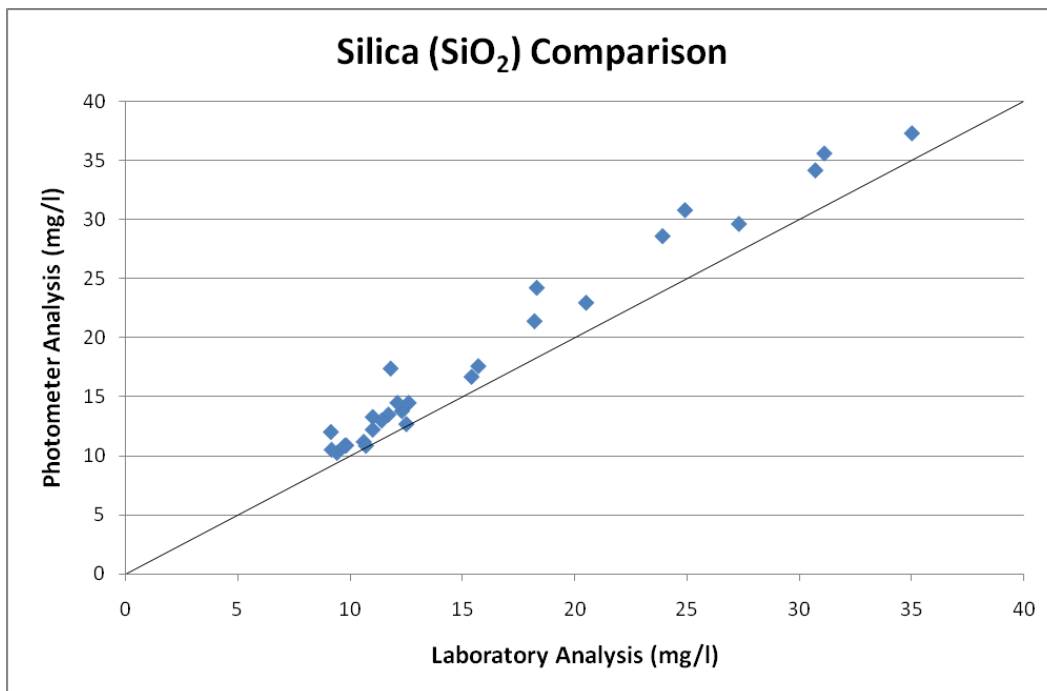


Figure 22. Silica laboratory comparison.

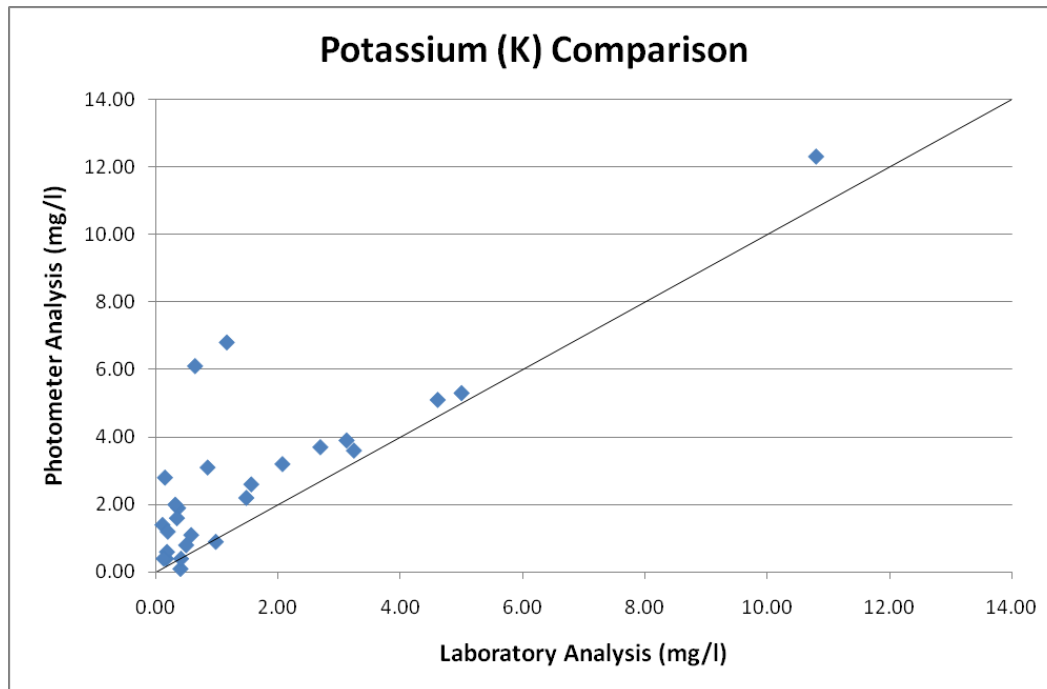


Figure 23. Potassium laboratory comparison. Single high point corresponds to spring at GPS location #10.

### Turbidity, TDS, Conductivity and pH results

Turbidity results (Figure 24) show a high bias in the photometer results below 1.0 FTU, suggesting that the laboratory method is less sensitive than the photometer at low values. Laboratory results show a slight high bias between 4.0 and 10.0 FTU, but this disappears and results become comparable above 16.0 FTU.

Conductivity, TDS and pH (Figure 25 to Figure 27) show good correlations between field and laboratory determinations. Conductivity, expressed in microsiemens or  $\mu\text{S}$  (Figure 25) displays a strong correlation with no bias. Total dissolved solids results (Figure 26) also show no discernible bias, but the values have a greater spread around the X=Y line indicating a greater discrepancy between the two methods. Nevertheless, the absolute difference between the two sets of values is less than 10%.

Water pH results (Figure 27) show larger differences between the field and laboratory measurements. The differences are more apparent at lower, more acidic pH values and could reflect changes in water chemistry between the field and the laboratory.

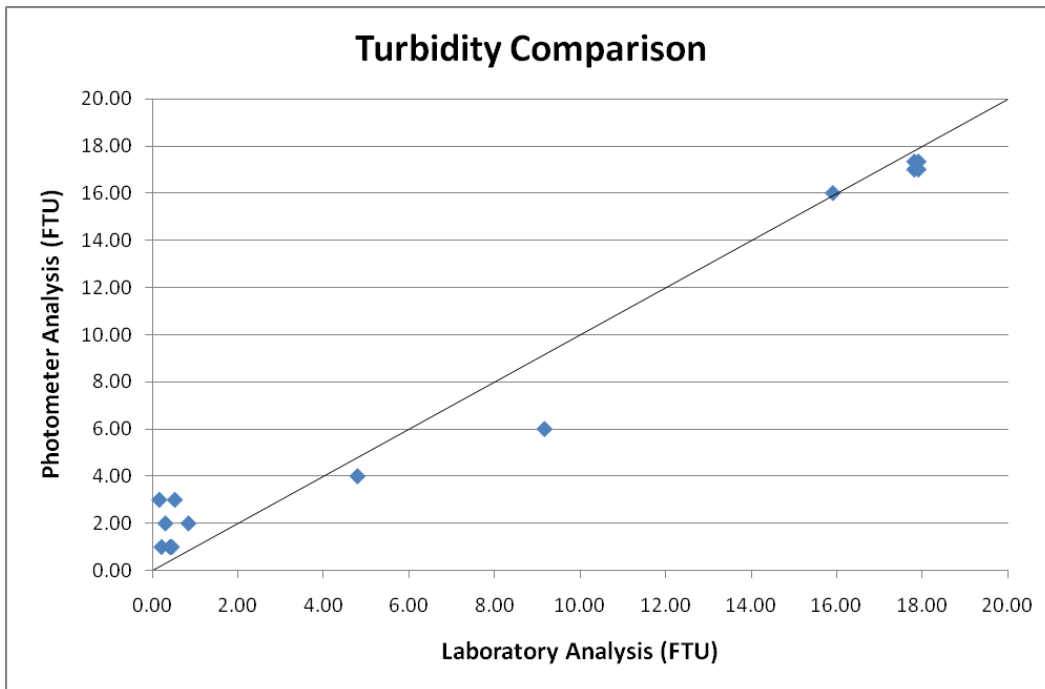


Figure 24. A Comparison of field and laboratory turbidity measurements.

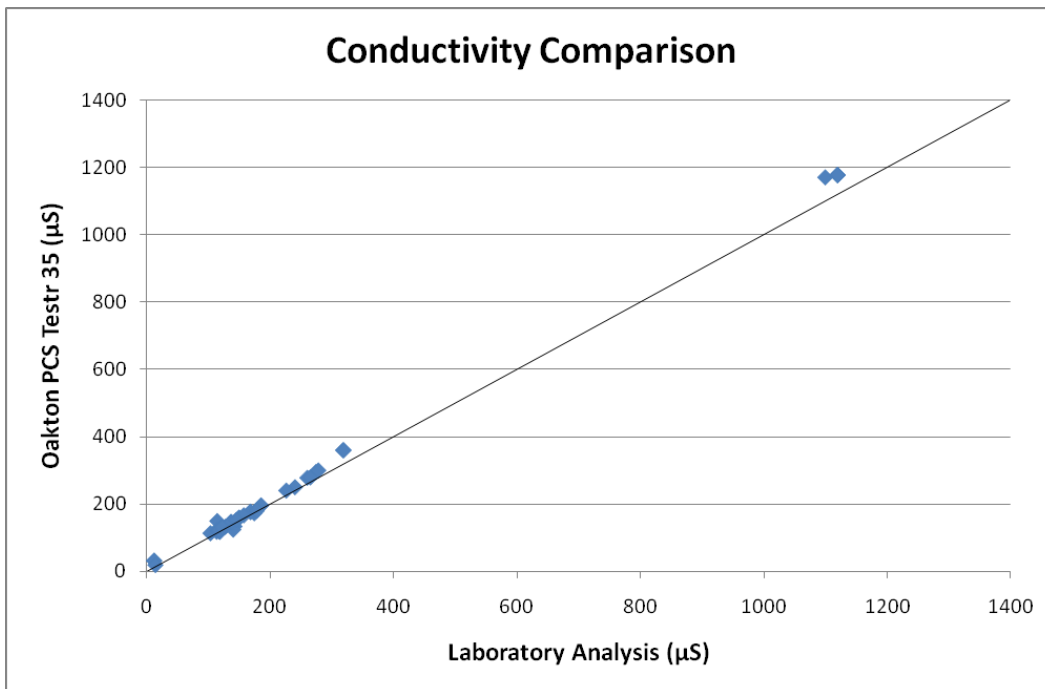


Figure 25. A Comparison of field and laboratory conductivity measurements.

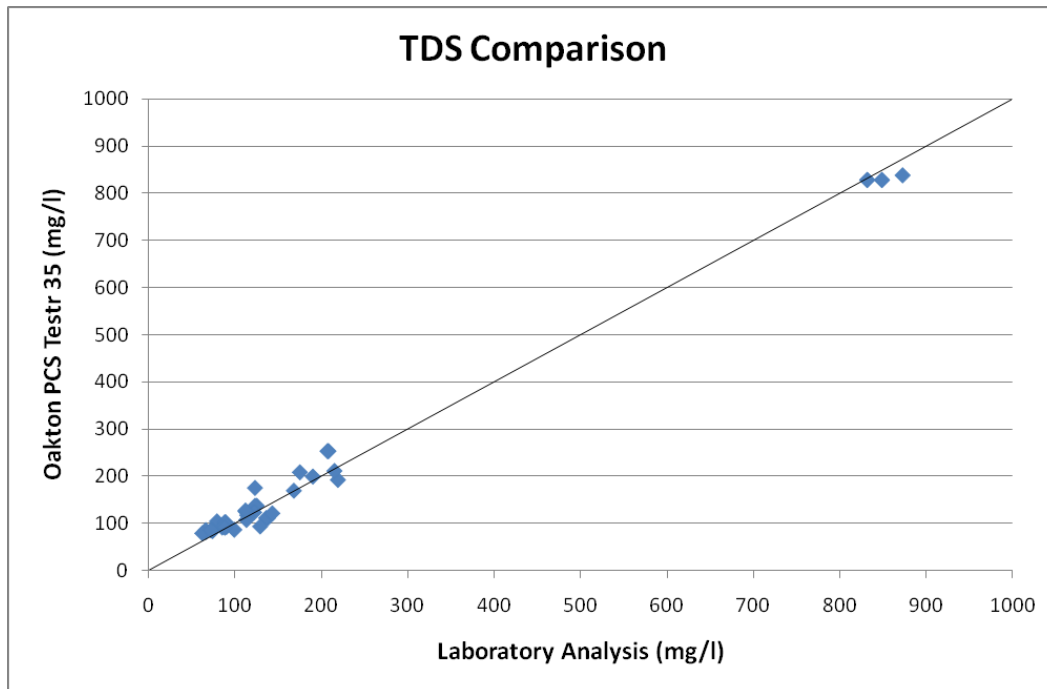


Figure 26. A Comparison of field and laboratory TDS measurements.

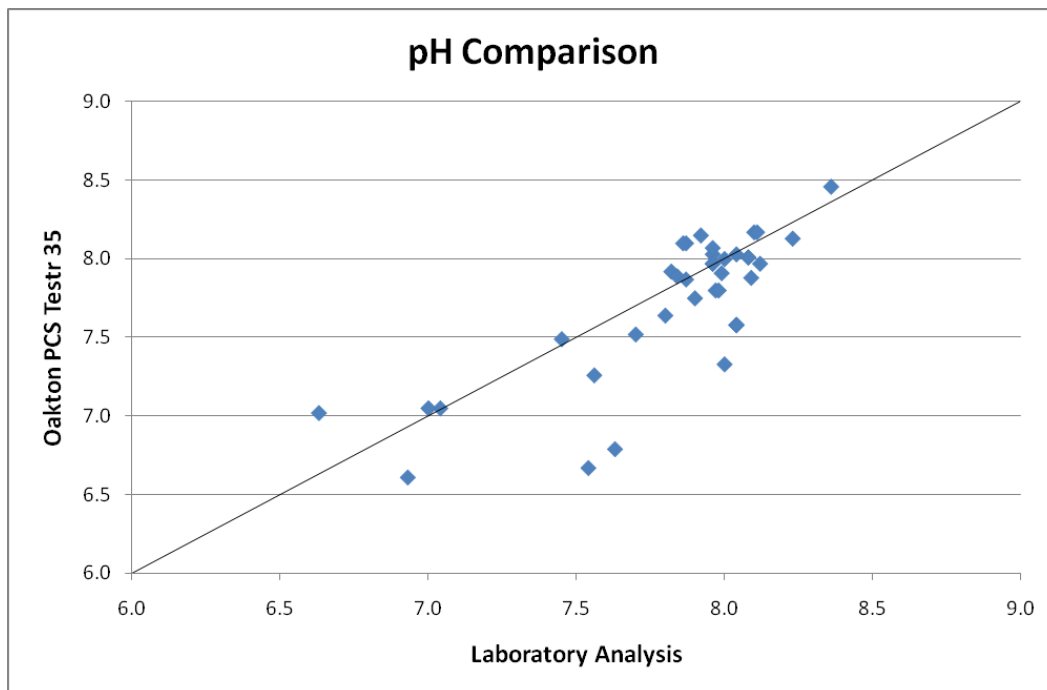


Figure 27. A Comparison of field and laboratory pH measurements.

## Inconsistent Results

### Photometer

While the comparisons between the photometer and laboratory results are reasonably good for many of the analytes some unusual readings were observed in both the photometer and laboratory results that merit examination. These are listed in Table 7.

The first suspect reading is for  $\text{SO}_4$  in sample L141016170051 (collected in October), which produced an initial value of 19.0 mg/l. This result is quite different from the analysis from the same sample location collected in October (50 mg/l) and the August laboratory result (62.1 mg/l). A second test was performed to check the of the original photometer reading. This time a reading of 66.0 mg/l was obtained, which is more consistent with the laboratory and August results. The cause of this apparent error is not understood but human error cannot be discounted. The second analysis of 66.0 mg/l was used for the interpretation.

The second unusual result from the October sampling is for mineral spring sample L140835470043 which recorded an initial Mg value of 4.67 mg/l. This is anomalously low compared to the laboratory result of 26.90 mg/l and the August photometer reading of 34.0 mg/l. We conclude that this result is also erroneous.

Regardless of causes, proper application of QA/QC procedures identified these anomalies. In the case of  $\text{SO}_4$  the anomalous reading was identified during the analysis when compared to August and was rectified by performing a second test. In the case of Mg, the irregular reading was discovered after analysis was completed and the solution discarded; consequently the test could not redone. This is one of the advantages of doing the analysis at the field location: it allows for suspect results to be identified at the time of analysis and the test repeated if necessary. Field based analysis also allows for re-collection of samples if a sample appears compromised even after the original sample has been discarded.

### Laboratory

Unusual results were also obtained from the laboratory, which resulted in re-analysis of some of the sample batches (Table 5).

October sample L141032630068 and its laboratory counterpart LB14103263033 display large differences in their Mg concentrations (73.0 mg/l vs. 6.41 respectively). The August photometer result for the same location was 62.7 mg/l, which is consistent with the October reading and suggests that the laboratory result is suspect. Investigation of this discrepancy did not come up with an obvious explanation.

Results for sample LB14102339023 and its field duplicate, LB14102339024, show marked differences in turbidity as well as discrepancies in their Al and Fe concentrations. This could indicate failure to acidify

one of the samples in the field, or a sample mix-up in the field or at the laboratory. However, the decision to not acidify the samples does not explain the large difference in the turbidity. Another likely explanation is inconsistent sampling where more suspended material was included in the second bottle as a result of site disturbance during collection of the first sample.

For stream sediment field duplicates SL1408413212 and SL1408413213, the Mn values are an order of magnitude apart (449 ppm versus 4120 ppm respectively), despite being collected at the same location. This observation could reflect presence of MnO<sub>2</sub> coatings in the sediment. Cobalt and Ba also show discrepancies that are significantly larger than most other field duplicates.

Table 7. Inconsistent Analyses.

Sample ID	Test	Type	Result	Comments
L141016170051	Photometer	SO <sub>4</sub>	19.0 (mg/l)	First run
L141016170051	Photometer	SO <sub>4</sub>	66.0 (mg/l)	Second run
LB14101617025	ALS Environmental	SO <sub>4</sub>	62.1 (mg/l)	Lab duplicate of 0051
L140816170018	Photometer	SO <sub>4</sub>	50.0 (mg/l)	August analysis
L140835470043	Photometer	Mg	4.67 (mg/l)	
LB14103547021	ALS Environmental	Mg	26.90 (mg/l)	Lab duplicate of 0043
L140835470010	Photometer	Mg	34.0 (mg/l)	
L140835470011	Photometer	Mg	34.0 (mg/l)	Duplicate of 0010
LB14083547005	ALS Environmental	Mg	27.0 (mg/l)	Lab duplicate of 0010 and 0011
LB14083547006	ALS Environmental	Mg	26.8	Lab duplicate of 005
L141032630068	Photometer	Mg	73.0 (mg/l)	
LB14103263033	ALS Environmental	Mg	6.41 (mg/l)	Lab duplicate of 068
L140832630005	Photometer	Mg	62.7 (mg/l)	August analysis
LB14102339023	ALS Environmental	Turbidity	7.98 (FTU)	Lab duplicate of 0048
LB14102339024	ALS Environmental	Turbidity	0.82 (FTU)	Duplicate of 023
L140823390015	Photometer	Turbidity	1 (FTU)	August sample
L140823390048	Photometer	Turbidity	0 (FTU)	October sample
LB14102339023	ALS Environmental	Al	0.297 (mg/l)	Lab duplicate of 0048
LB14102339024	ALS Environmental	Al	1.34 (mg/l)	Duplicate of 023
L140823390015	Photometer	Al	0.0467 (mg/l)	August sample
L140823390048	Photometer	Al	0.0500 (mg/l)	October sample
LB14102339023	ALS Environmental	Fe	0.240 (mg/l)	Lab duplicate of 0048
LB14102339024	ALS Environmental	Fe	1.65 (mg/l)	Duplicate of 023
L140823390015	Photometer	Fe	0.140 (mg/l)	August sample
L140823390048	Photometer	Fe	0.150 (mg/l)	October sample
SL1408413212	ALS Minerals	Mn	449 (ppm)	
SL1408413213	ALS Minerals	Mn	4120 (ppm)	Duplicate of 13
SL1408413212	ALS Minerals	Mn	402 (ppm)	ALS rerun of 12
SL1408413213	ALS Minerals	Mn	4240 (ppm)	ALS rerun of 13
SL1408413212	ALS Minerals	Co	55.9 (ppm)	
SL1408413213	ALS Minerals	Co	108.5 (ppm)	Duplicate of 13
SL1408413212	ALS Minerals	Co	49.7 (ppm)	ALS rerun of 12
SL1408413213	ALS Minerals	Co	116 (ppm)	ALS rerun of 13
SL1408413212	ALS Minerals	Ba	130 (ppm)	
SL1408413213	ALS Minerals	Ba	190 (ppm)	Duplicate of 13
SL1408413212	ALS Minerals	Ba	130 (ppm)	ALS rerun of 12
SL1408413213	ALS Minerals	Ba	200 (ppm)	ALS rerun of 13

## Field Test and Photometer Results

In the following sections, the analytical results are presented as scaled symbol plots based on percentile breaks (Table 8). Stream waters and springs are assigned different colours. Percentiles were calculated separately for each analyte. Calculations were performed on a spreadsheet and mapping was done using Quantum GIS (QGIS) v. 2.4 using the NAD83 UTM Zone 10 projection.

### Field Tests

Water pH values in springs over the mineralized zone are more acidic than those from background areas (Figure 28). The oxidizing sulphide mineralization beneath 'Copper Creek' appears to be the cause of groundwater acidification, which is then reflected in the surface water pH. Water pH values over the mineralized zone are up to two pH units lower than background values on the east side of Poison Mountain (7.49, defined by the 50<sup>th</sup> percentile October concentration). The trend of lower pH readings continues downstream to the confluence of Poisonmount Creek where they remain about half a pH unit below background levels. Values were slightly more acidic in October when water levels were lower. Slightly elevated pH values to the east of Poison Mountain in August likely indicate the presence of groundwater springs in an un-mineralized area.

Total dissolved solids (Figure 29) and conductivity (Figure 30) generally correlate well. Both variables show patterns of higher values over the mineralized zone and gradually diminishing downstream as far as Poisonmount Creek in both August and October. Elevated values noted southeast of Poison Mountain could indicate proximity to springs, or the presence of mineralized springs further upstream.

Temperature (Figure 31) correlates well with TDS and conductivity in both springs and surface waters. It is an important field observation that can indicate proximity to springs, which can be slightly warmer than surface waters, or variations in local conditions such as snow melt, precipitation or warming due to exposure to sunlight. Sub-surface sulphide oxidation, as an exothermic reaction, can also cause warming of ground waters and the creeks they drain into. Figure 31 shows that the temperatures over the mineralized zone in Copper Creek are on average slightly warmer than elsewhere in the survey area. The highest water temperatures however, were recorded from two springs in the Churn Creek drainage situated above the confluence with Poisonmount Creek. Temperatures were generally comparable between the August and October and range between 3.3° and 12.2 °C in August and 2.8° and 11.3°C in October. One notable exception is the lower spring on Churn Creek, which was cooler in October.

Turbidity (Figure 32) was generally quite low throughout the study area. It is a good indicator of the presence of suspended material in the water such as mineral particulates, precipitates, colloids and organics. Results show that spring waters in lower 'Copper Creek' and in Poisonmount Creek have higher turbidity values than Upper Poisonmount creek waters. Elevated values in springs could indicate Fe hydroxide precipitation as slightly reduced ground waters mix with oxidized surface waters.

Table 8. Percentiles distribution.

Analyte* (mg/l)	August							October								
	50%	75%	90%	95%	97%	98%	99%	100%	50%	75%	90%	95%	97%	98%	99%	100%
pH	7.85	7.66	6.79					5.70	7.91	7.49	6.67					5.29
TDS	112.0	152.5					203.0	829.0	120.0	170.0					254.0	839.0
Cond. (µS)	157.7	215.0					286.0	1177.0	168.6	239.0					359.0	1170.0
Temp (°C)	6.2		7.8					12.2	5.3		7.0					11.3
Turbidity (FTU)		2				21		30		1				7		16
Cu		0.0600	0.1493	0.3410				1.5500		0.0874	0.1170	0.6135				1.6000
Fe		0.0300	0.0520	0.0980				0.3100		0.0200	0.0470	0.1370				0.2200
MoO <sub>4</sub>	0.3400	0.4967	0.7500	0.9833				1.3733	0.0100	0.0731	0.1870	0.2763				0.7433
Zn (EDTA)			0.0098	0.0145				0.0200			0.0085	0.0110				0.0129
Br	0.020	0.058	0.117					0.353	0.030	0.050	0.079					0.207
Cl <sup>-</sup>	0.40	0.60	0.97	2.01				10.23	1.05	1.85	5.07	5.79				8.53
F <sup>-</sup>	0.223	0.375	0.534	0.614				1.153	0.150	0.283	0.468	0.587				0.97
K	1.10	2.65	3.55	4.74				12.30	2.40	4.13	6.59	8.41				11.90
SO <sub>4</sub>	2.0	54.0	87.1	107.4				300.0	5.6	62.8	107.5	121.6				290.0
SiO <sub>2</sub>	14.50	26.37	30.48	34.60				38.87	14.45	28.45	33.76	34.42				37.30
Al			0.0100					0.1000			0.0100					0.3000
B	0.103	0.145	0.220					0.540	0.160	0.250	0.330					0.580
Ca	16.0	21.8	31.4		42.1			95.7	16.6	23.7	34.4		49.7			114.4
CaCO <sub>3</sub>	49.0	75.0	102.9		140.1			523.0	57.5	72.6	109.0		136.1			448.3
Mg	3.0	6.2	22.3	29.8				62.7	6.0	7.0	10.0	26.3				73.0
Mn			0.0032	0.0115				0.0467			0.0010	0.0027				0.0090
Ni		0.0200		0.0910				0.2367		0.0100		0.0673				0.1367

\*In order of figures.

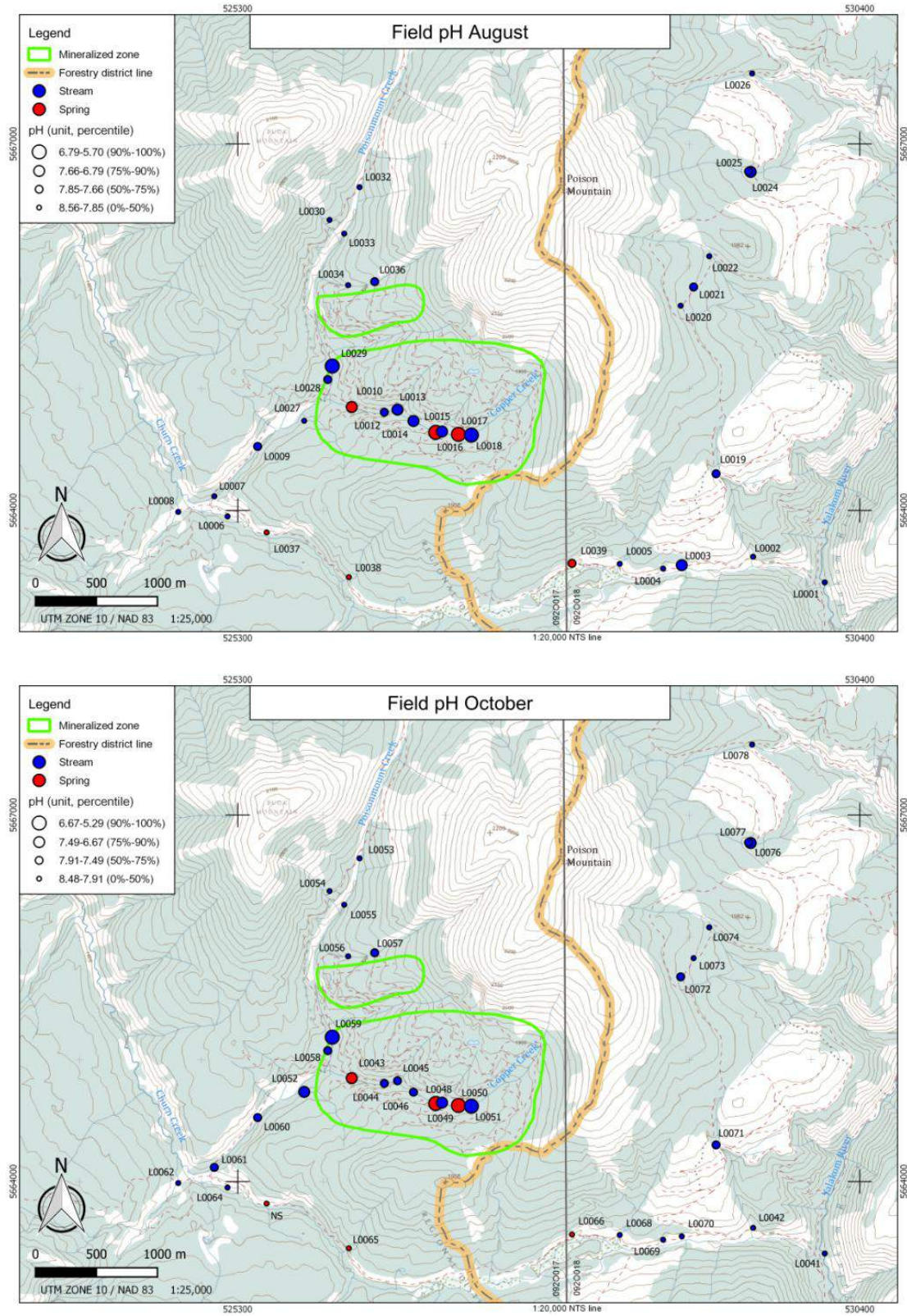


Figure 28. Field pH results August (top) and October (bottom).

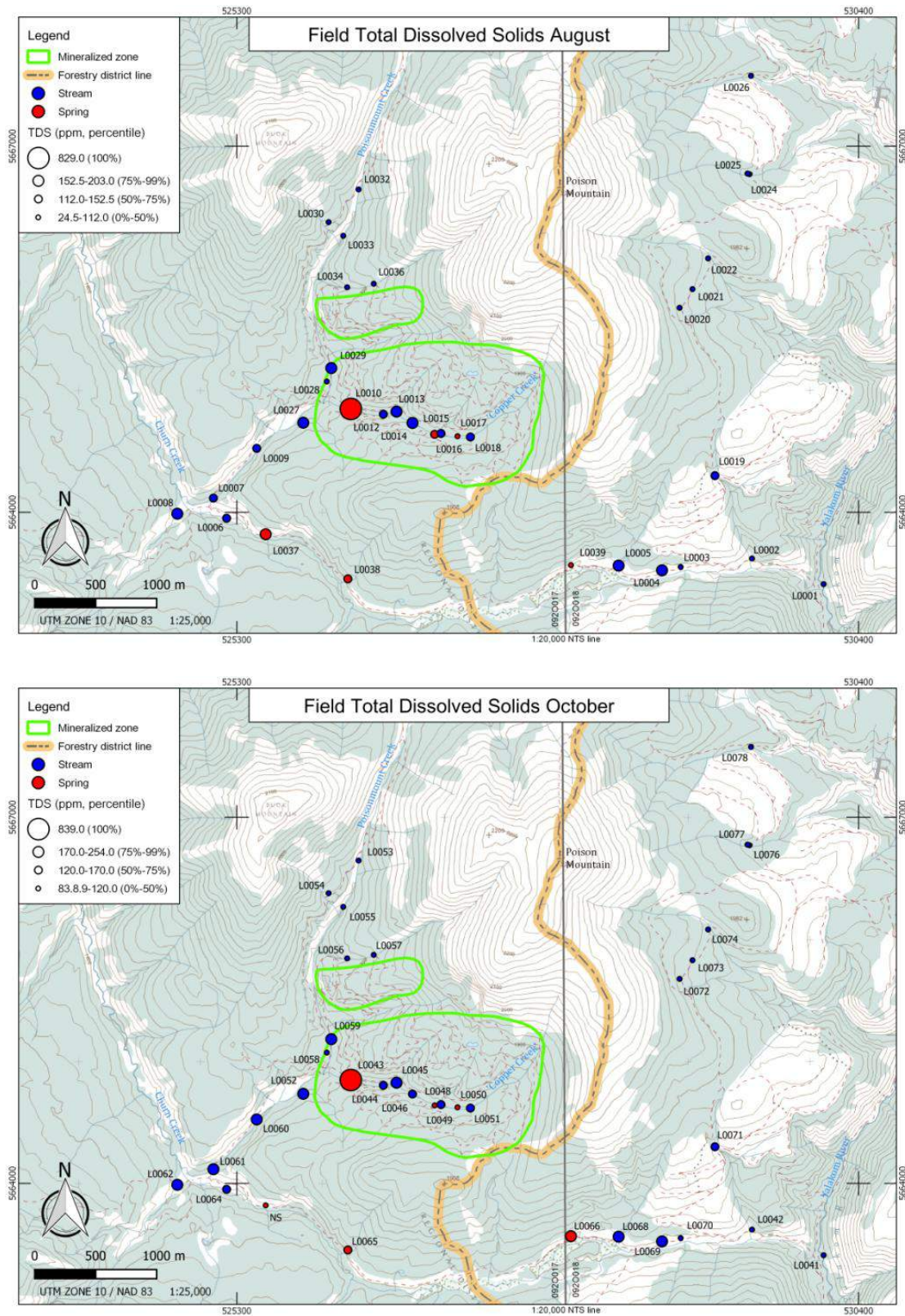


Figure 29. Field TDS Oakton PCS Testr 35 August (top) and October (bottom).

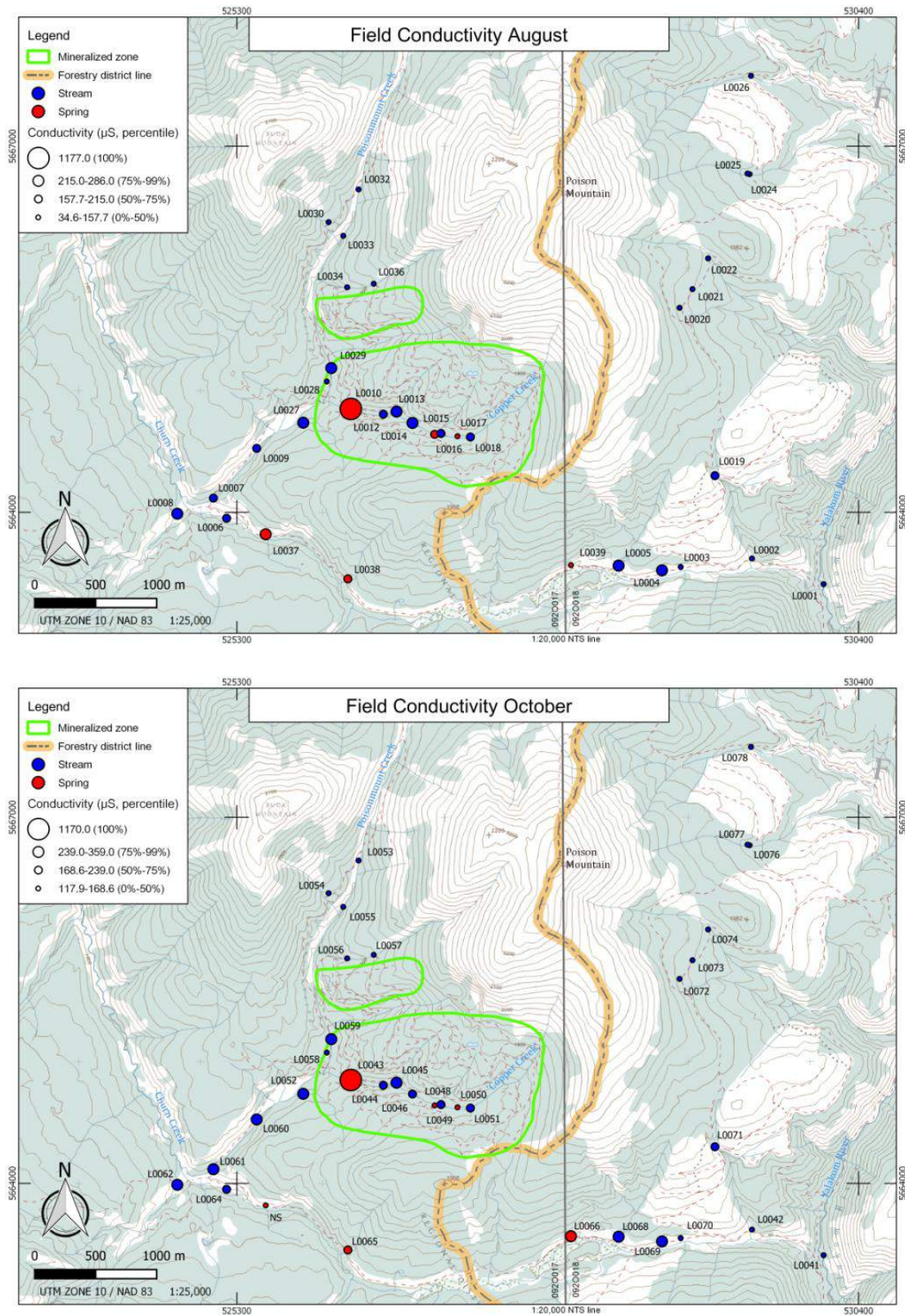


Figure 30. Field conductivity Oakton PCS Testr 35 August (top) and October (bottom).

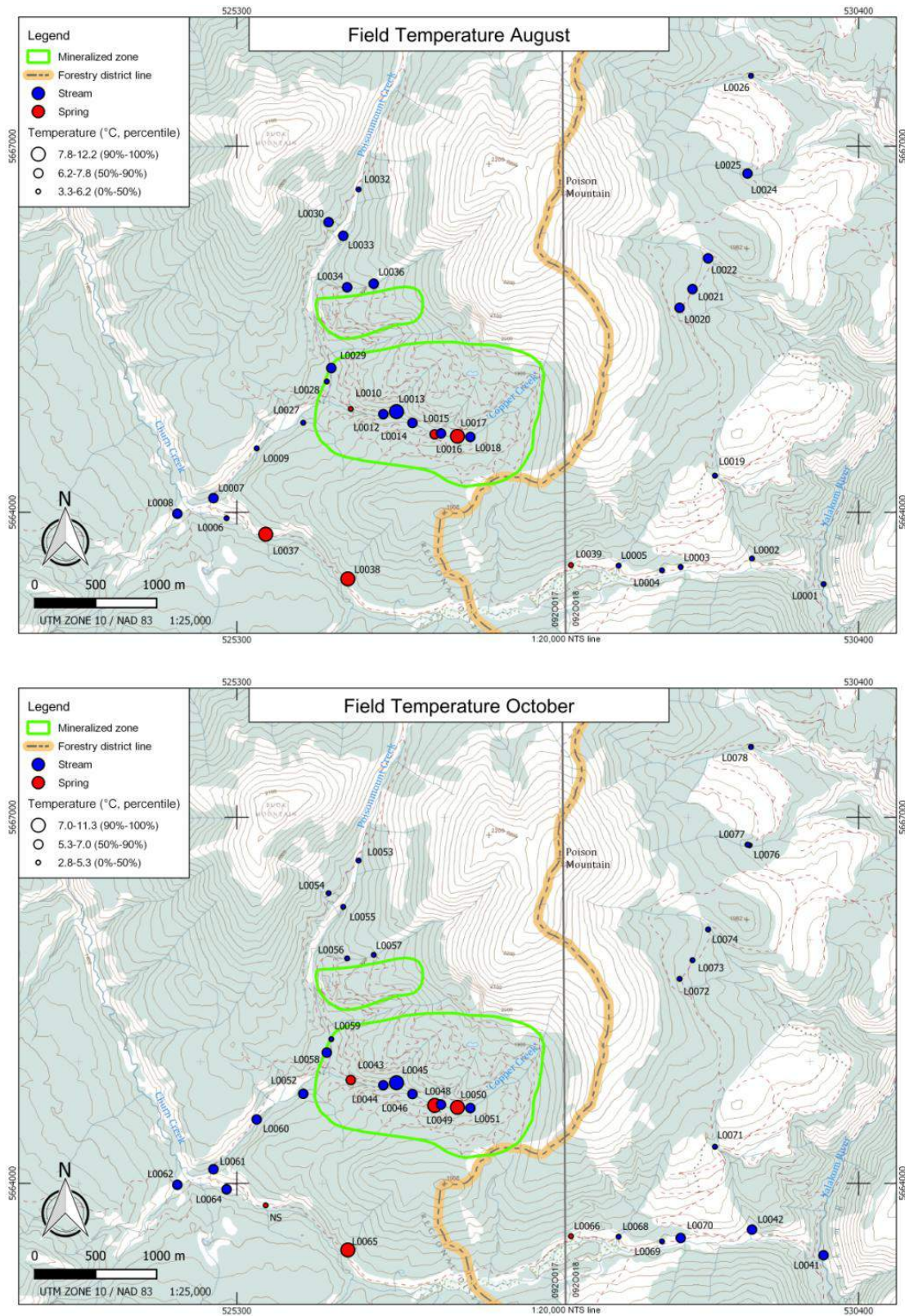


Figure 31. Field temperature Oakton PCS Testr 35 August (top) and October (bottom).

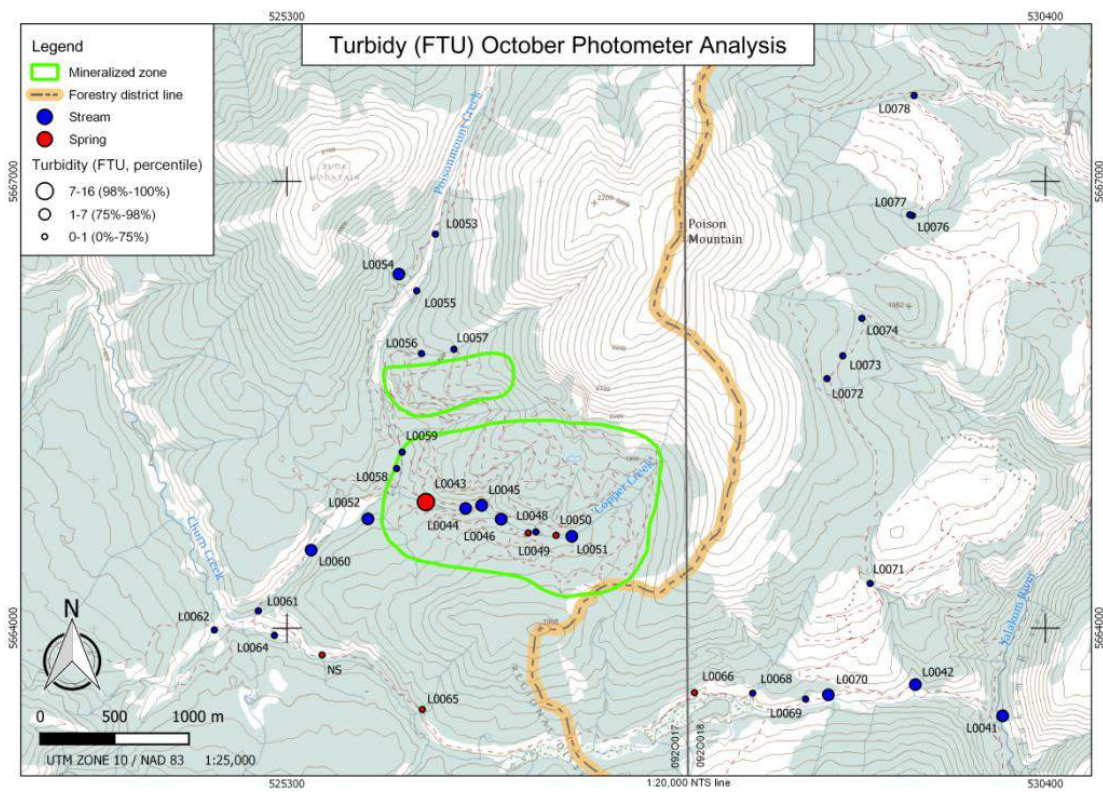
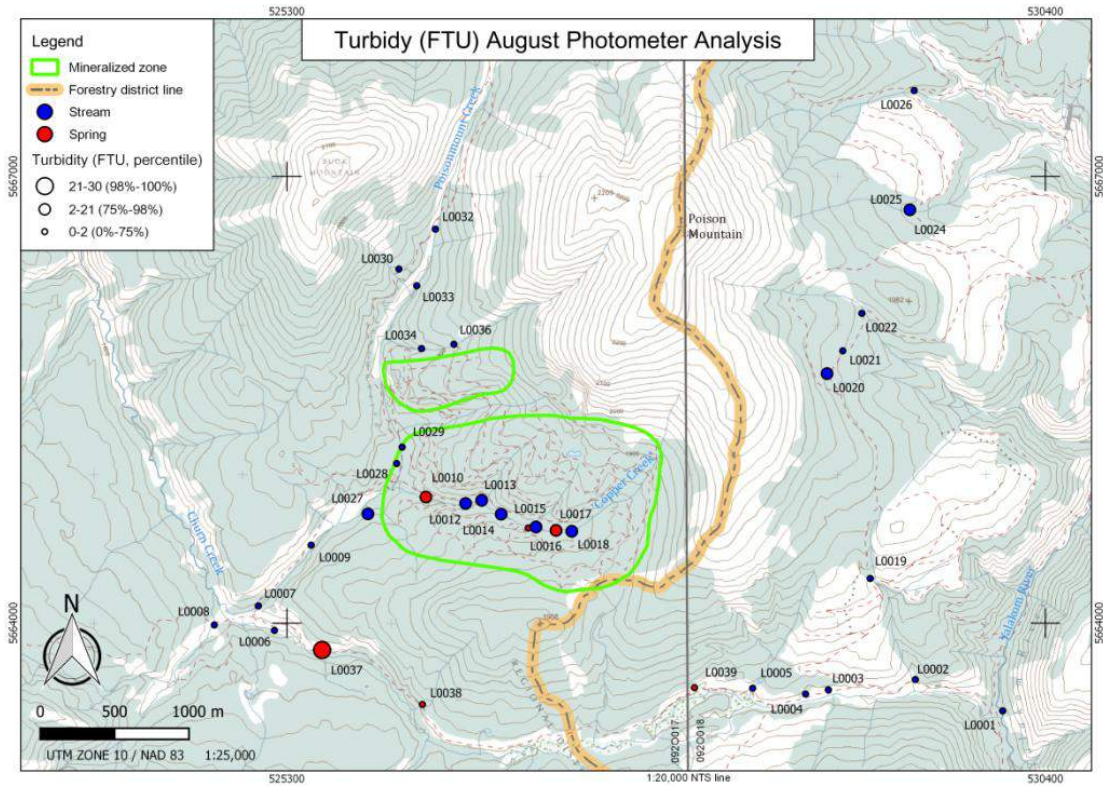


Figure 32. Turbidity photometer analysis August (top) and October (bottom).

## Photometer Results

### Commodity Elements

Elevated values for Cu (Figure 33), Fe (Figure 34), MoO<sub>4</sub> (Figure 35) and Zn EDTA (Figure 36) correlate well with the mineralized zones but do not show much downstream dispersion outside the deposit area. Background is defined as the 50<sup>th</sup> percentile unless otherwise stated. (Refer to Table 8.)

#### *Copper*

Copper (Figure 33) values are elevated over the mineralized zone in both sampling campaigns. Highest concentrations occur in the two springs in the upper part of 'Copper Creek'. A very slight response occurs downstream from the springs in sample L0027 (Figure 33 top) and L0052 (Figure 33 bottom), near the confluence with Poisonmount Creek. Maximum concentrations reach 0.060 mg/l and 0.875 mg/l. Concentrations in October are slightly higher than in August due to lower stream levels (meaning less dilution). The high concentration identified in sample L0037 (Figure 33 top) may be a response to higher turbidity in the sample medium.

#### *Iron*

Iron (Figure 34) displays comparable patterns of enrichment to Cu albeit at much lower concentrations. This is probably due to the preservation issue identified above. Maximum concentrations reach 3 to 11 times background levels (0.02 mg/l and 0.03 mg/l). As with Cu, sample L0027 in August (Figure 34 top) and L0052 in October (Figure 34 bottom), shows a subtle response above the confluence with Poisonmount Creek. In sample L0037 (Figure 34 upper), the elevated concentration is possibly caused by higher turbidity in the sample. Unlike Cu, Fe does not show significant seasonal differences.

#### *Molybdate*

Molybdate (Figure 35) is another analyte with a positive response over the mineralized zone. It is one of the more interesting results in this study. Another interesting observation is the markedly different MoO<sub>4</sub> concentrations between the August and October results. For August (Figure 35 upper) maximum concentrations are only 3 to 4 times background (0.3400 mg/l), while concentrations in October (Figure 35 bottom) are 27 to 74 times higher than background (0.0100 mg/l). Again (Figure 35 upper), the high concentration for sample L0037 (Figure 35 upper) is likely due to higher turbidity in the water. Elevated MoO<sub>4</sub> values present outside the mineralized zone may also be reflecting low-grade Mo mineralization in the porphyritic intrusions (Figure 3).

#### *Zinc*

Zinc (Figure 36) results after correction for Cu interfere with EDTA show that for the August there is a depletion of Zn in stream waters over mineralized zone. Values are slightly higher below the confluence with Poisonmount Creek. The two spring samples within the mineralized zone both show elevated values (0.0100 & 0.0200 mg/l). The October results show almost no variation in either stream or spring

waters inside or outside the mineralized zone. One spring (0.0129 mg/l) and one water sample (0.0100 mg/l) from the highest reaches of 'Copper Creek' show a slightly elevated values.

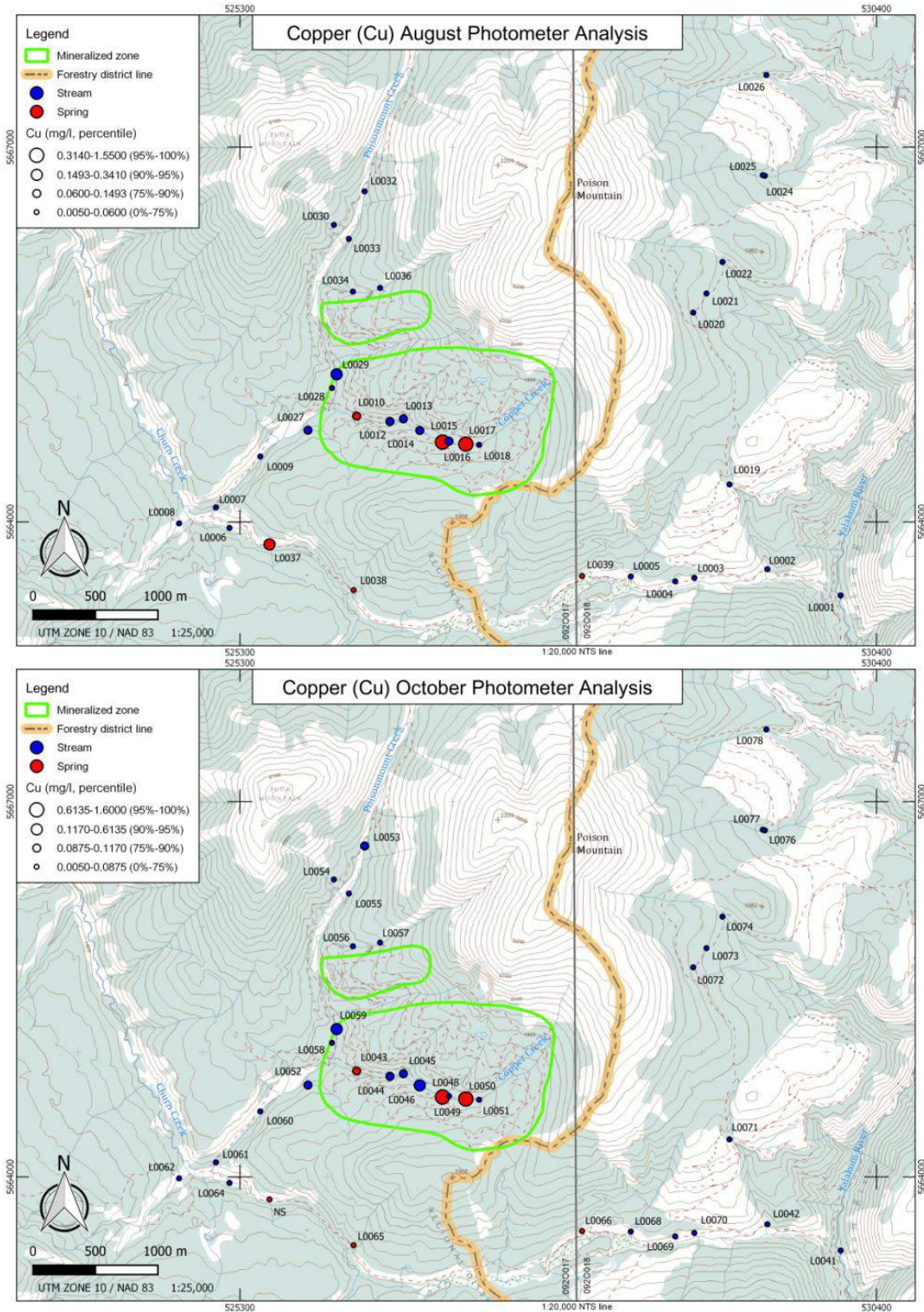


Figure 33. Copper photometer analysis August (top) and October (bottom).

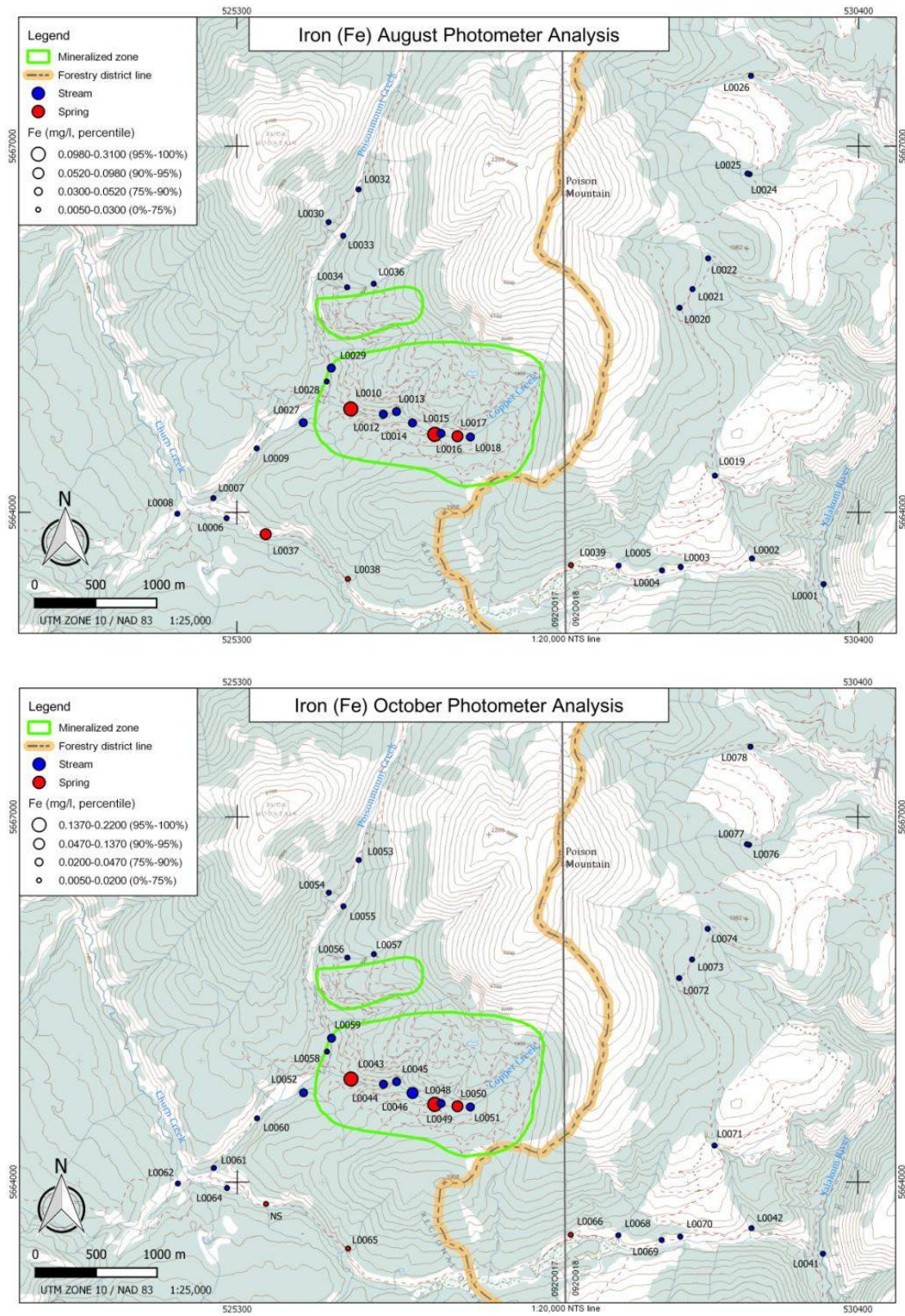


Figure 34. Iron photometer analysis August (top) and October (bottom).

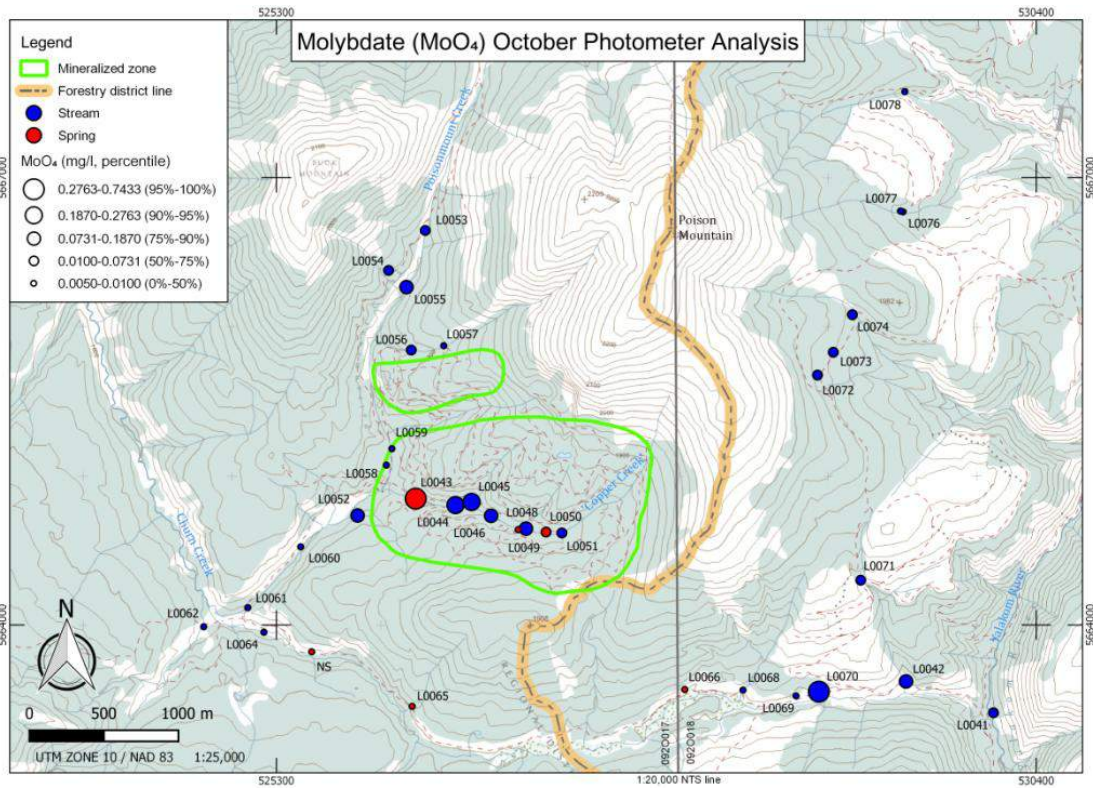
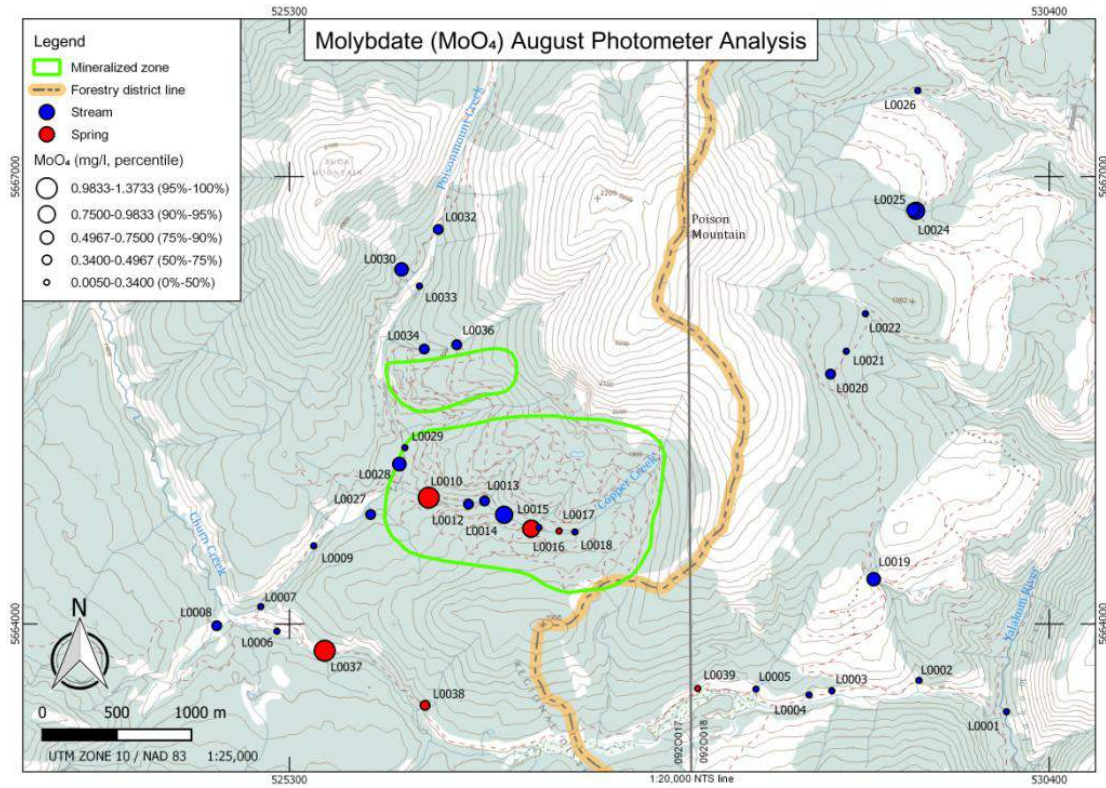


Figure 35. Molybdate photometer analysis August (top) and October (bottom).

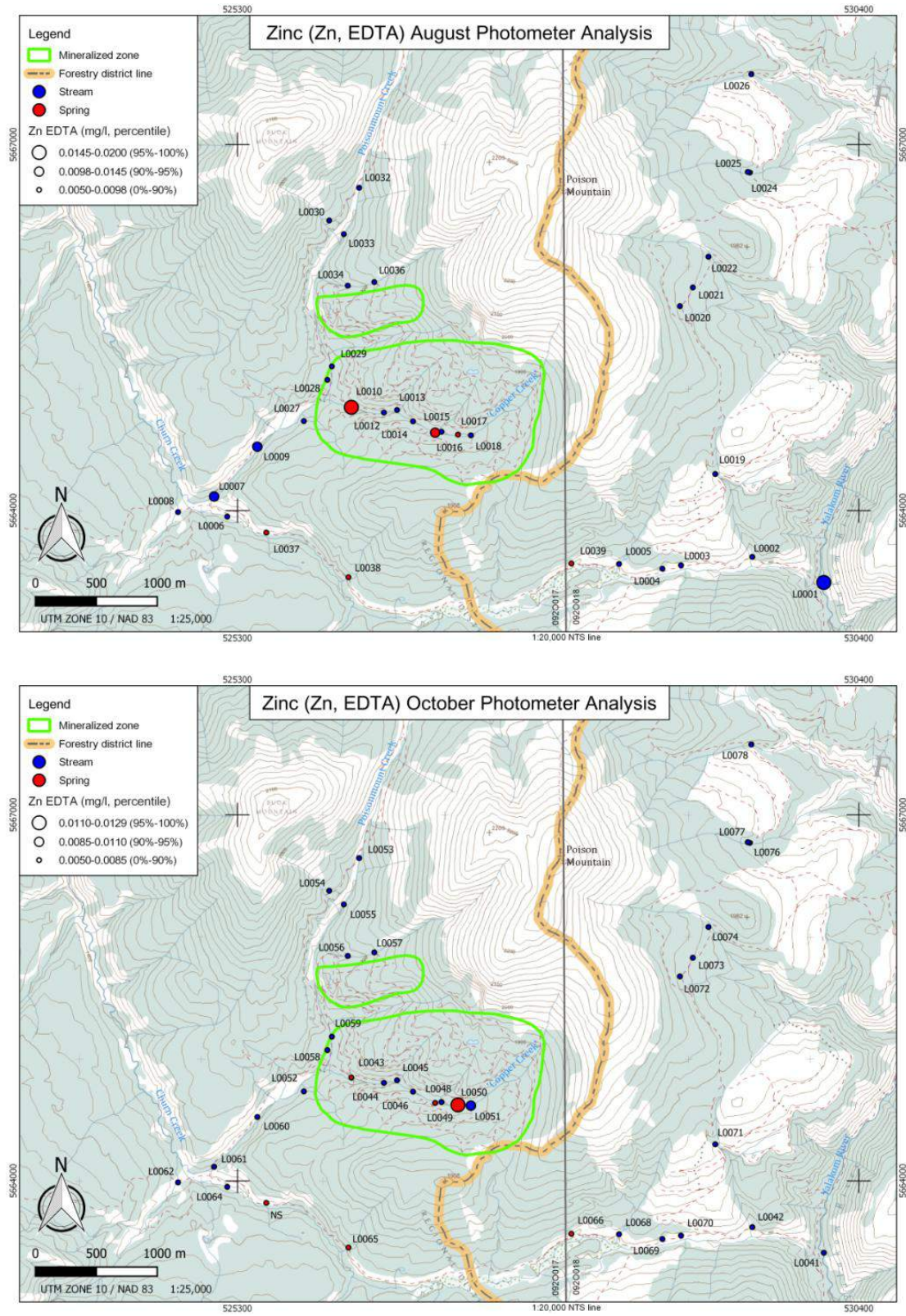


Figure 36. Zinc EDTA photometer analysis August (top) and October (bottom).

## Halogens and other analytes

Bromine (Figure 37), Cl<sup>-</sup> (Figure 38), F<sup>-</sup> (Figure 39), K (Figure 40), SO<sub>4</sub> (Figure 41), and SiO<sub>2</sub> (Figure 42) are stable ions that correlate well with the mineralization zone. All six show dispersion. Also for F<sup>-</sup>, K, SiO<sub>2</sub> and SO<sub>4</sub> high concentrations for sample L0029 in August and L0059 in October are evident in Poisonmount Creek at the northwest border of the mineralized zone. Except for SiO<sub>2</sub>, all register highest percentile concentrations in the mineralized spring in both August (L0010), and October (L0043).

### *Bromine*

Bromine (Figure 37) has an ambiguous response. In the August results, stream waters do not show a definitive response over the mineralized zone. Concentration ranges observed within the mineralized area are similar to those from supposedly background areas along Churn Creek and on the east side of Poison Mountain. Two of the three spring water samples do appear to highlight the mineralized zone however their response is diminished by an anomalous spring located to the south on Churn Creek. The elevated value for this sample (L0037) correlates with a high turbidity reading and may therefore be a false positive.

The October results show a slightly better response to the mineralized area. Values in both stream and spring waters are slightly elevated over the mineralized area and elevated concentrations appear to persist downstream as far as Churn Creek. Contrast is very low as isolated stream water samples with similar concentrations occur southeast and northeast of the mineralized area in inferred background locations.

### *Chloride*

Chloride (Figure 38) displays noisy results outside the limits of the projected mineralization, but consistently elevated values over the mineralized zone. Good downstream dispersion is observed especially in the August results (Figure 38 top). Maximum concentrations are 5 to 26 times higher than background (0.40 mg/l and 1.05 mg/l). Of note are the three higher concentrations in the creek just above the smaller northern mineralized zone (samples L0057, L0058 and L0060; Figure 38 bottom) along Poisonmount Creek. Sampled in August, Mineral spring L0037 high concentration is suspect due to high turbidity in the sample medium.

### *Fluoride*

Fluoride (Figure 39) values are elevated in the mineralized zone and show some good dispersion downstream to Poisonmount Creek. Unlike Br and Cl<sup>-</sup>, the F<sup>-</sup> results are less noisy outside the zone. Maximum concentrations are 4 to 6 times background (0.223 mg/l and 0.150 mg/l).

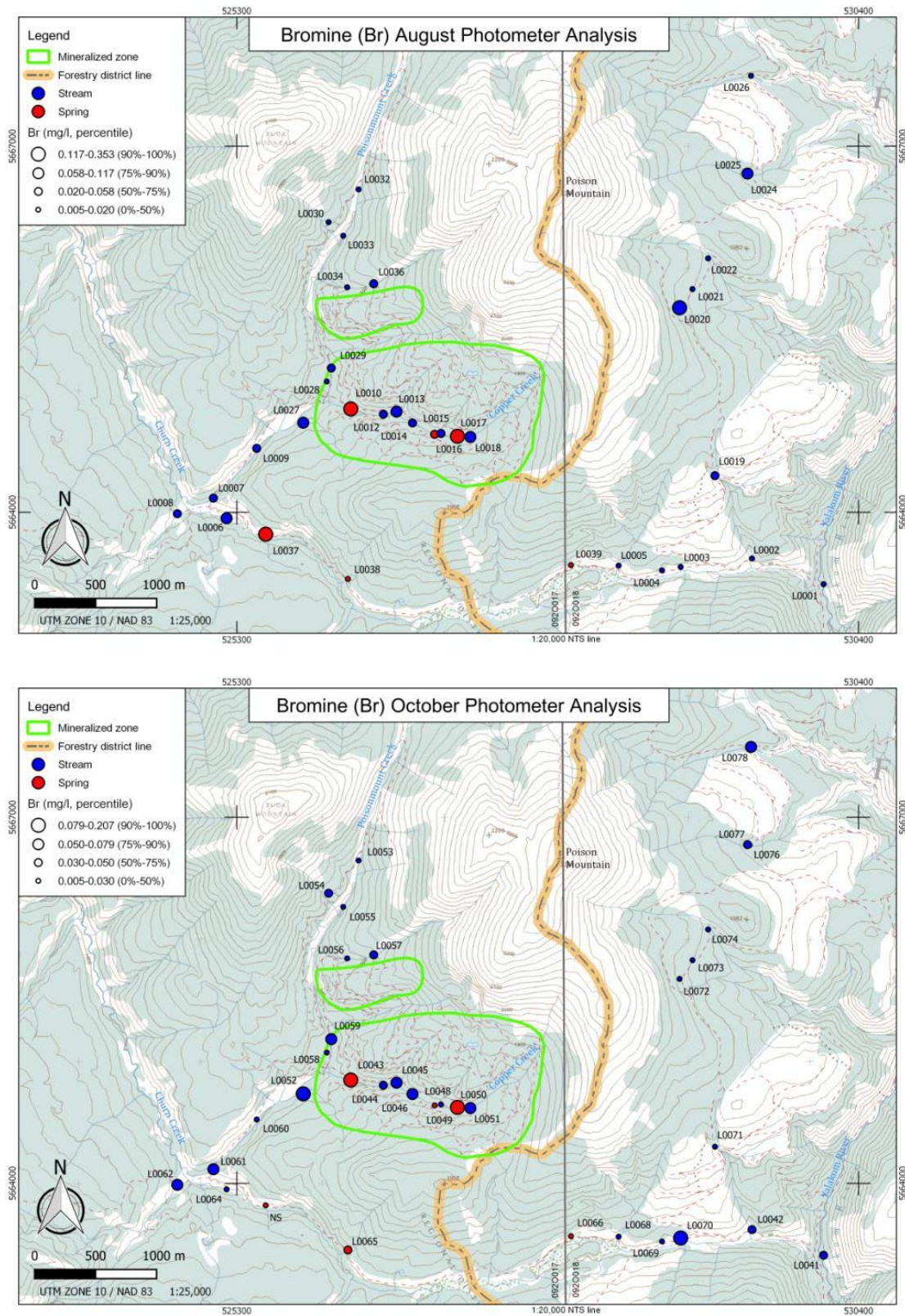


Figure 37. Bromine photometer analysis August (top) and October (bottom).

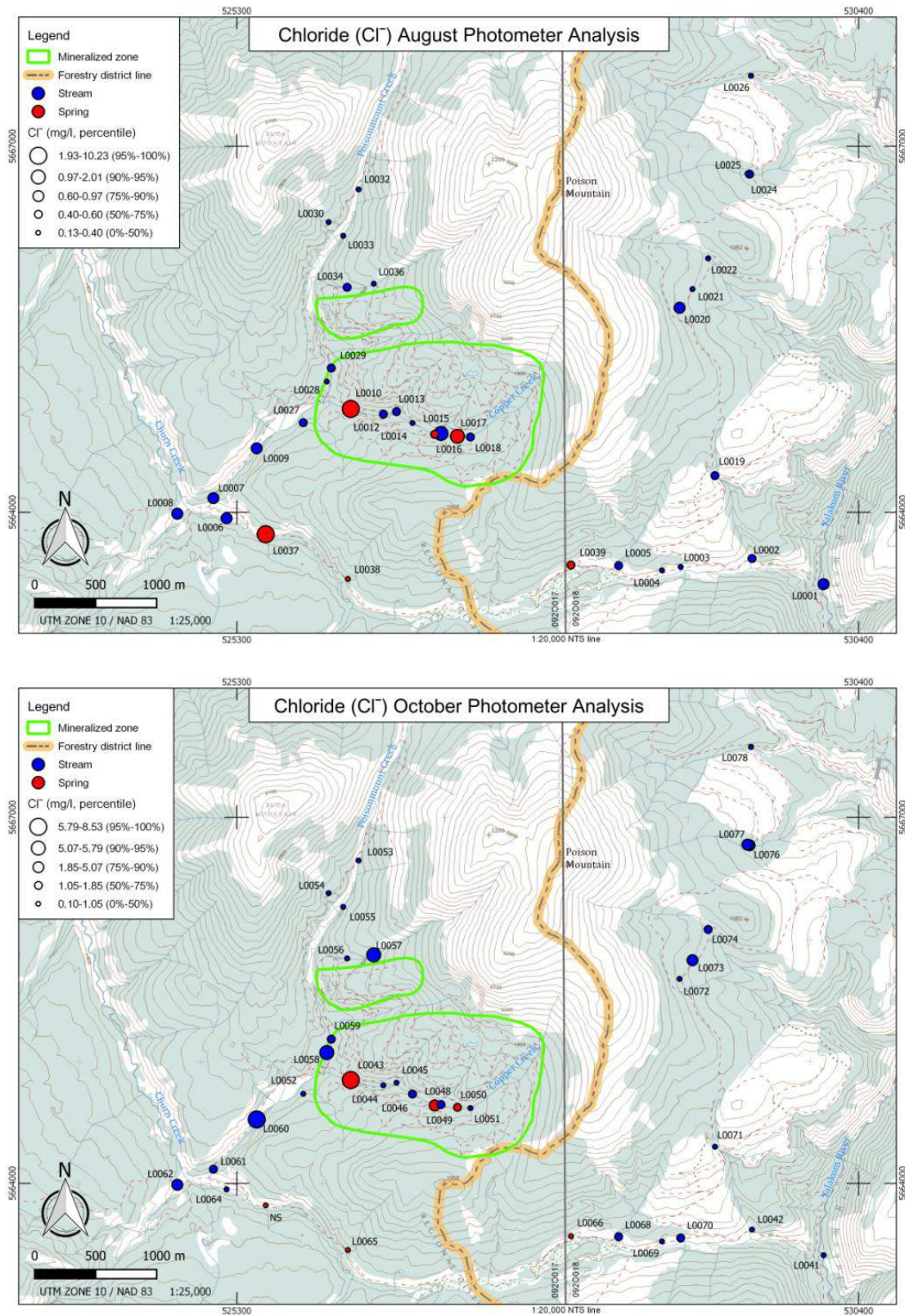


Figure 38. Chloride photometer analysis August (top) and October (bottom).

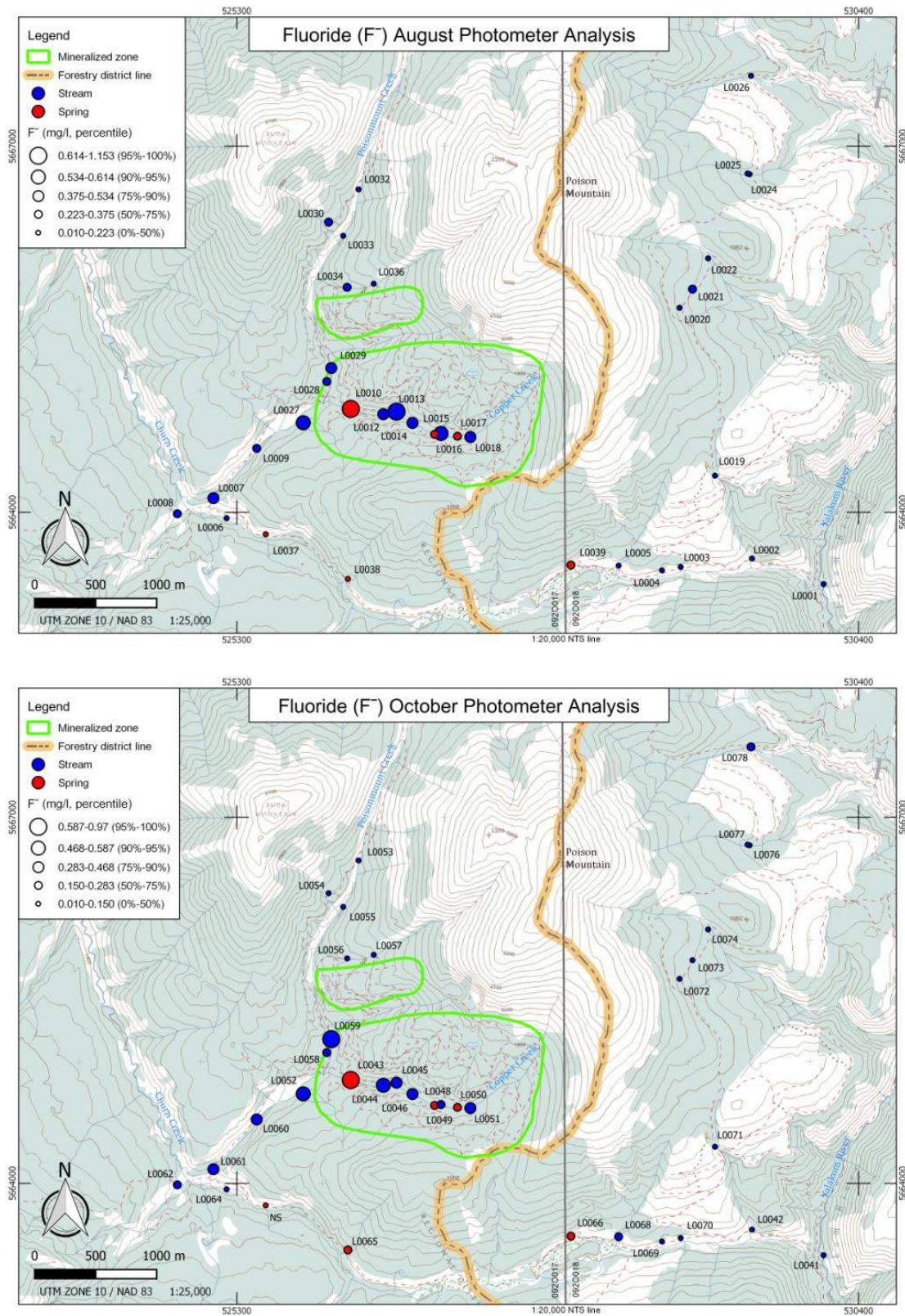


Figure 39. Fluoride photometer analysis August (top) and October (bottom).

## Other Elements and Anions

### *Potassium*

Potassium (Figure 40) shows a good correlation with the mineralized zone and has good dispersion down Poisonmount Creek. Maximum concentrations are 4 to 11 times higher than background (1.10 mg/l and 2.40 mg/l). Overall, K displays higher concentration for October, which is probably a result of less dilution due to lower water levels.

### *Sulphate*

Sulphate (Figure 41) has a good correlation with the mineralized zone and defines a strong downstream dispersion trend along Poisonmount Creek. Slightly higher concentrations are evident northwest of Poison Mountain along Poisonmount Creek. Maximum concentrations reach 21 to 150 times background levels (2.0 mg/l and 5.6 mg/l).

### *Silica*

Silica (Figure 42) also displays a good correlation with mineralized zone and slightly elevated values along Poisonmount Creek. Maximum concentrations are 2 to 3 times maximum the background level (<14.45 mg/l and 14.50 mg/l). Note also that of the entire suite of reagent tests employed, SiO<sub>2</sub> displays the most stable concentrations for both August and October, including all percentiles.

### *Aluminum*

High Al values (Figure 43) occur over the mineralized zone. This is especially true for the October results even though concentrations are lower when compared to lab results as discussed above. This element did not show sufficient variation to allow for calculation of its contrast over background.

### *Boron*

Boron (Figure 44) displays elevated concentrations from two springs over the mineralization, but shows noisy patterns outside the zone. August (Figure 44, top) results show a better correlation with the mineralized zone. The majority of elevated concentrations outside the zone are in the southwest and southeast of the Poison Mountain. October (Figure 44 bottom) concentrations are not as elevated in the zone in upper 'Copper Creek' as in August, and elevated results are mostly in the northern west and east flank of Poison Mountain. Concentrations vary between 2 to 5 times background (0.103 mg/l and 0.160 mg/l).

### *Calcium and Hardicol*

Calcium, derived from the Calcicol test, (Figure 45) and Hardicol results (Figure 46) both correlate with the mineralized zone and show downstream dispersion (especially in Hardicol) to Poisonmount Creek. Both also have a strong signature in the drainage to the south of Poison Mountain. Contrast for Ca is 3 to 7 times background (<16.0 mg/l and 16.6 mg/l) and for Hardicol, it is 2 to 11 times background (<49.0 mg/l and 57.5 mg/l). Both tests have stable results for August and October.

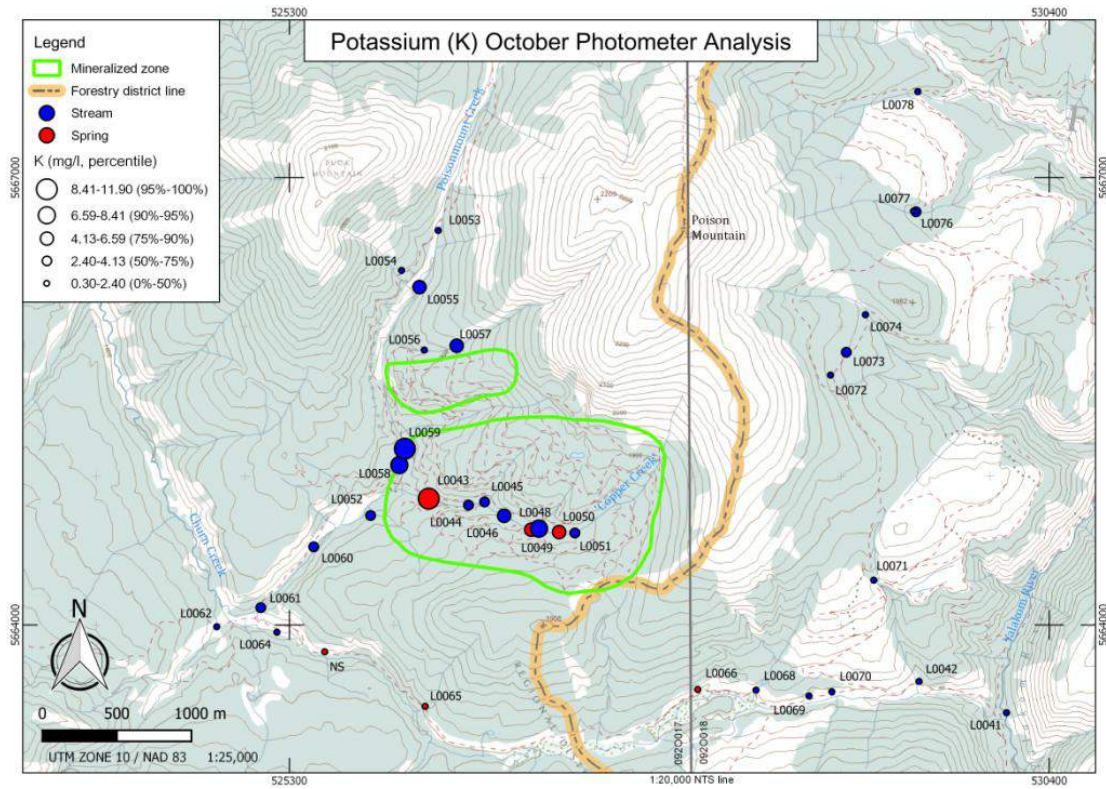
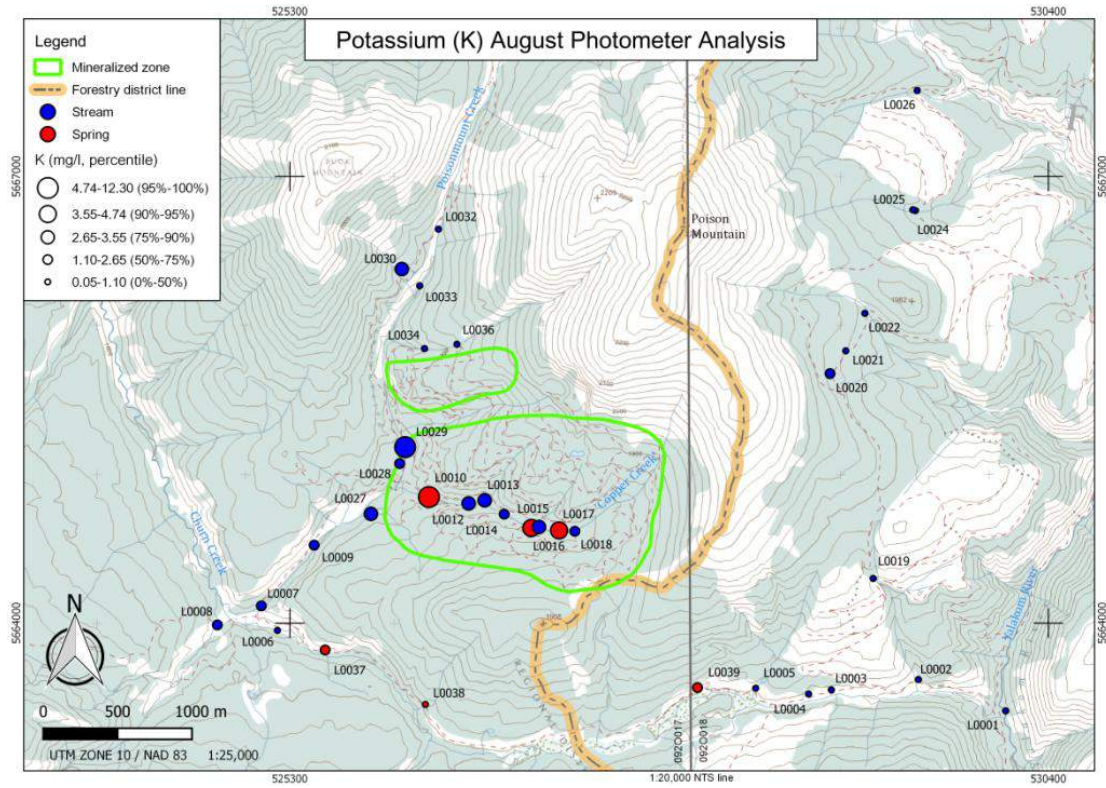


Figure 40. Potassium photometer analysis August (top) and October (bottom).

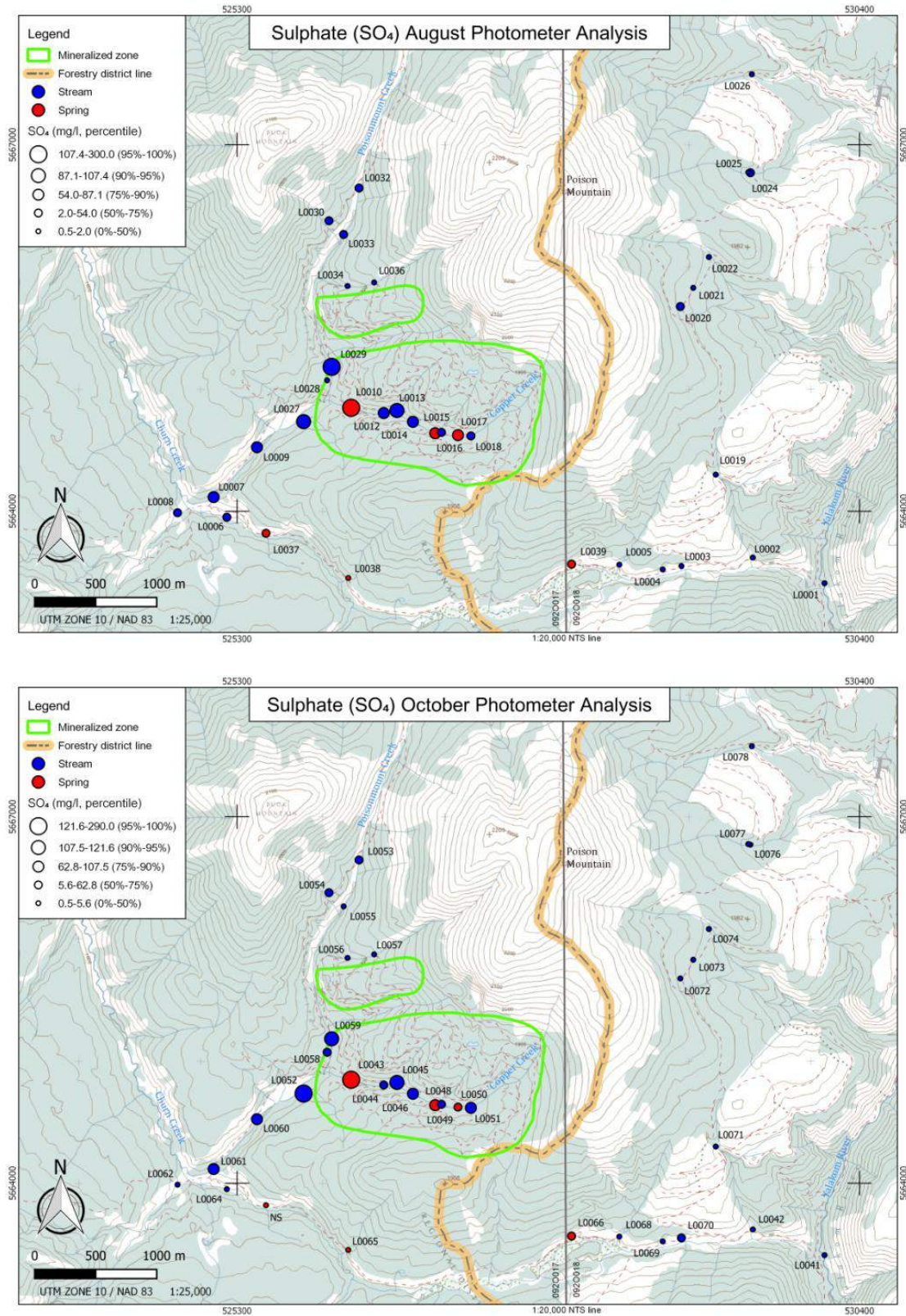


Figure 41. Sulphate photometer analysis August (top) and October (bottom).

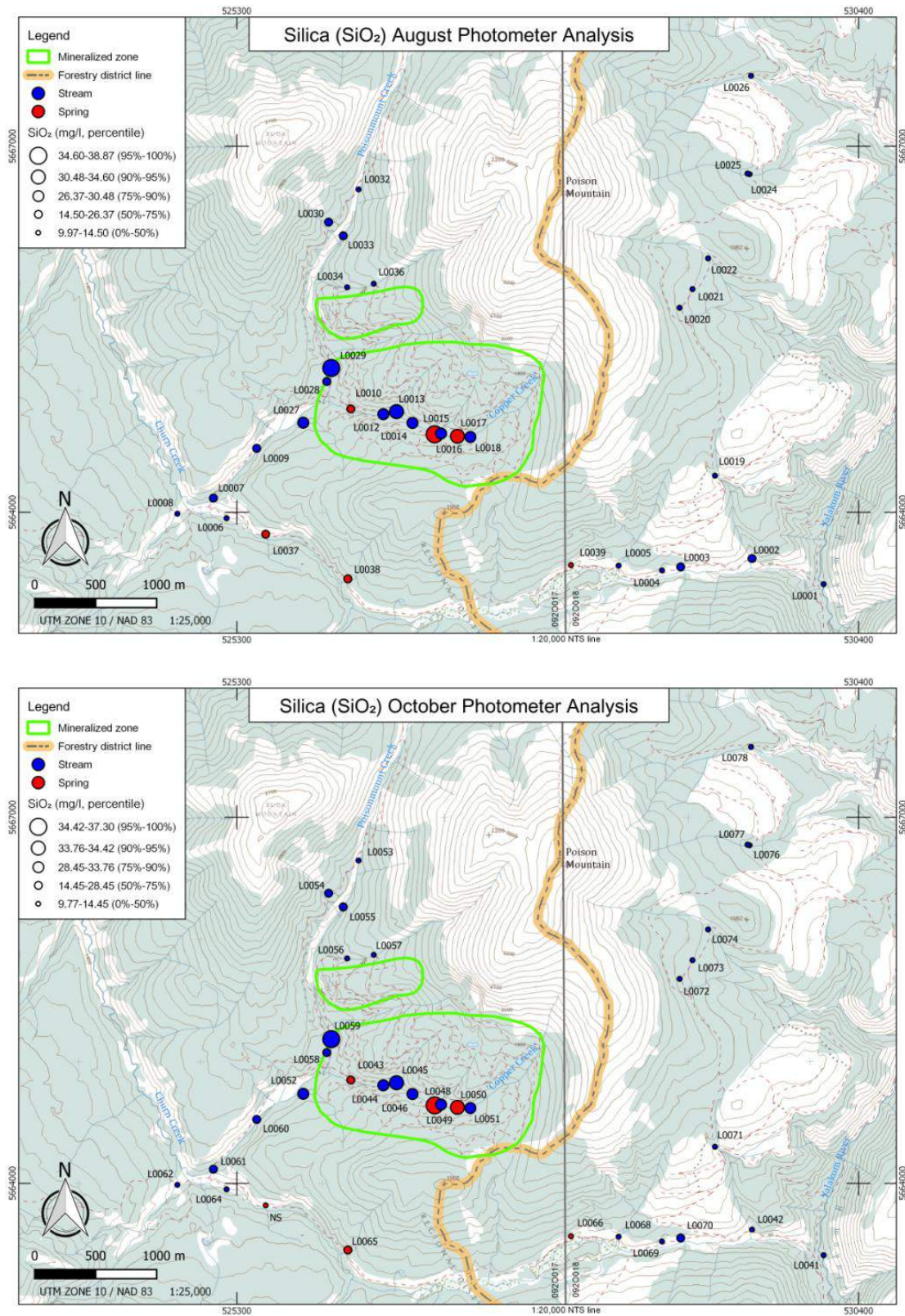


Figure 42. Silica photometer analysis August (top) and October (bottom).

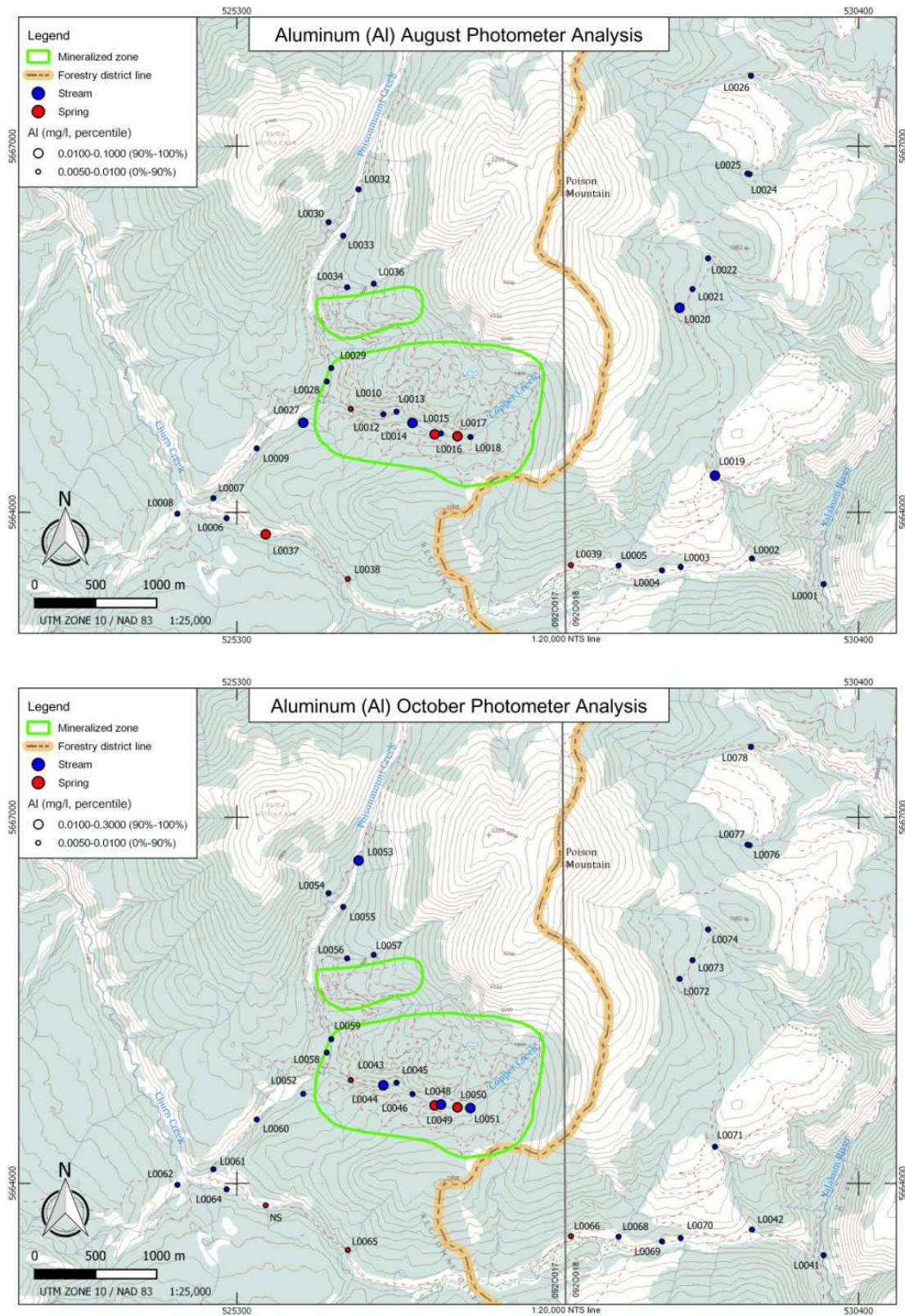


Figure 43. Aluminum photometer analysis August (top) and October (bottom).

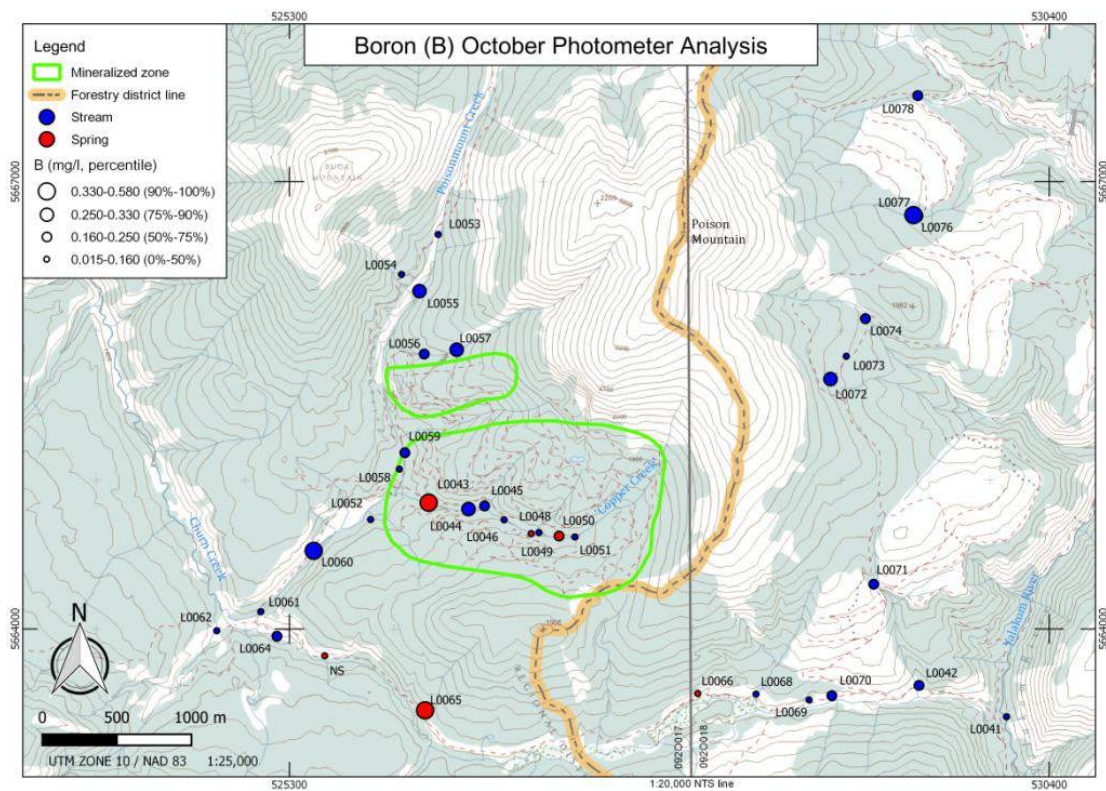
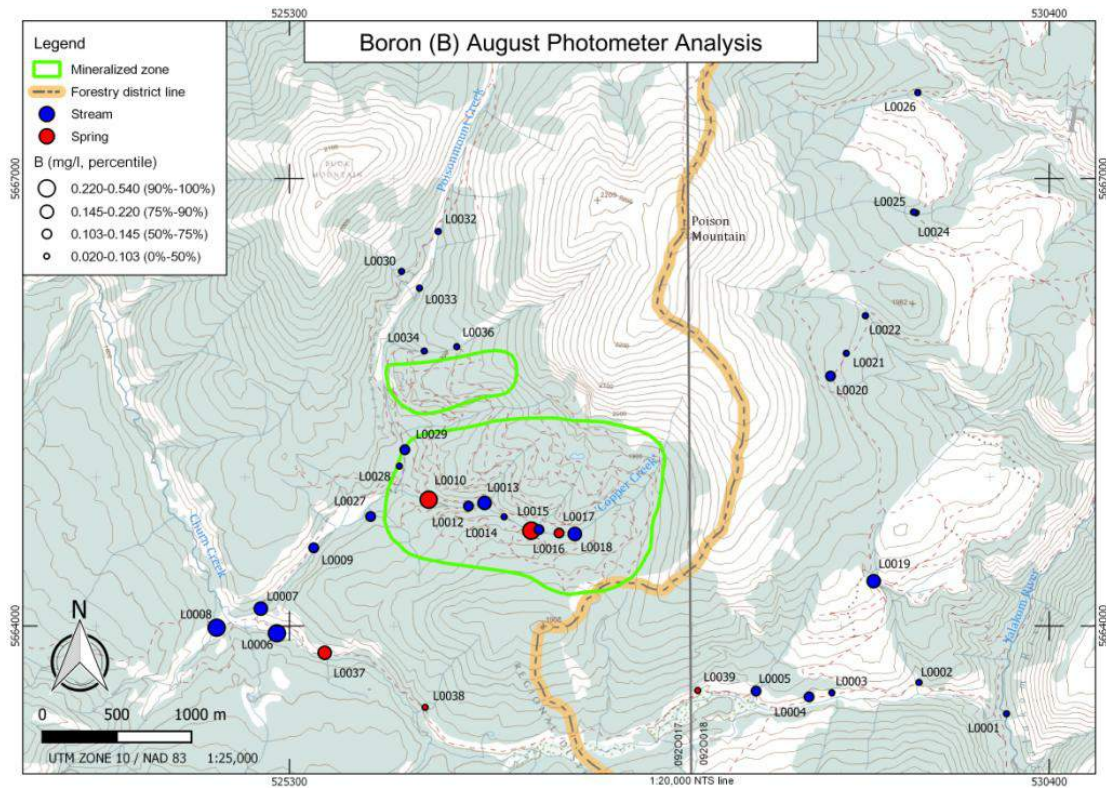


Figure 44. Boron photometer analysis August (top) and October (bottom).

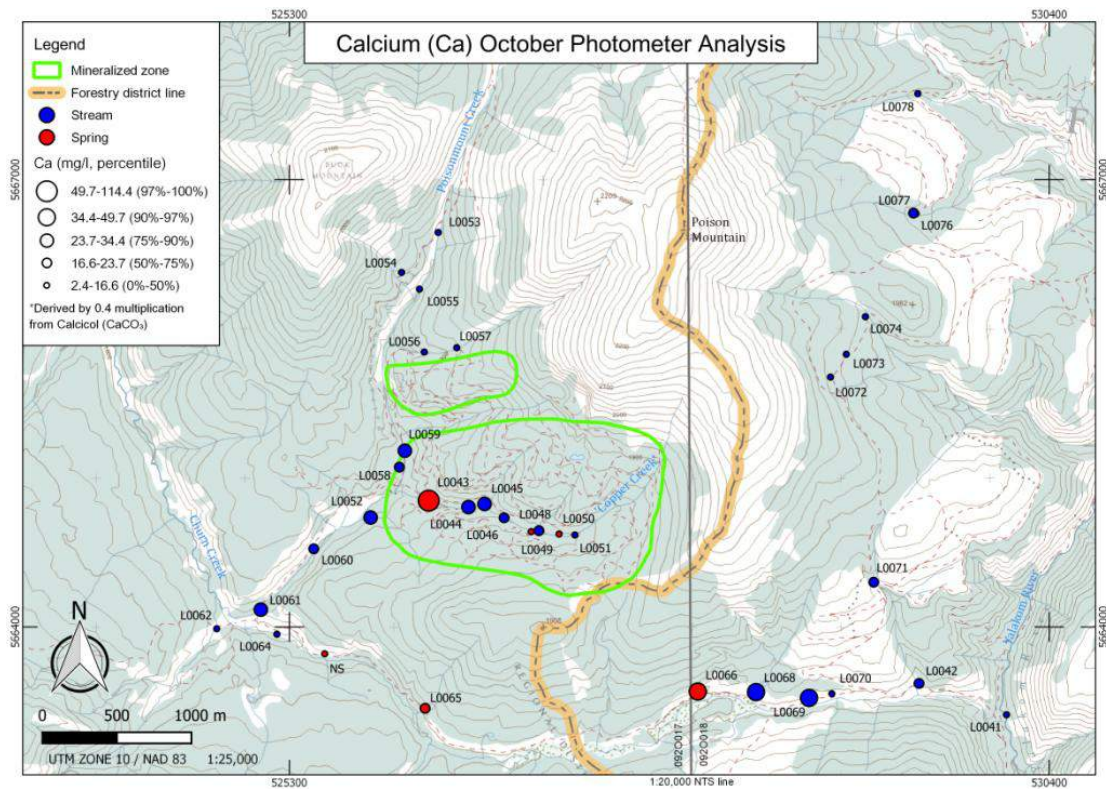
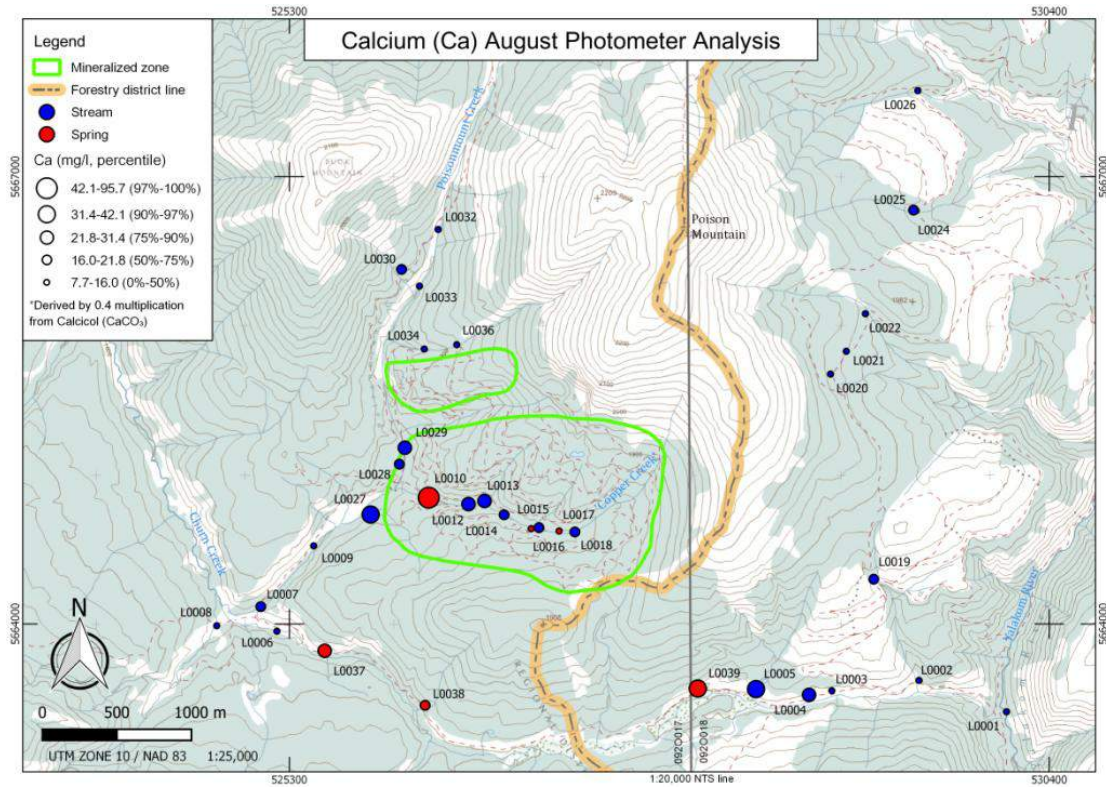


Figure 45. Calcium photometer analysis August (top) and October (bottom).

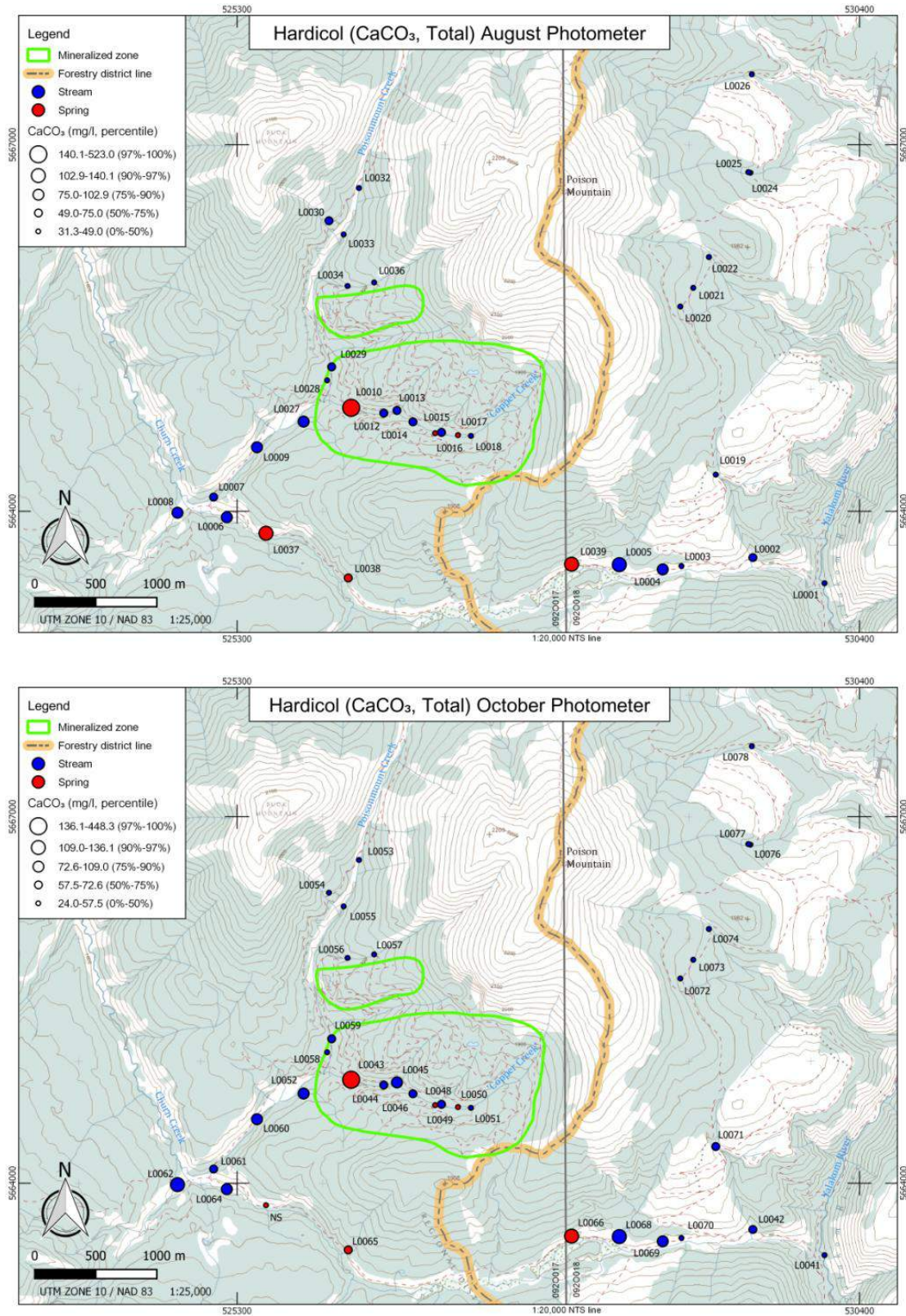


Figure 46. Hardicol photometer analysis August (top) and October (bottom).

### ***Magnesium***

Magnesium (Figure 47) correlates well with the mineralized zone and to springs in the drainage to the south of Poison Mountain in both months. The October result for spring sample L0043 is unusual. Its result is anomalously low compared to the equivalent sample in August (sample L0010). This anomaly is described in more detail in Figure 47. Results correlate well with Ca and Hardicol described above. Maximum concentrations are 4 to 21 times background (<3.0 mg/l and 6.0 mg/l).

### ***Manganese***

Considering the low concentrations measured for Mn (Figure 48), the test demonstrates a good correlation with the mineralized zone for the October results but less convincing results for the August campaign (Figure 48 bottom). Concentrations are higher in August (top) compared to October. As in the case of Al, low concentrations and small percentile breakdown make maximum concentrations versus background calculation not possible.

### ***Nickel***

Nickel yielded consistently low concentrations (Figure 48), although slightly elevated values are present over the mineralized zone in Copper Creek. The high concentration (0.2367 mg/l) in the August spring sample L0037 is likely to be caused by high turbidity in the spring water.

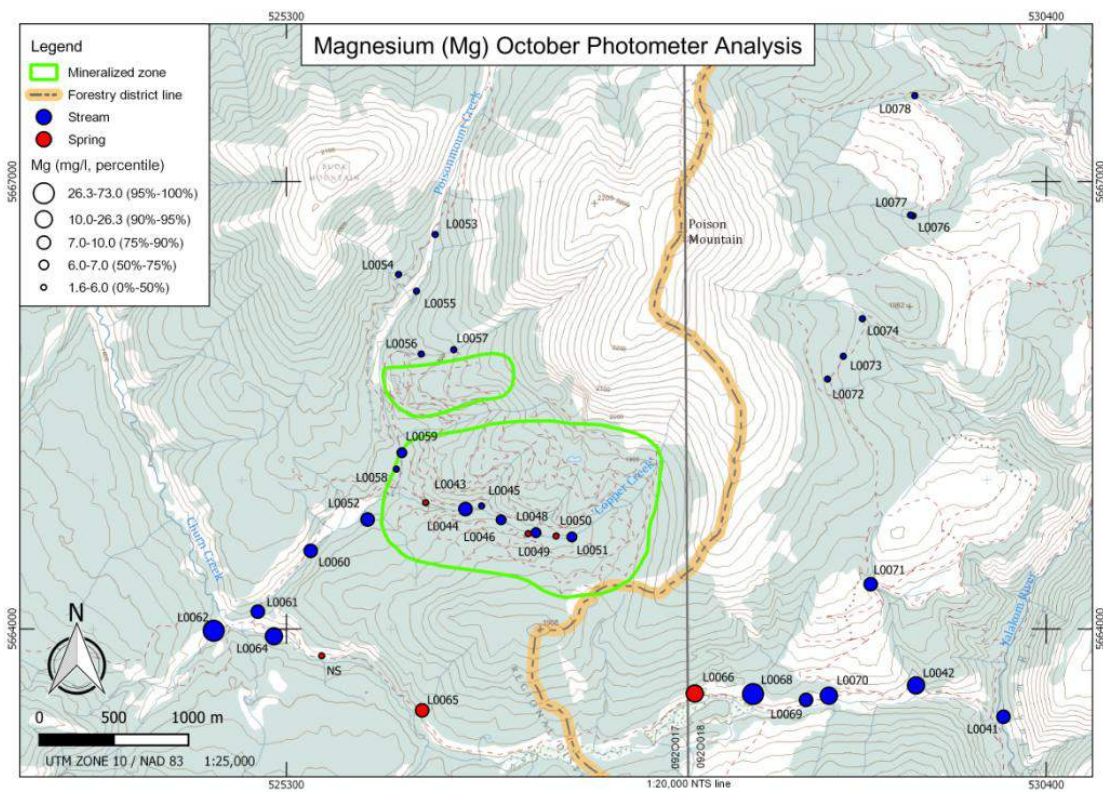
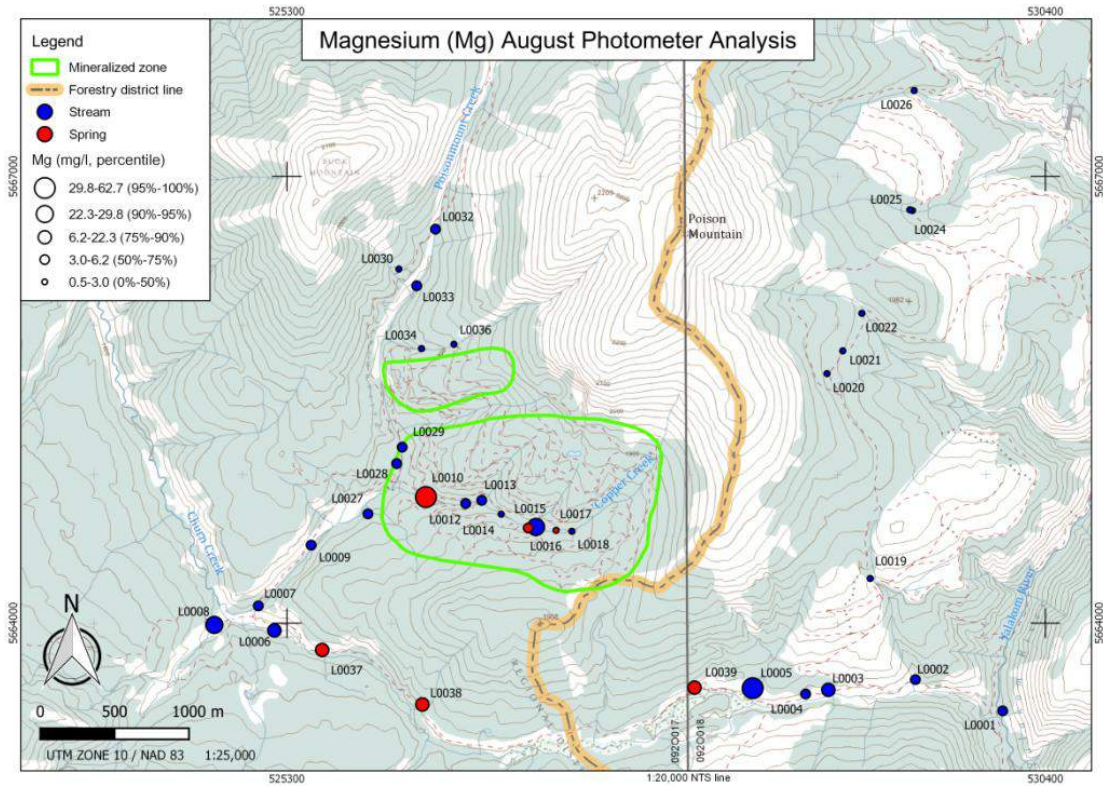


Figure 47. Magnesium photometer analysis August (top) and October (bottom).

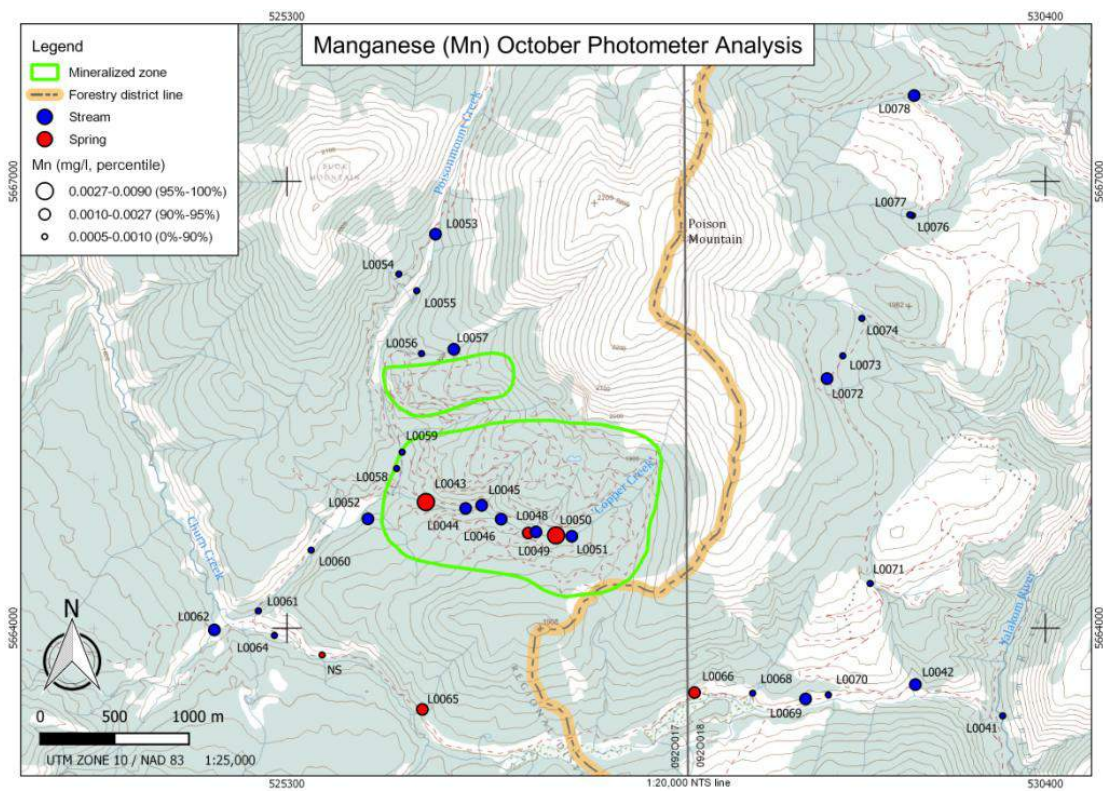
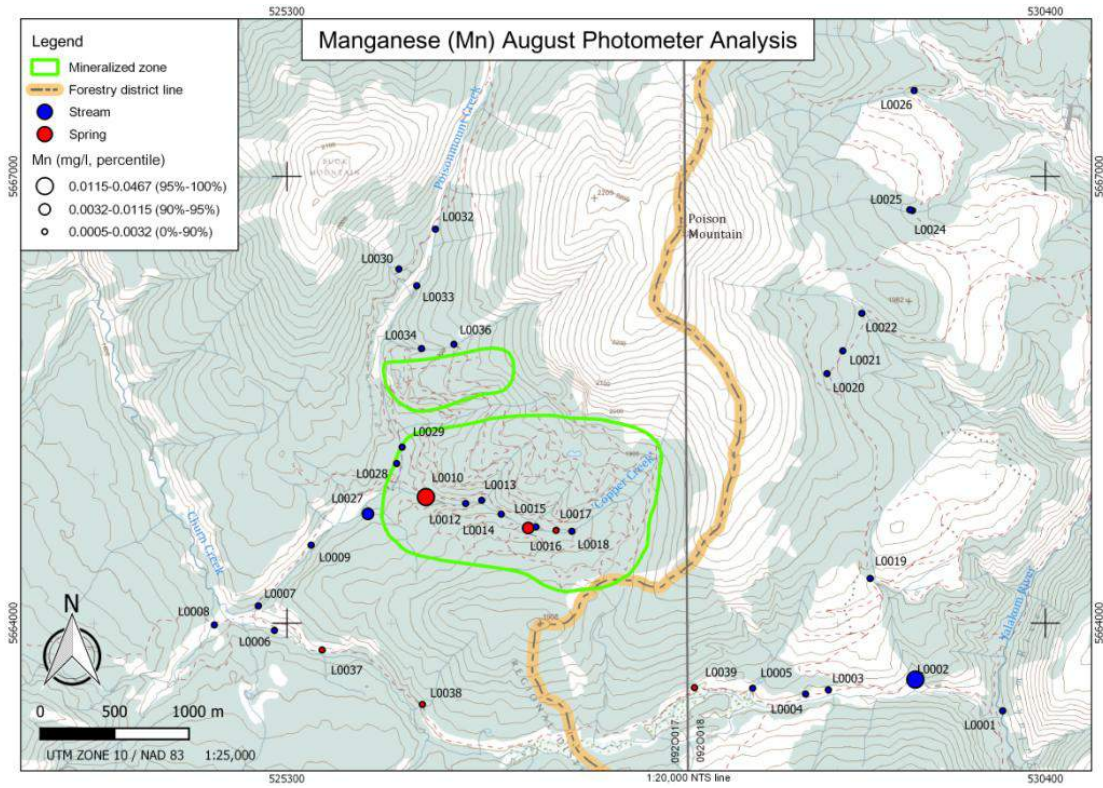


Figure 48. Manganese photometer analysis August (top) and October (bottom).

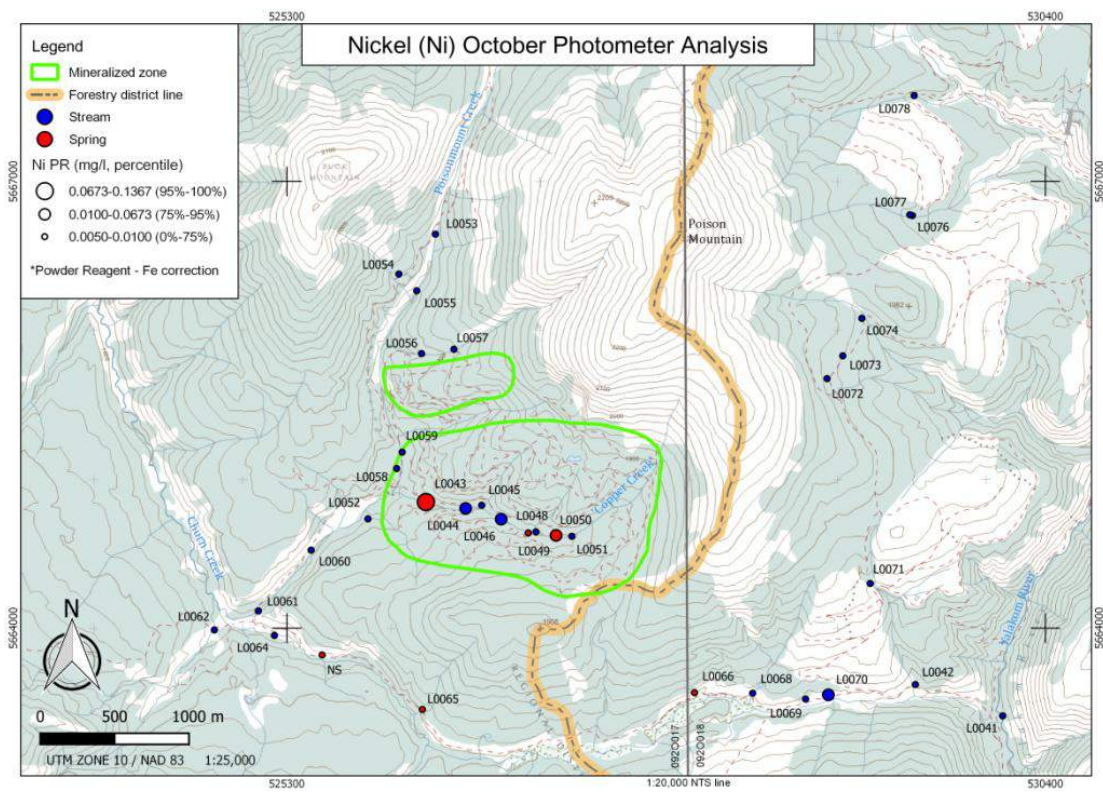
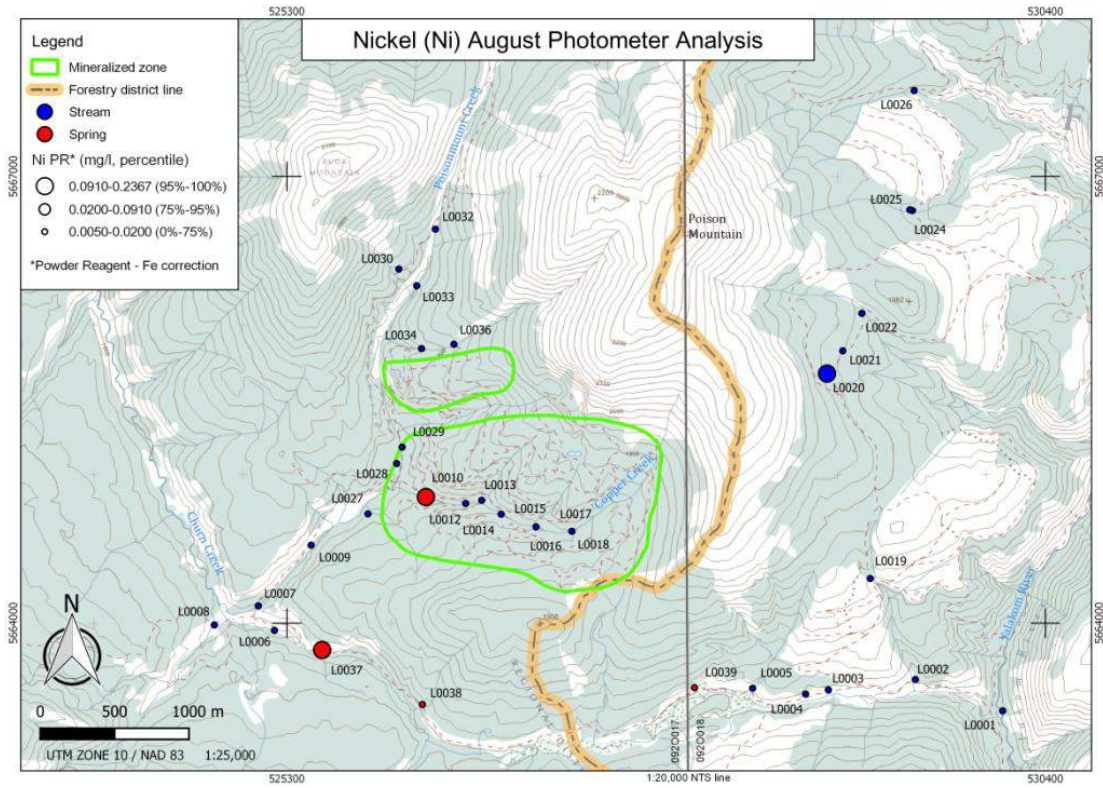


Figure 49. Nickel photometer analysis August (top) and October (bottom).

## Stream Sediment Results

Stream sediment results for a selection of elements corresponding to the photometer analyte suite are shown in Figure 50 to Figure 60. For ease of discussion, the elements are grouped into commodity, pathfinder and other categories. The figures are paired to show the results for the August (top) and October (bottom) sampling campaigns.

### Commodity Elements

#### *Copper*

Copper (Figure 50) shows a good correlation between the August and October sampling campaigns. Highest concentrations occur directly over the southern mineralized zone along Copper Creek, where the maximum concentration (6860 ppm in August and 5040 ppm in October) reaches 122 and 78 times the background (56.8 ppm and 64.7 ppm; defined by the 50<sup>th</sup> percentile concentration). Elevated values also occur on Poisonmount Creek above the confluence with Copper Creek, downstream from the northern mineralized zone. Values remain elevated above regional background levels downstream to the confluence with Churn Creek. East of Poison Mountain, concentrations show little variation and remain at background levels.

#### *Molybdenum*

Figure 51 shows that Mo has much the same pattern as Cu. Over the southern mineralized zone, concentrations reach highs of 39.0 ppm in August and 41.7 ppm in October, which are 45 and 44 times the regional background (0.86 and 0.98 ppm). Below Copper Creek, Mo concentrations remain elevated as far as the confluence with Churn Creek. The northern mineralized zone has a more subdued downstream expression for Mo than Cu. Samples from the unnamed drainage on the north side of the northern mineralized zone are weakly anomalous, with values of up to 12.2 ppm in August and 11.35 ppm in October, or 14.2 and 11.6 time background. Only background values occur in the drainages east of Poison Mountain.

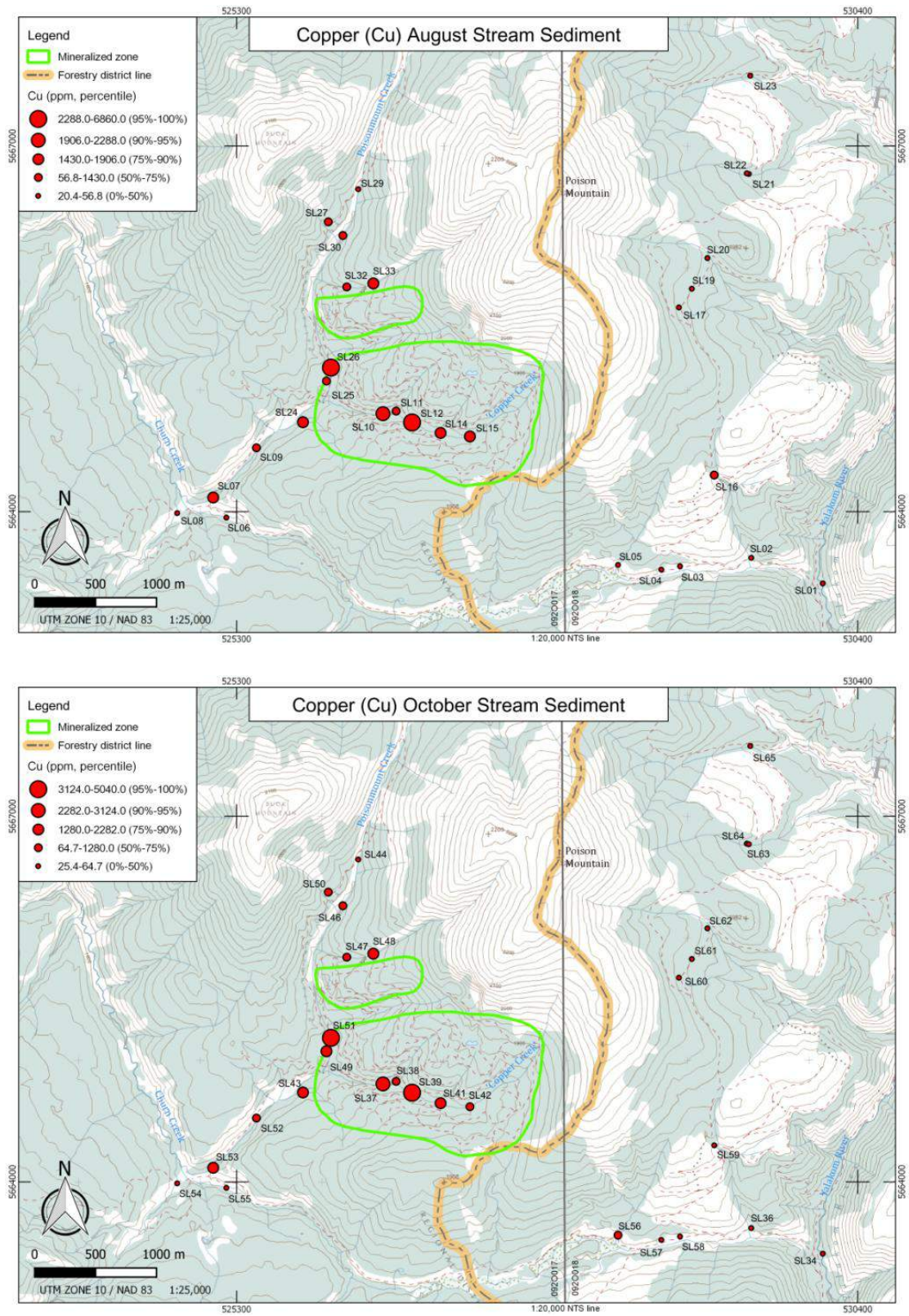


Figure 50. Copper stream sediment August (top) and October (bottom).

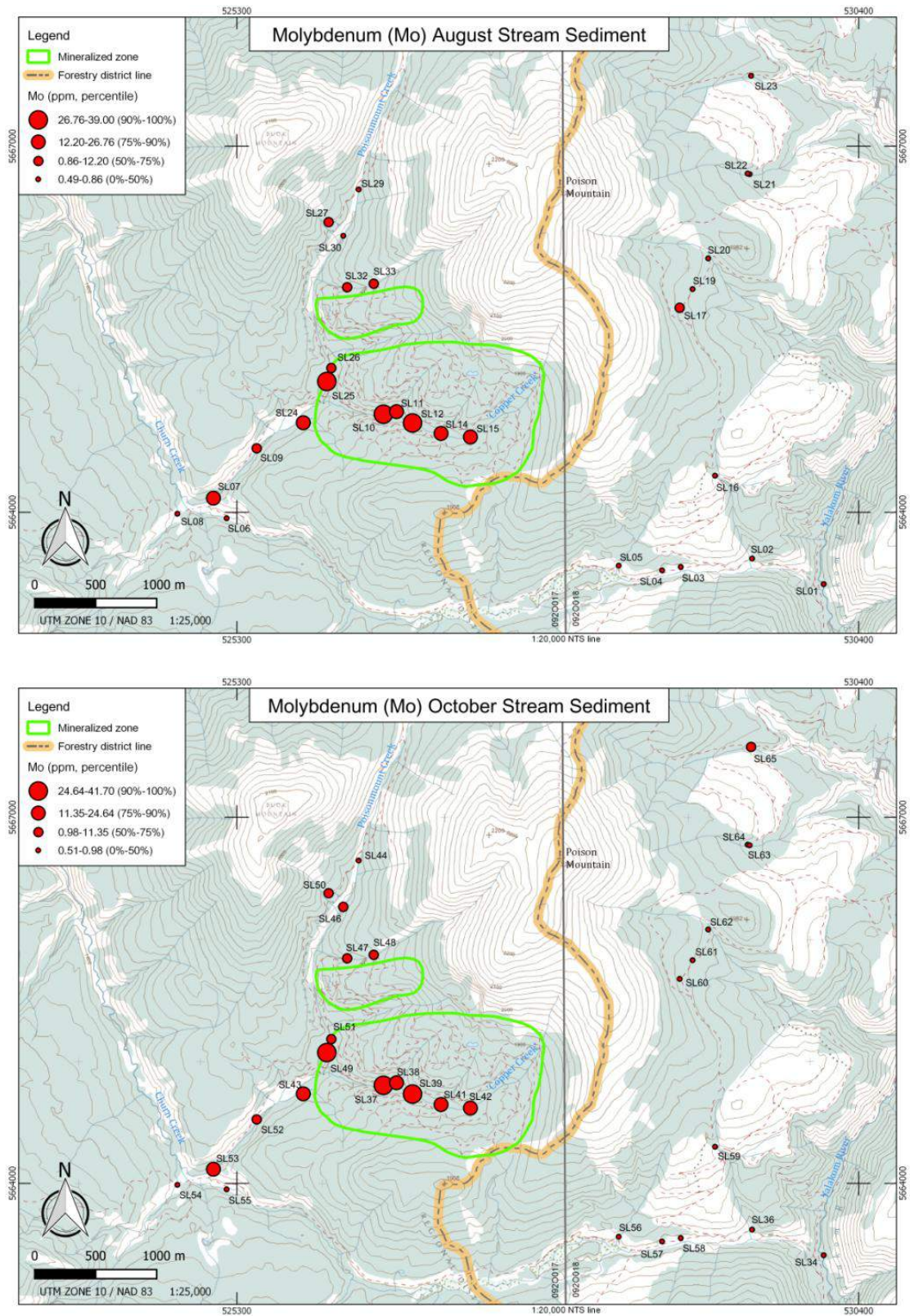


Figure 51. Molybdenum stream sediment August (top) and October (bottom).

## Pathfinder Elements

### *Iron*

Iron (Figure 52) shows a somewhat different pattern to Cu and Mo. All of the samples collected from Copper Creek and the Poisonmount Creek display moderately to highly anomalous concentrations of this element. Whereas for Cu and Mo the highest concentrations occur over the mineralized zone, Fe shows only a weak response over the mineralization and a gradual increase in concentration downstream. Maximum values (6.79% in August and 6.67% in October) occur below the confluence of Poisonmount and Churn Creeks. This pattern displays a close relationship with stream pH (Figure 28), which is slightly more acidic over the mineralization (pH of 6) and becomes more neutral to slightly alkaline (pH 7) downstream towards the confluence with Churn Creek. This relationship is most clearly visible in the October results. The enrichment of Fe with increasing water pH suggests that it is being transported in solution under slightly acidic conditions and hydromorphically precipitating in the sediments (presumably as hydroxides) where the pH reaches near neutral values.

East of Poison Mountain, Fe values are at regional background levels (3.42% in August and 3.30% in October) and show no systematic variations with pH.

### *Manganese*

Manganese shows a similar pattern to Fe (Figure 53), but unlike Fe it displays considerable differences between the two sampling campaigns. Results from August (Figure 53; top) show elevated values over the southern mineralized zone as well, as along the lower reaches of Poisonmount Creek and at the confluence with Churn Creek. The maximum concentration of 897 ppm (or 1.6 times background) occurs over the southern mineralized zone but a similar value is also present on Poisonmount Creek below the confluence with Copper Creek.

In the October results, the Copper Creek response is muted, and concentrations at the confluence between Poisonmount and Churn Creeks are enhanced. The maximum concentrations (to 808 ppm or 1.5 times background) occur immediately adjacent to the confluence in both drainages. Once again, this pattern is consistent with hydromorphic dispersion where Mn appears to be deposited from solution and where the drainage pH rises to neutral or slightly alkaline levels.

Manganese also has slightly elevated concentrations along Churn Creek in the southeast of the study area and in some of the drainages to the east of Poison Mountain. The Churn Creek anomalies are most pronounced in the October results. A lack of sampling along Churn Creek between the confluence with Poisonmount Creek and the anomalous samples makes it difficult say with certainty whether the elevated values are truly anomalous, or just represent variations in local background.

### *Nickel*

Nickel shows a strong hydromorphic response (Figure 54). Values over the mineralization in Copper Creek and immediately below the confluence with Poisonmount Creek are at background levels for both

campaigns. The low values coincide with samples from the more acidic parts of the drainage system (Figure 28). Concentrations are significantly in the lower parts of Poisonmount Creek and at the confluence with Churn Creek where pH values become neutral to slightly alkaline. Here concentrations reach 666 ppm in August and 570 ppm in October (or 25 and 21 times background respectively).

Elevated Ni values also occur along Churn Creek in the southeastern part of the survey, in the same area where higher Mn values are observed. There is no obvious Ni source in the immediate vicinity, but the correlation with Mn suggests that the elevated values could also be a hydromorphic response. An alternative explanation for the Ni values is the presence of detrital material derived from the Shulaps Metamorphic Complex that crops out 2.5 kilometres south of the study area.

### **Zinc**

Zinc results are illustrated in Figure 55. They show similar patterns in August and September. A notable feature of the Zn distribution is an apparent depletion in the centre of the study area in the vicinity of the porphyry Cu-Mo mineralization. Samples in Copper Creek over the southern mineralized zone have consistent values below the 50<sup>th</sup> percentile concentration (74 ppm). Similar values are present in the unnamed drainage on the north side of the northern mineralized zone, as well as in Poisonmount Creek upstream from the Copper Creek confluence.

Elevated values occur in the lower reaches of Poisonmount Creek and at its confluence with Churn Creek. As discussed in the case of Cu, Fe and Mn, this area of enrichment is likely to be a hydromorphic concentration caused by Fe hydroxide scavenging in the lower more neutral part of the drainage.

Highest Zn concentrations occur in the drainages on the east side of Poison Mountain and include the maximum values of 145 and 144 ppm for the respective campaigns. These concentrations are relatively low and are likely to indicate the regional background levels for the Jackass Mountain Formation rather than a mineralized source.

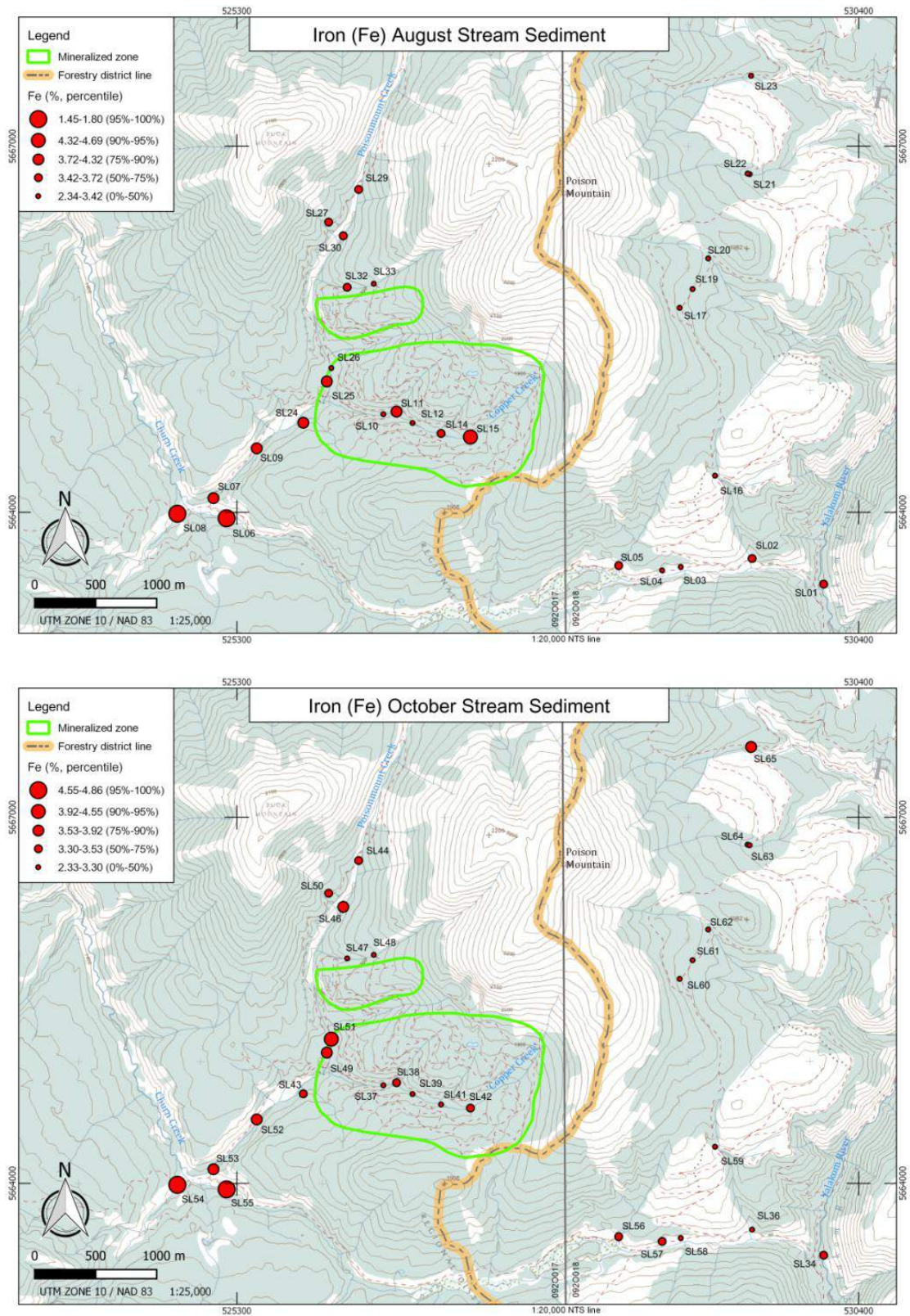


Figure 52. Iron stream sediment August (top) and October (bottom).

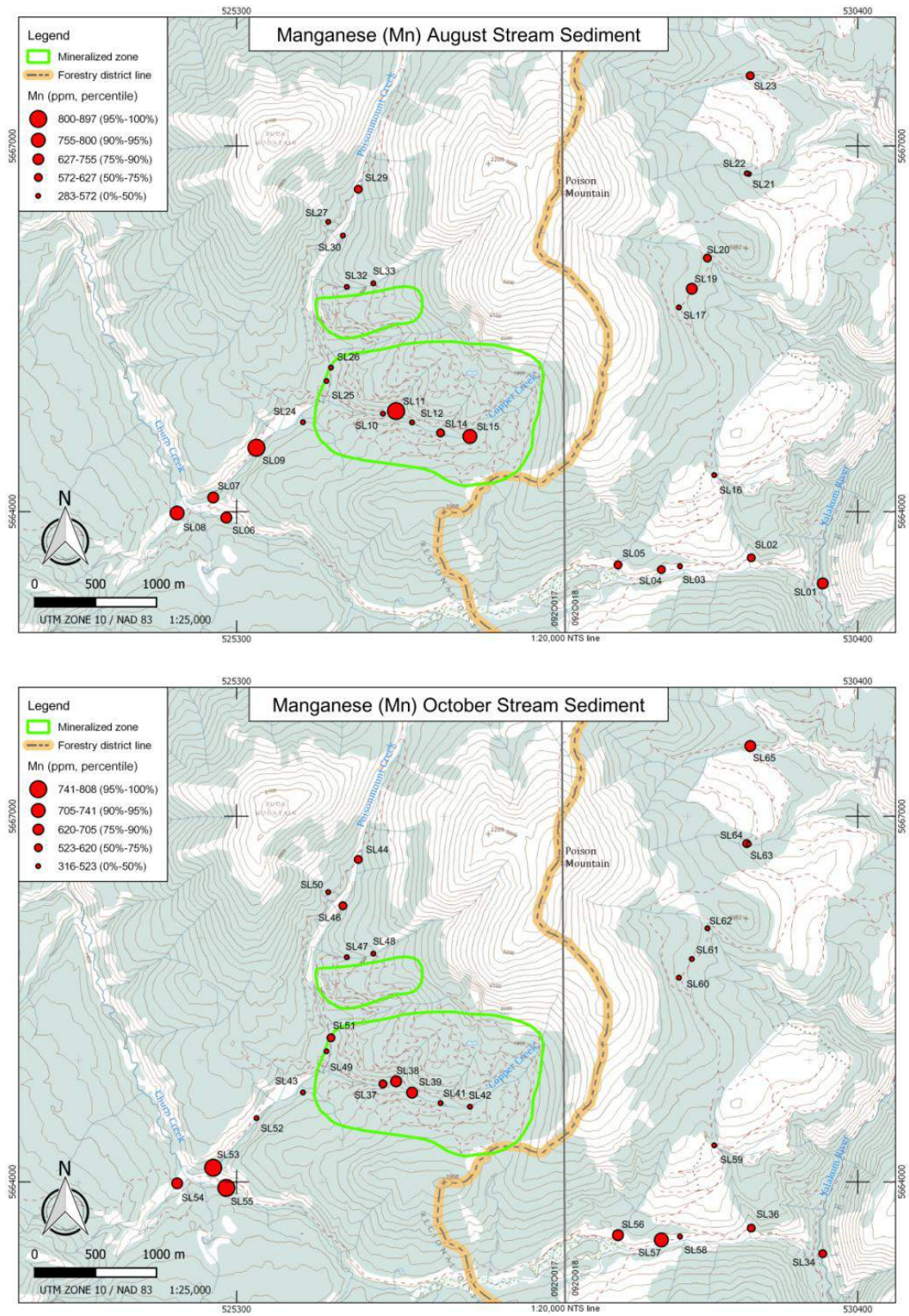


Figure 53. Manganese stream sediment August (top) and October (bottom).

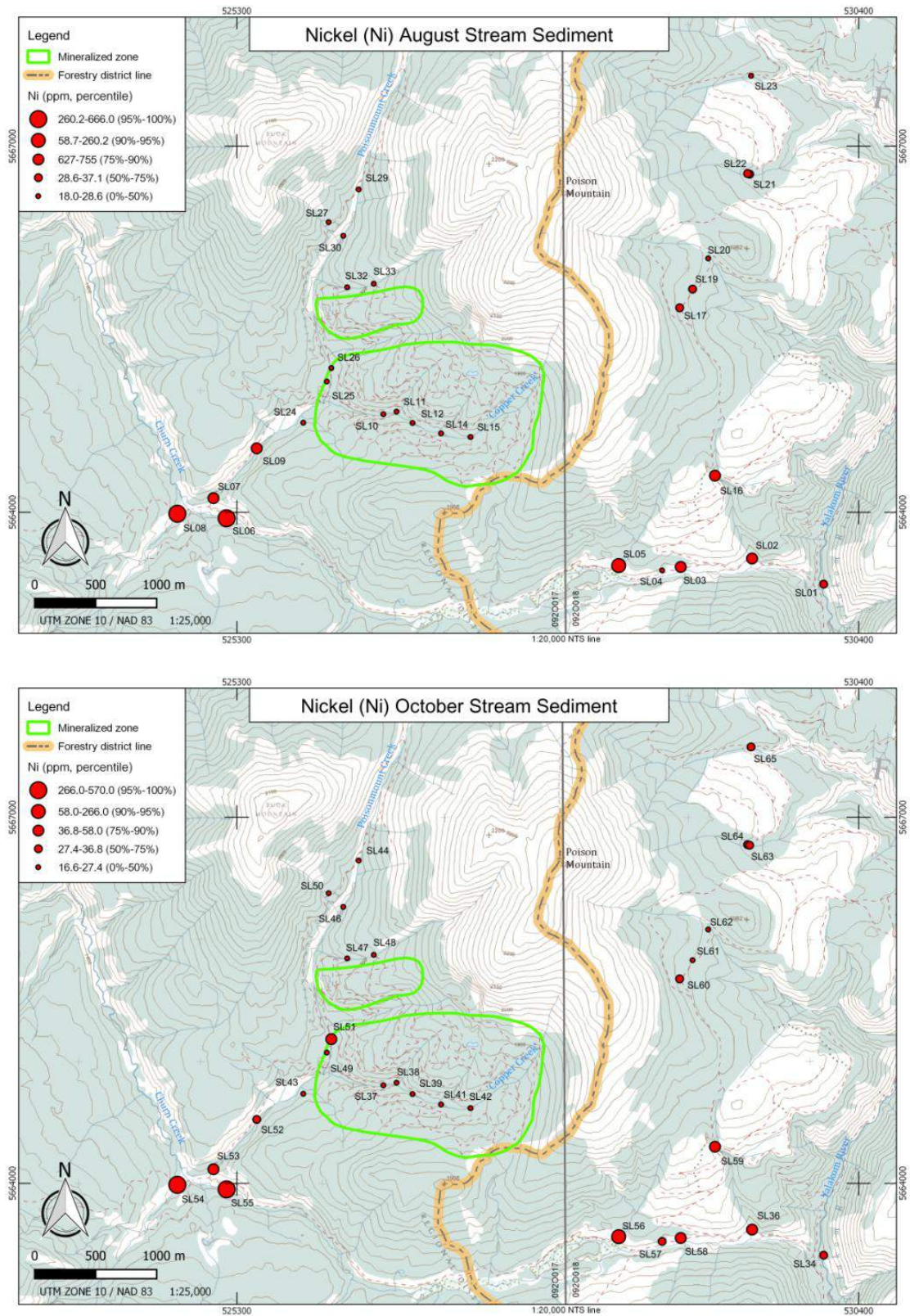


Figure 54. Nickel stream sediment August (top) and October (bottom).

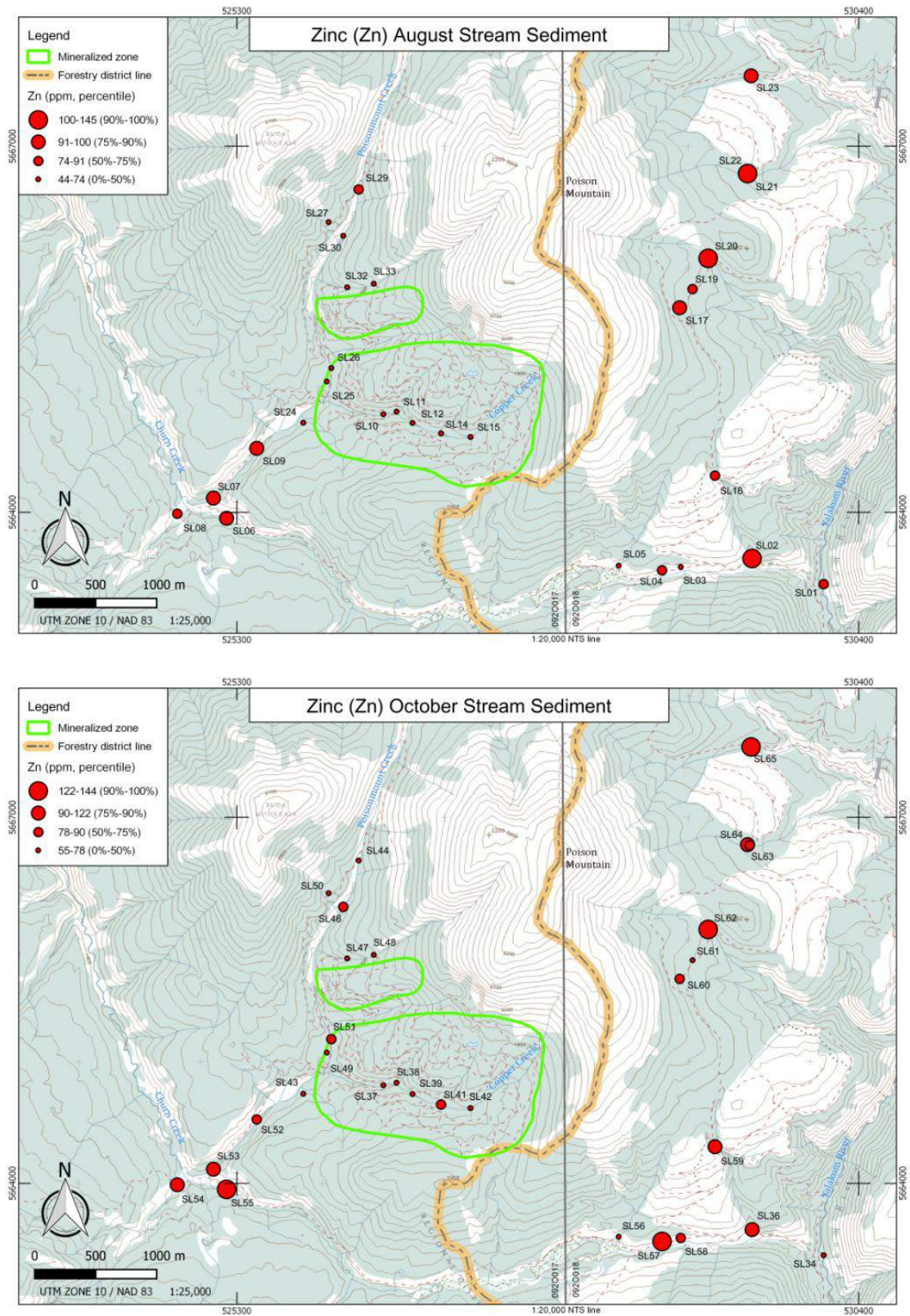


Figure 55. Zinc stream sediment August (top) and October (bottom).

## Other Elements

Other elements that also occur in the photometer analyte suite are Al, B, Ca, K and Mg. Boron results, with a couple of exceptions, are consistently at or below the analytical method detection limit and therefore do not show any useful patterns; this element will not be discussed any further in this report. Results for the other element are presented in Figure 56 to Figure 60 and discussed below.

### *Aluminum*

Patterns for Al are nearly identical between the two sampling campaigns. This element also appears to show a relative depletion over the mineralized zones (Figure 56). Samples along Copper Creek have values consistently below the 50<sup>th</sup> percentile (2.05% - August; 1.86% - October). Similar levels are also observed in the unnamed drainage adjacent to the northern mineralized zone. In Poisonmount and Churn Creeks, concentrations are marginally higher (2.05 to 2.55%) and show only minor variation, which is interpreted to represent the local background. The Al content of the stream sediments most likely reflects the amount of clay minerals weathered from the exposed bedrocks in the catchment basins. The low Al concentration over the mineralized zones is consistent with sediment derived from the unweathered feldspar porphyry intrusions. Higher values in Poisonmount and Churn Creeks almost certainly indicate input from mudstones and shales, which are widespread in the surrounding Jackass Mountain Formation.

### *Calcium*

Calcium results are presented in Figure 58. Patterns show little change between the August and October sampling campaigns. Concentrations below the 50<sup>th</sup> percentile (0.95% - August; 0.66% - October) characterize samples collected in Copper Creek and the lower parts of Poisonmount Creek. The low values are believed to reflect the relatively Ca-poor sediments derived from the intrusive rocks exposed in the Copper Creek catchment basin. Lower Ca values may also be attributed to the slightly acid waters encountered over and downstream from the southern mineralized zone (see earlier).

Samples collected on Poisonmount Creek to the north of the porphyry mineralization and on the eastern and southeastern slopes of Poison Mountain have higher Ca concentrations, most likely reflecting the calcareous nature of the Jackass Mountain Formation sedimentary units in that area.

### *Potassium*

Potassium is another element that appears to highlight lithological differences in the catchment basins. Figure 59 shows that the highest values (0.28% - August and 0.24% - October) occur along Copper Creek and the unnamed drainage adjacent to the northern mineralized zone. Both of these areas are underlain by, or are adjacent to, feldspar porphyry intrusions that show varying degrees of potassic and sericitic alteration. Both the August and October results show a steady decline in concentrations downstream towards the confluence of Poisonmount and Churn Creeks. This is almost certainly caused by dilution of the porphyry-derived sediment by sedimentary material from the Jackass Mountain Fm.

East of Poison Mountain, K values are uniformly low, falling below the 50<sup>th</sup> percentile (0.10%). The low levels indicate the background concentration of sediments derived from the Jackass Mountain Fm.

### ***Magnesium***

Magnesium, not surprisingly, displays similar patterns to Ca. Figure 60 shows that concentrations and patterns are similar in both sampling campaigns. Elevated concentrations occur mostly in the western part of the study area along Poisonmount Creek. Maximum values (1.20%) occur in samples along Churn Creek near to the confluence with Poisonmount Creek. Over the mineralized zone in Copper Creek, concentrations are depressed below the 50% percentile (0.89% and 0.85%). As mentioned in the case of Ca, this is likely to be a response to the weakly acidic water pH values encountered over the mineralized zone.

Sporadic elevated Mg values in the southeast part of the survey area coincide with the higher Ni concentrations mentioned earlier (Figure 54). They are likely to be caused by the input of ultramafic material from the Shulaps Ultramafic Complex that crops out a short distance to the south of the study area.

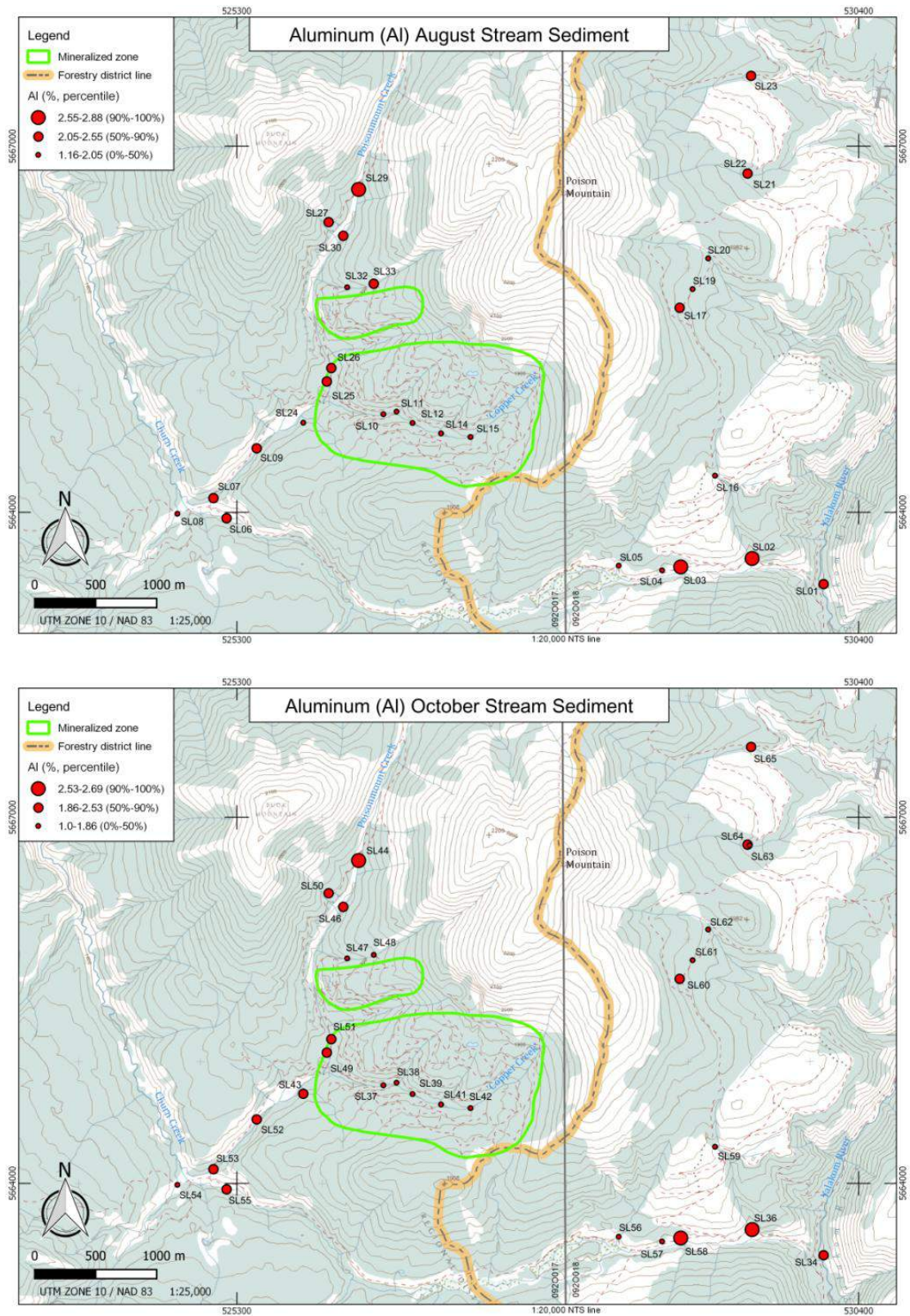


Figure 56. Aluminum stream sediment August (top) and October (bottom).

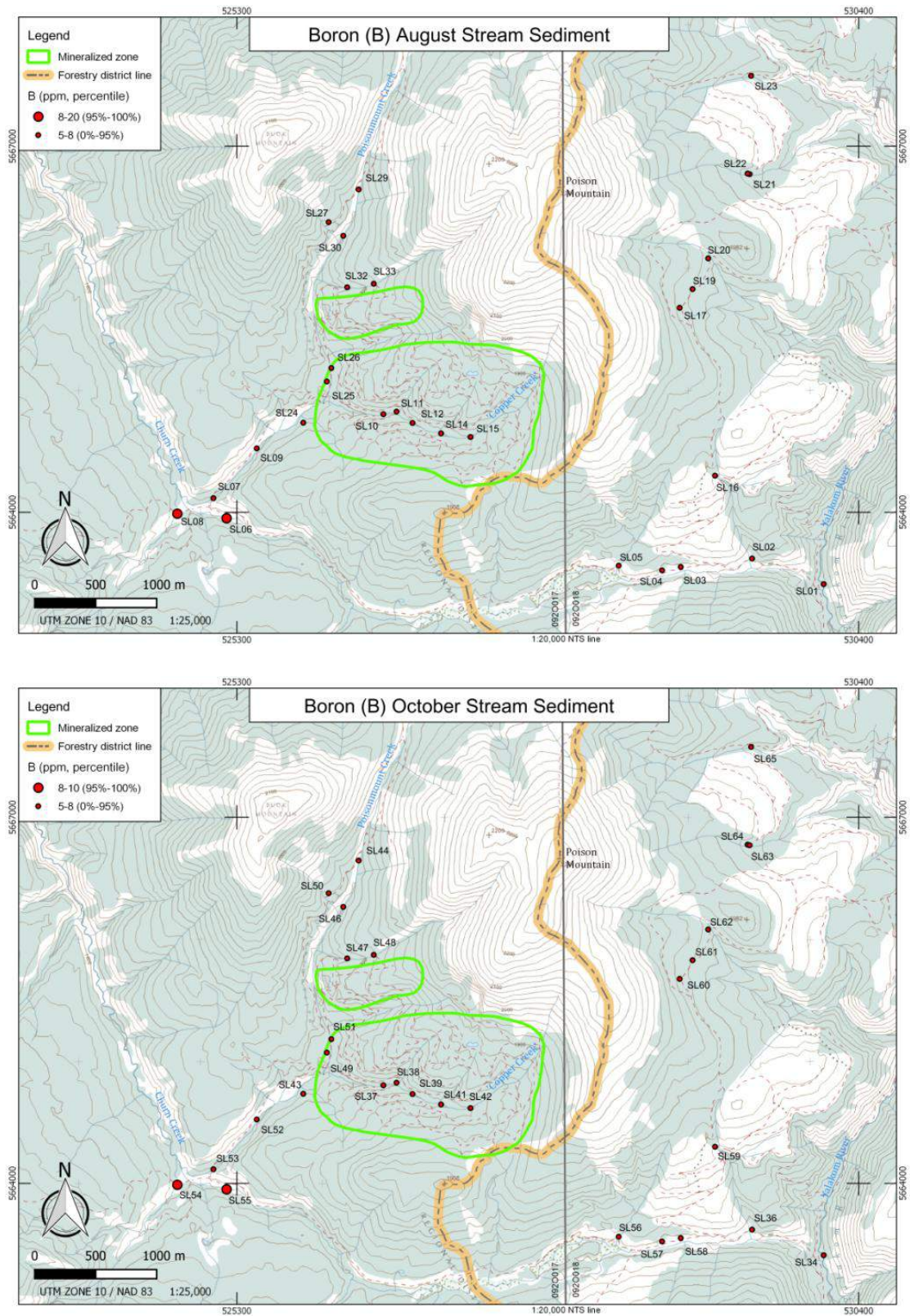


Figure 57. Boron stream sediment August (top) and October (bottom).

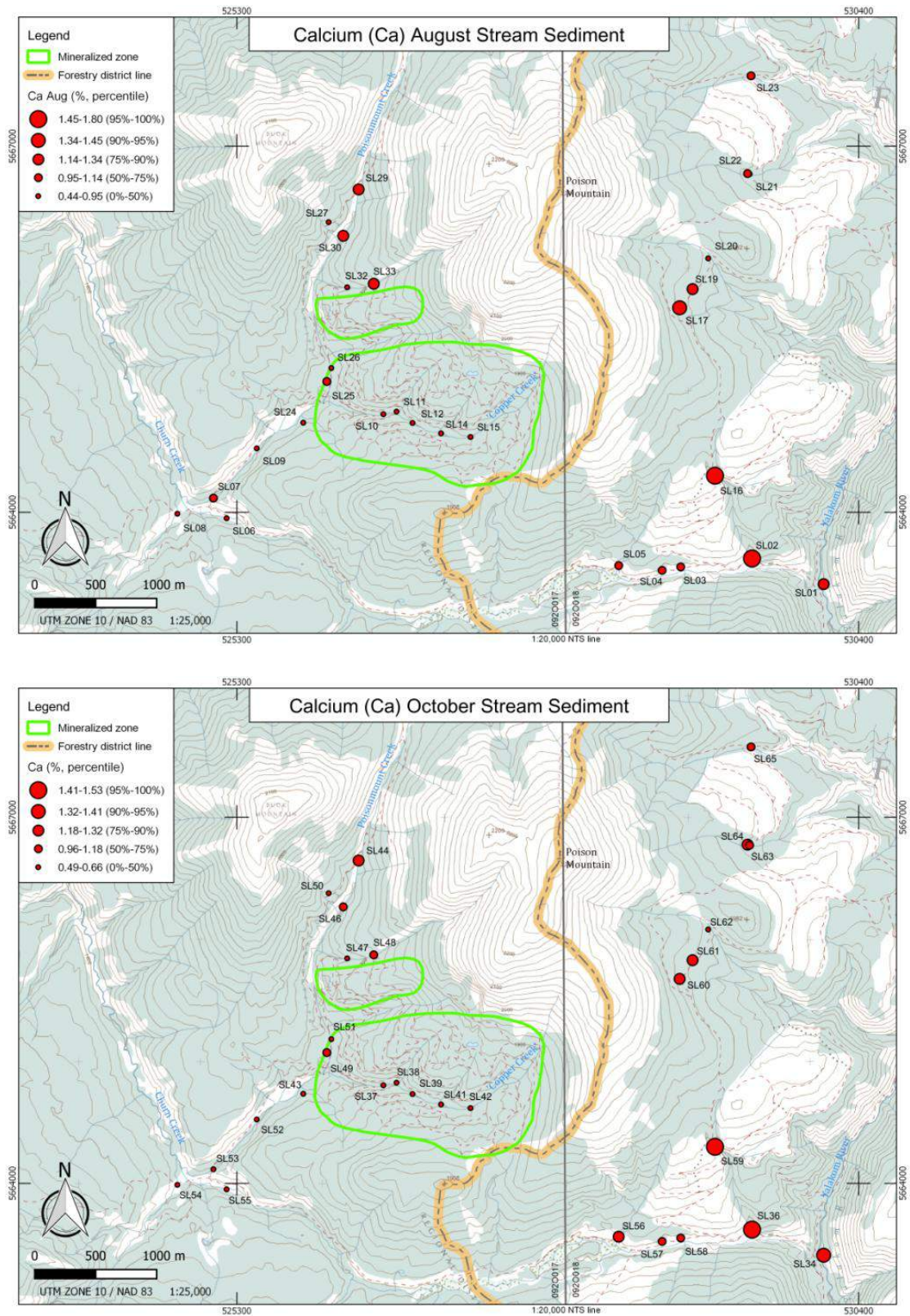


Figure 58. Calcium stream sediment August (top) and October (bottom).

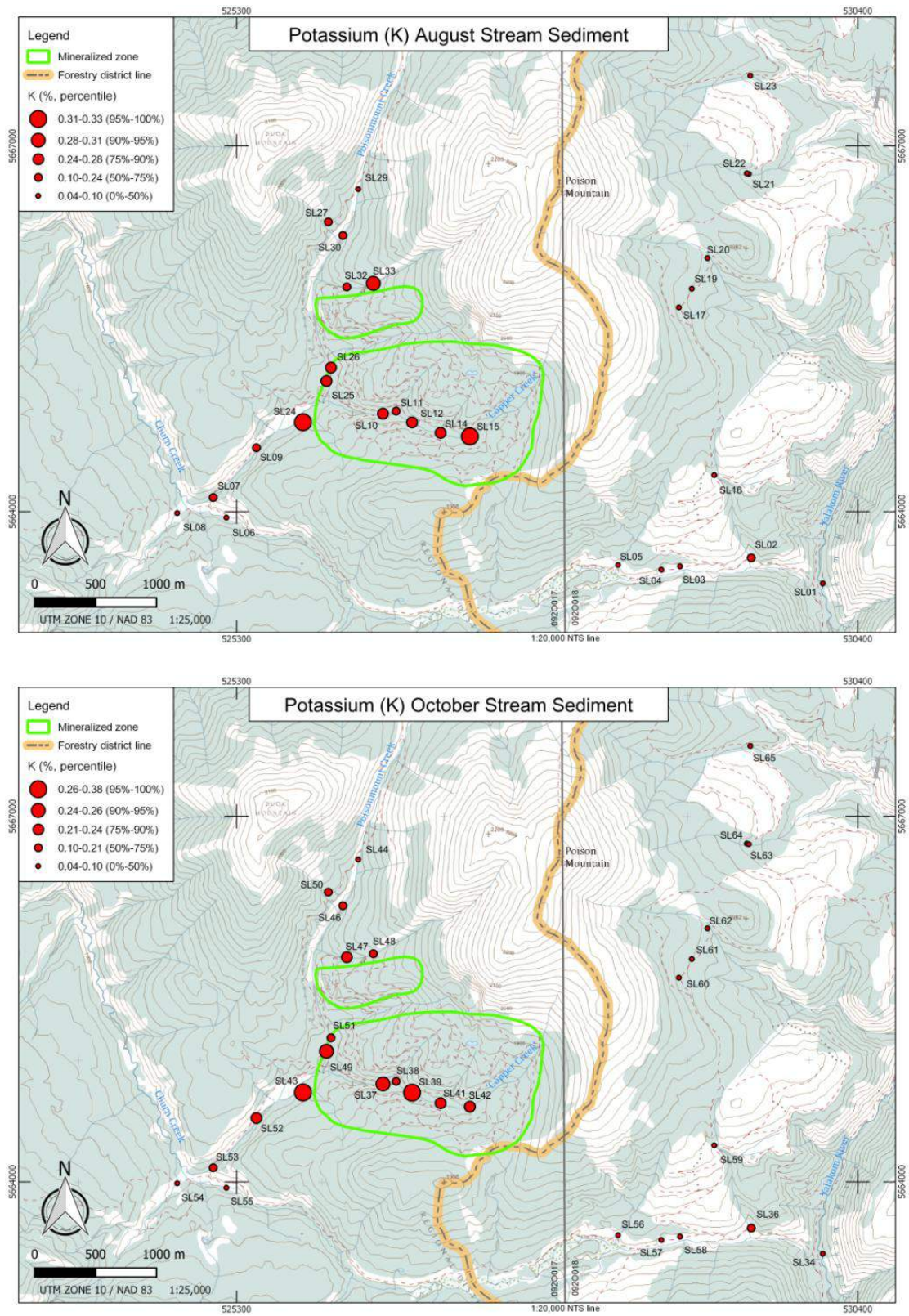


Figure 59. Potassium stream sediment August (top) and October (bottom).

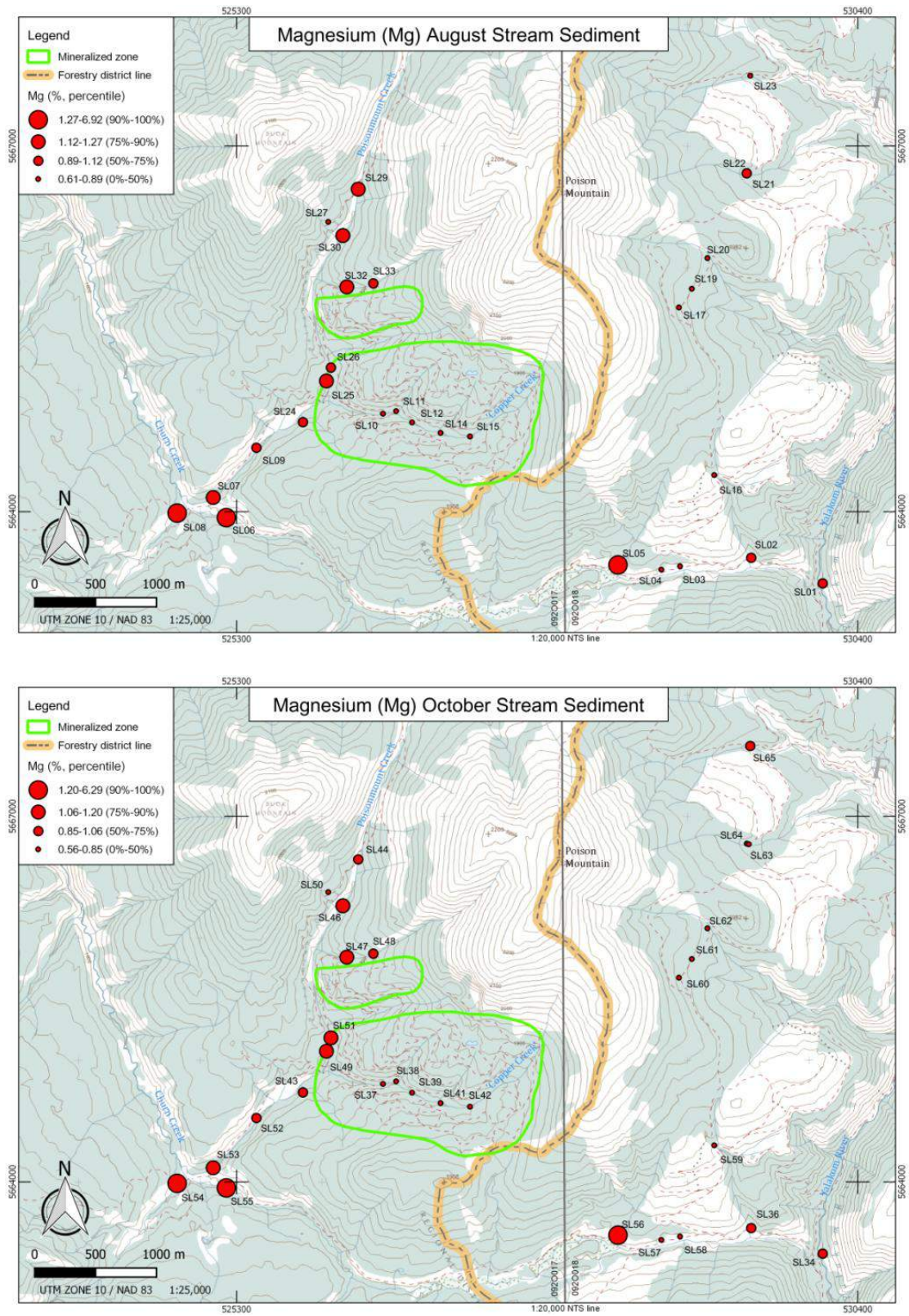


Figure 60. Magnesium stream sediment August (top) and October (bottom).

## Downstream Dispersion

One way of comparing the effectiveness of water geochemistry versus stream sediment geochemistry for detecting sulphide mineralization is by looking at downstream dispersion distances from the mineral source. Longer dispersion distances effectively enhance the footprint of the mineralized zone and make it easier to detect with drainage geochemistry. Elements are dispersed downstream either mechanically or hydromorphically. Mechanical dispersion involves the physical transport of primary minerals and weathering products within the stream's sediment bed and suspended load. Hydromorphic dispersion involves the movement of soluble element complex and ion species in solution. Element concentrations that reflect both mechanisms are diluted downstream as a result of the input of unmineralized bank material and surface water run-off into the drainage.

In order to assess the characteristics of each dispersion mechanism, results are plotted along a profile of Copper Creek, beginning at the mineralized zone and extending downstream for about 3.5 km to the confluence with Poisonmount Creek. The distances referred to in the following paragraph are measured from the highest (eastern most) sample station on 'Copper Creek' (Figure 9).

Charts below compare pH, water and stream sediment concentrations for selected elements and ions along the stream profile. Due to the absolute concentration differences between stream sediment and water results, the photometer results are scaled to fit on the same axis as the stream sediment results. (The scaling factor is noted on the legend of each chart.) Stream flow direction is from left to right.

Copper (Figure 61) results show a classic dispersion profile in both media with highest concentrations occurring over the outcropping mineralization (425 to 1211) and gradually decreasing to background levels downstream. For the stream sediments, the Cu response is detectable as far as 3100 metres downstream where concentrations fall to background levels. Water samples show a similar profile, but with higher contrast than the stream sediments; the maximum concentration occurs over the mineralization between 425 and 1211 metres. Downstream from this point, values gradually decrease to detection limit values down to the limit of sampling at 3950 metres. Water clearly has a longer dispersion distance than the stream sediments in these results.

October results are slightly different. Copper concentrations in the stream sediments are marginally higher, with a maximum concentration of about 3400 ppm compared to 2400 ppm in August. The profile has the same smooth downstream attenuation pattern, but with greater contrast than the earlier results. Dispersion distance remains the same. Stream water shows a very different profile from the August results. Elevated values (up to 2500 ppm versus about 1700 ppm in August) occur between 750 and 2460 metres, but drop precipitously downstream from there. The change in profile is explained by an increase in the proportion of (Cu-bearing) ground water input from springs to that of surface runoff which cause a localized increase in Cu concentration. The stream sediment results have a longer dispersion distance in the October, which is the reverse of the August results. The change in dispersion distance in the water samples highlights how water geochemistry may be affected by the time of year when the sampling is done.

Molybdenum (Figure 62) shows a similar pattern to Cu. The August stream sediment results display a smooth downstream attenuation in concentration from a maximum of 39 ppm over the mineralization at 750 metres to inferred background levels of about 7 ppm at 3100 metres. Water results also show decreasing values downstream, but the profile is slightly noisier than that of the stream sediment results. The more erratic values in the water samples could be due to poorer precision at the much lower concentrations in the photometer readings, which have been multiplied by 100 for the August results and by 300 for October (Tables 4 and 5).

October results for the stream sediments are very close to those from August, although the maximum concentration is marginally lower at 34 ppm. Both sets of results show the same dispersion profile along the drainage. The profile for the water samples is smoother in the October results, but the maximum is displaced 461 metres downstream from the August maximum. Concentrations also show a slightly more rapid decrease to background levels.

Nickel results (Figure 63) show different profiles for the photometer and stream sediment results. In both campaigns, the stream sediment results display steadily increasing values downstream, with the highest concentrations (40 ppm and 38 ppm) occurring at the limit of sampling at 3950 metres. This increase parallels the trend of pH values, which rise from slightly acidic (6.8 and 6.6) at the top end of the profile to slightly alkaline (8.1 and 7.8) at the bottom. Thus the increase in Ni concentration in the stream sediments is likely caused by its decreasing solubility at more alkaline pH values.

By contrast, the water results do not show a systematic change in concentration along the profile. Instead, both campaigns define well-constrained Ni responses between 750 and 1211 metres, corresponding with the centre of the mineralized zone. Upstream and downstream values are at the photometer's detection limit. The October profile shows a rapid attenuation of values downstream to background levels; the dispersion distance is very short and does not extend beyond the limits of the subcropping mineralization. The water response is likely reflecting metal input into the stream from groundwater springs.

Calcium (Figure 64) displays gradual increases in concentration downstream in both media and water pH in the August results, but followed by reversal following 2460 metres. The stream sediment profile displays a sudden increase in concentration after 2460 metres. This is likely caused by a change in the bedrock geology from granodiorite to the Jackass Mountain Formation. sedimentary rocks. The change also corresponds with the point where the water pH, which also steadily increases downstream, reaches carbonate stable conditions (i.e. pH 7.5). The water results show a different pattern to the sediments. The reversal in Ca in solution below 2460 metres is consistent with the deposition of  $\text{CaCO}_3$  in the drainage, removing Ca from solution.

Patterns are slightly different in the October results. Stream pH becomes weakly alkaline between 759 and 1211 metres. This increase, which was not present in the August results appears to be caused by additional input of ground water from springs and reduced input from surface runoff. The locally increased pH coincides with a subtle dip in the stream sediment Ca concentration at 1211 metres. The

reason for this is dip is not readily apparent. Water results appear to be unaffected by the pH increase and show similar profiles in both sampling campaigns.

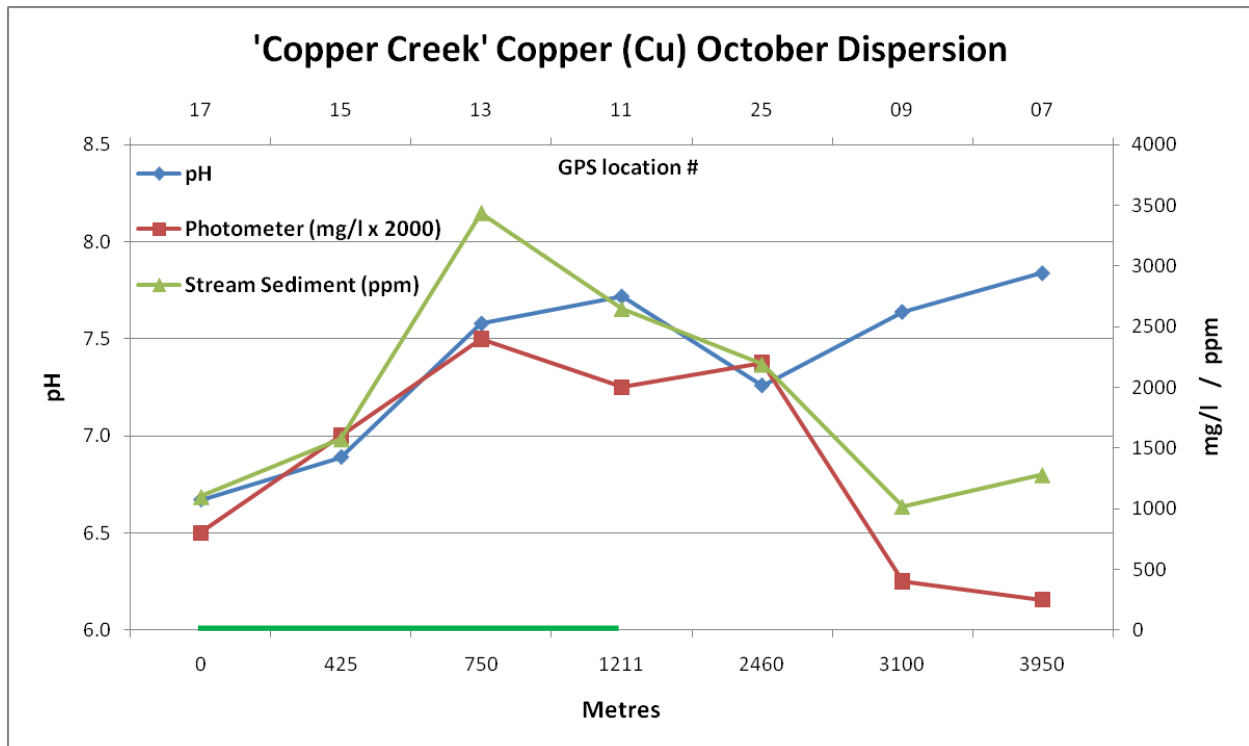
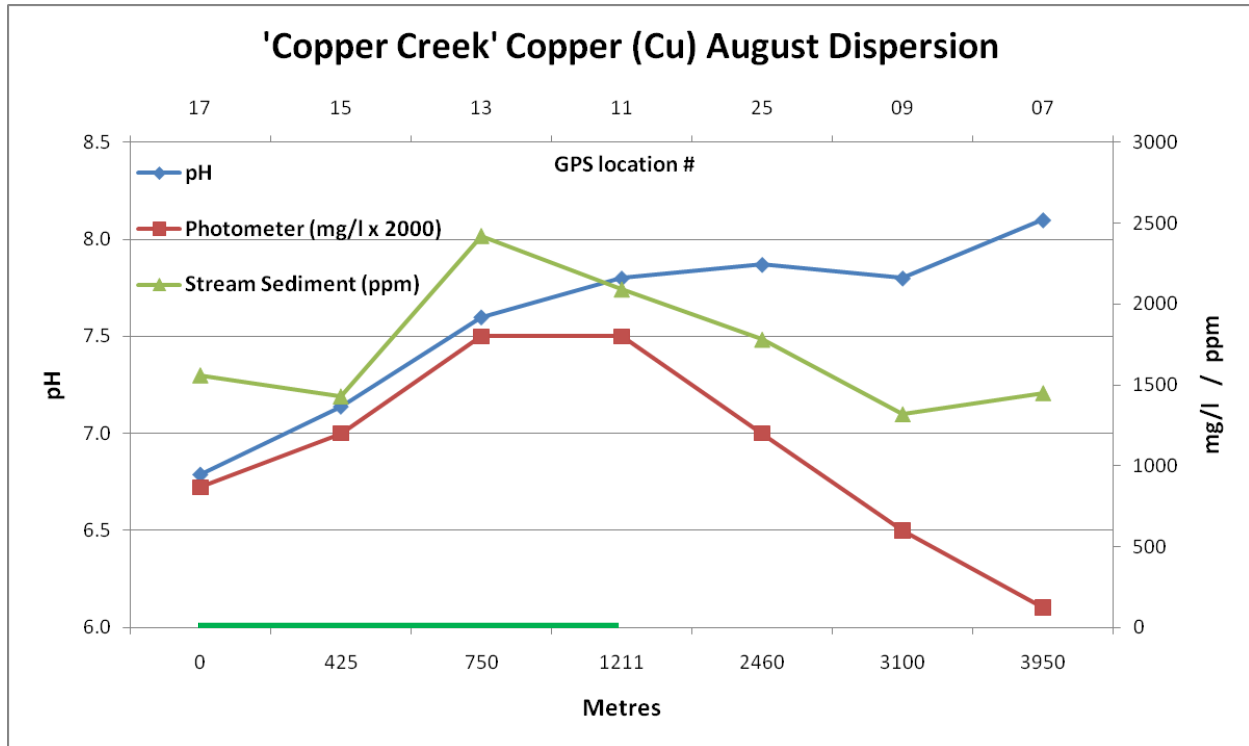


Figure 61. Copper 'Copper Creek' dispersion August (top) and October (bottom). Coloured bar on this and subsequent diagrams indicates the position of the mineralized zone.

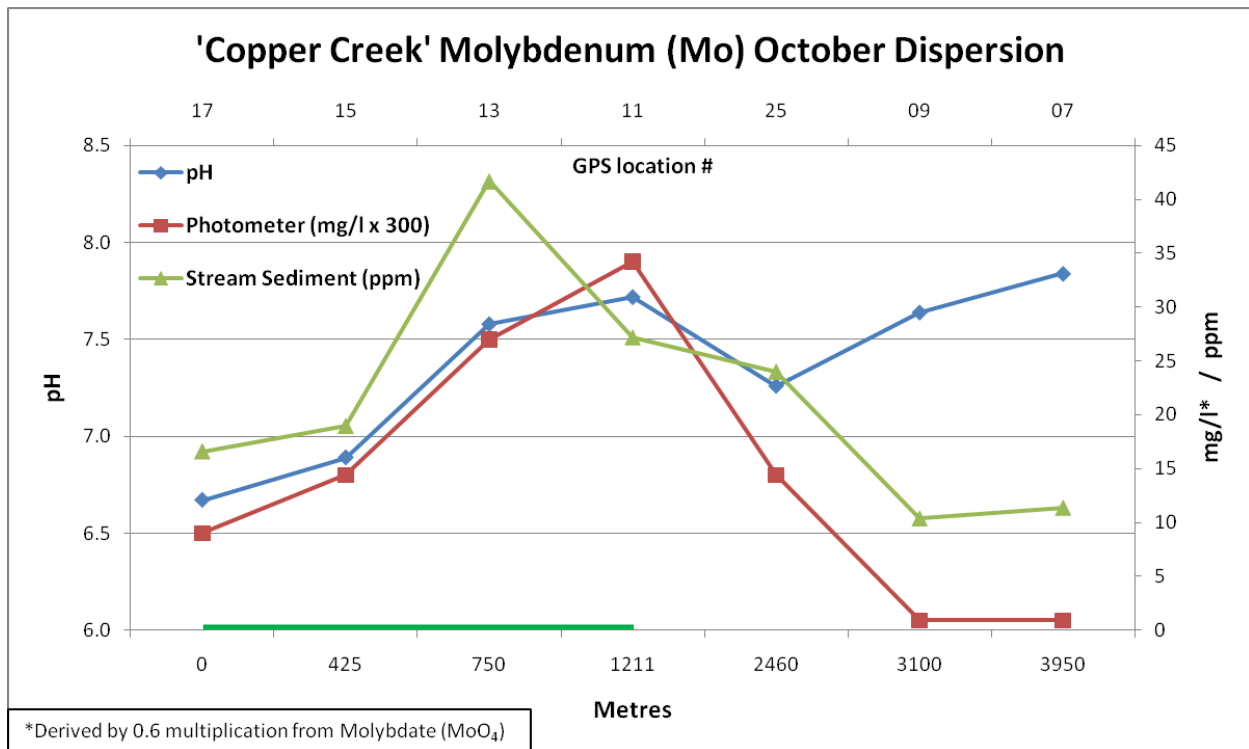
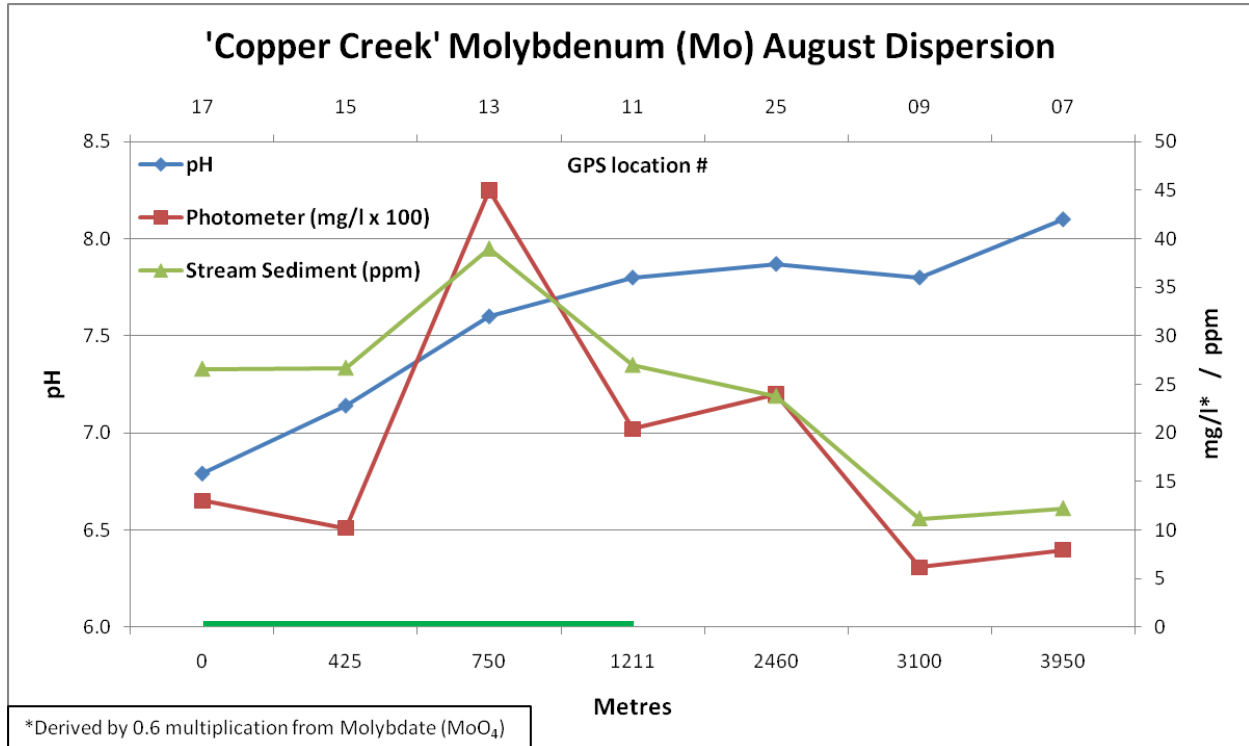


Figure 62. Molybdenum 'Copper Creek' dispersion August (top) and October (bottom).

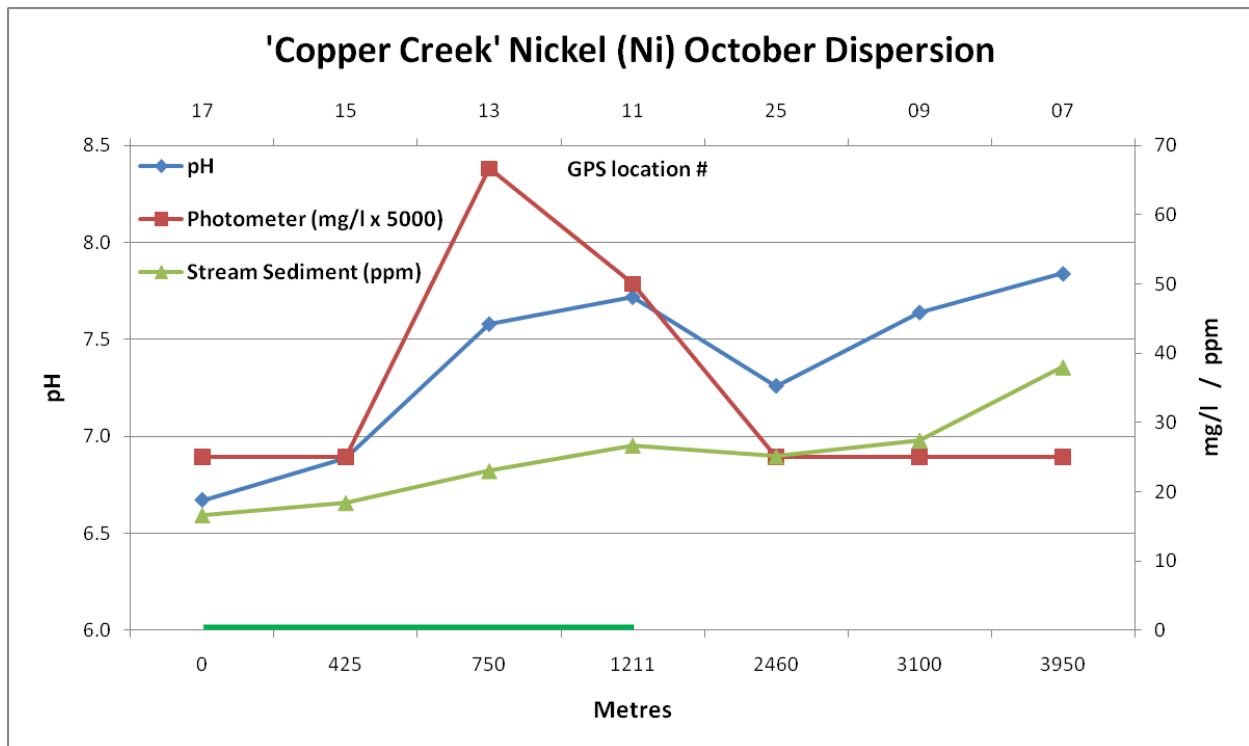
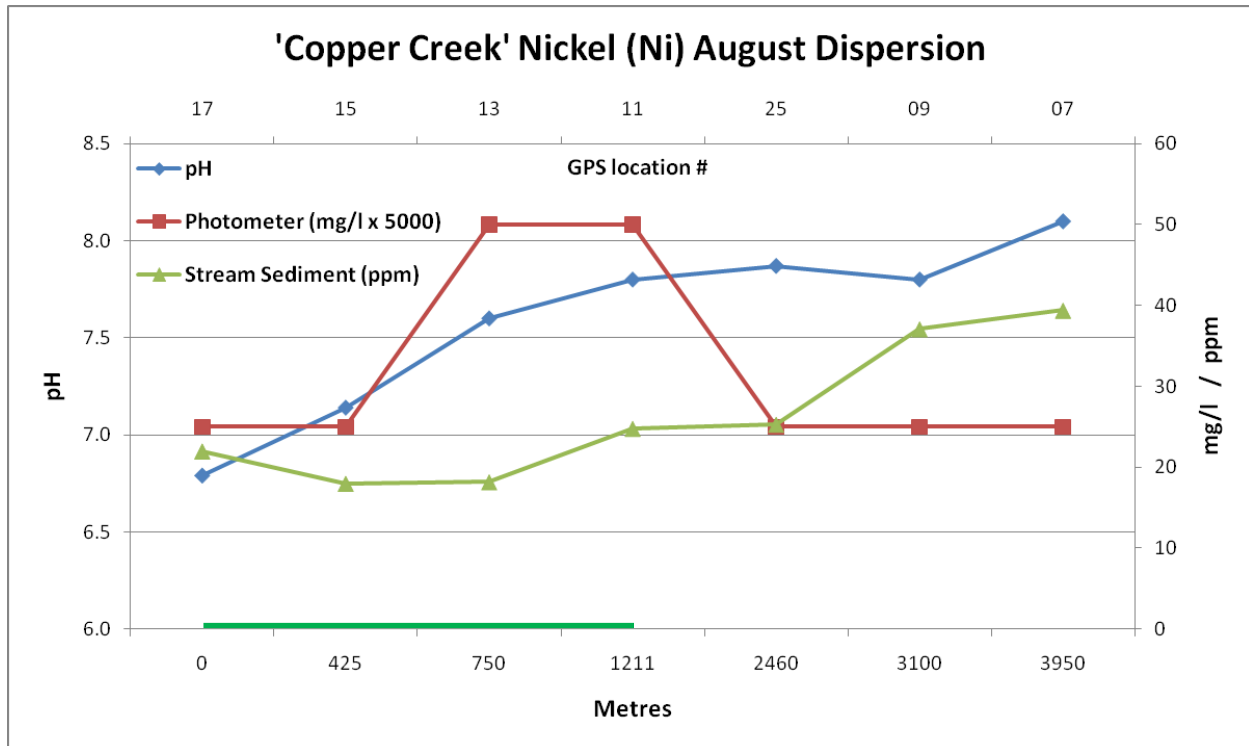


Figure 63. Nickel 'Copper Creek' dispersion August (top) and October (bottom).

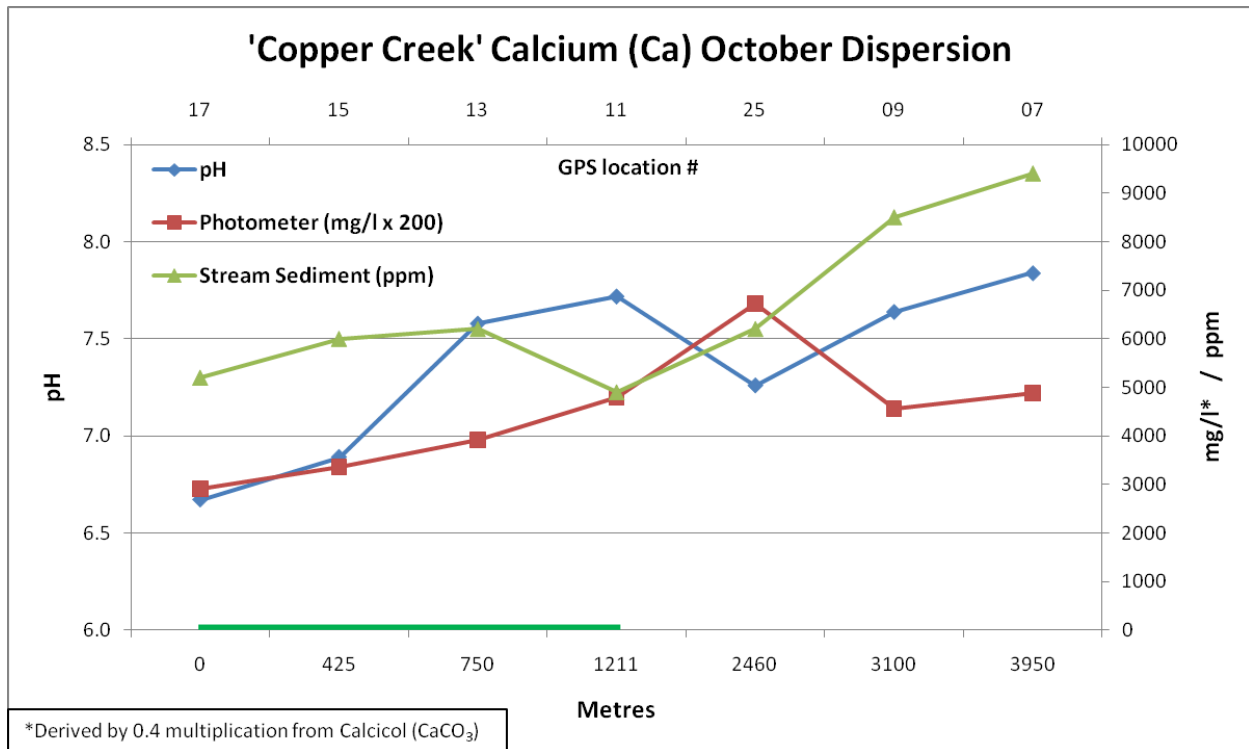
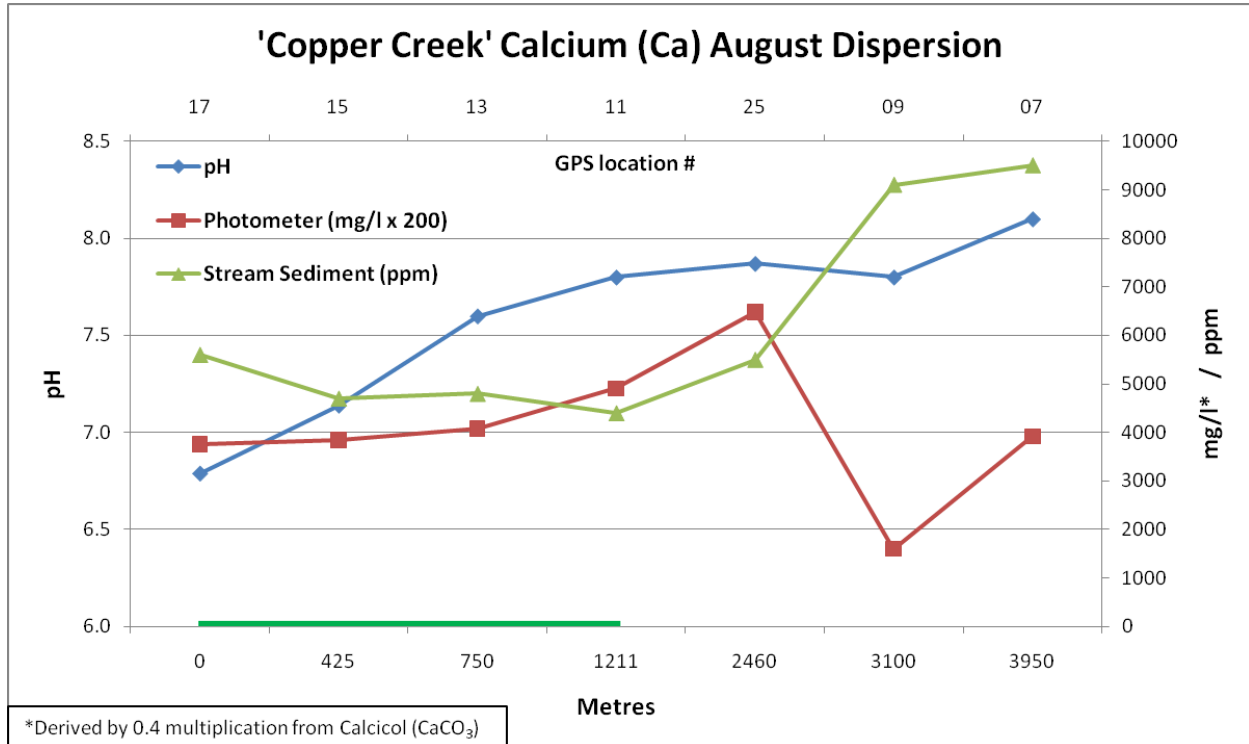


Figure 64. Calcium 'Copper Creek' dispersion August (top) and October (bottom).

## Discussion

Two objectives of this study were to examine the practicality of using a photometer for near real-time field water surveys, and to test the photometer's reliability when compared to traditional stream sediment geochemistry and laboratory water analysis. An added component was to compare stream sediment chemistry with the chemistry of the stream waters. The results presented here show that the photometer can produce rapid and meaningful analyses for some analytes at relatively low cost when compared with conventional laboratory-based methods.

The most attractive aspect of this methodology is its near real-time capability. Analyses can be carried out within a few hours of sample collection, which during an exploration program could allow for rapid identification of priority areas for follow-up. The low detection limits for some analytes provides sufficient contrast that enable detection of geologically meaningful patterns. Another advantage of the photometer is the capability to perform error correction during a survey, with the possibility of returning to sample locations for further examination or re-sampling if a problem occurs.

Unexplained data irregularities are a concern. Inconsistent values encountered between photometer campaigns and with the laboratory analyses may be explained by human error. Discrepancies described earlier could either be caused by sample mix-ups or by sampling errors. In the latter case there is reasonable evidence to indicate that two field duplicate samples might be compromised by disturbance caused whilst collecting the original sample, which could affect results in the second. Such disturbance of the stream bed or spring can cause elevated turbidity (due to the inclusion of suspended particles) that could negatively impact the photometer readings and degrade precision.

Operator errors during analysis are unlikely but could occur since the procedure for measuring a large number of analytes is complicated and precise order and timing is necessary. However, procedures have been designed in such a way as to minimize the possibility of these errors occurring.

Another potential source of error is inconsistencies in the test reagents (Table 6). While the manufacturer produces a high quality product, differences were noted in the performance of individual tests. When suspect results were identified by the quality control procedures, the tests were repeated with fresh reagents. Routine use of triplicate readings was also helpful in identifying potential inconsistencies in the reagents.

An important outcome of this study is the observation of systematic differences or biases between the photometer readings and laboratory analyses. These differences were particularly notable for B, Al, Mo, Fe and Mn. For B, the laboratory analyses failed to detect meaningful concentrations when the photometer results did so. The same was true for Mo. The lack of a response for the latter in the laboratory analysis is somewhat of a mystery. Investigations carried out by the laboratory did not reveal any procedural or calibration errors to explain it. We are therefore left with the unsatisfactory conclusion that Mo was lost from the solution despite the use of nitric acid preservation for those samples. In the case of Al, the photometer failed to detect the low concentrations reported by the laboratory, suggesting that either the real detection limit for the test is higher than reported by Palintest

or that there are interferences in play that have not been identified or corrected for. Again, this is an unsatisfactory result.

Low biases in the photometer results for Cu, Fe and Mn are likely attributable to the decision not to acidify the photometer samples. The original premise that acidification and filtration would not be needed because the time between sample collection and analysis is short (within 48 hours) is somewhat supported by the results. It appears that appreciable metal loss (up to 80% for Fe and 20% for Cu) through adsorption and hydroxide precipitation does occur before photometer analysis, which undoubtedly has a negative impact on the sensitivity and contrast of the results. Experimentation with acidification of the photometer samples in the field is necessary to quantify the magnitude of the metal loss and to determine whether this step should be included in future surveys.

Based on the results and issues described above, modification of the methodology needs to be considered. Experimentation is needed to evaluate the benefits of acidification of the photometer samples at the collection site. Improved methodologies for the photometer readings are also needed in order to reduce the risk of operator error. One obvious improvement is to analyze a smaller suite of analytes. This study, as a proof of concept project, included the maximum number of analytes that the instrument is capable of reading. As a result the procedure for reading each sample was overly complex and potentially error-prone. A smaller suite of relevant analytes per operator would reduce the risk of human error and improve turnaround time on a real exploration program, thus accelerating the process and lowering the cost per sample.

### **Comparison of Photometer and Stream Sediment Results**

This study shows that water and stream sediment geochemistry can produce comparable results. What is not known is how the two media would respond at different times of the year and from year to year. This study found that the results were, for the most part, comparable between late summer and autumn, but more information is needed to assess the differences over longer periods of time (for instance between spring and autumn, when stream flows are at their maximum and minimum).

Another potential advantage of water sampling over stream sediment geochemistry is the detection of non-outcropping mineralization. Analysis of emergent ground waters from springs and seeps could detect mineralization that has interacted with the groundwater on its way to the surface. This study shows that when stream levels are low, spring waters produce generally higher contrast responses than the stream sediments for some elements. One drawback is that dispersion distances in waters appear to be shorter than those of stream sediments when water levels are low. More work is needed to better understand how the metal input from seeps and springs changes over the course of the year.

One lesson learned from this study is that it is not necessary to analyze all of the available analytes. Future studies should be carefully designed to include only the relevant analytes (i.e., those that have signals derived from the target mineralization). This will reduce costs, speed up turnaround time, and reduce the potential for errors. Moreover photometer analysis should always be accompanied by field

measurements of water pH, electrical conductivity, TDS and temperature; these are all parameters that help to establish the chemical environment of the stream and thus aid interpretation.

Some tests revealed interesting results for the project area. Copper, Fe, and Mo correlate well with the mineralized zone in 'Copper Creek', but do not show downstream water dispersion along Poisonmount Creek. Molybdenum displays some correlation with its stream sediment equivalent on the northeast flank of Poison Mountain, and to the west along Poisonmount Creek. Some elements, such as Al, Ca, Mg and Ni, display a clear inverse relationship with the mineralized zone, with lower values occurring over the mineralization and increasing downstream.

Boron had completely different results in water and stream sediments. The stream sediment analysis produced only two samples above the detection limit, while the water results revealed a robust pattern. This observation can be explained by the relative insolubility of B bearing minerals in an aqua regia digestion. Another issue may be the higher instrument detection limit for B by aqua regia-ICPMS (10 ppm).

### **Cost per sample**

There are various analytical options for water samples. The most expensive option (>\$200 per sample) would be an environmental laboratory that provides a full suite of cations, anions as well additional parameters such as pH, turbidity, TDS, and conductivity. A slightly less expensive option (\$40-\$50) would be the hydrogeochemical packages offered by some minerals laboratories. These provide high resolution ICP-MS analyses for up to 70 elements to very low detection limits but normally do not include anions or additional the parameters. The photometer is a third option, which is a compromise between speed and cost (~\$30 per sample) and a more limited selection of analytes.

### **Turnaround Time**

Although this is a relatively a small study it has provided a good baseline for comparisons of laboratory turnaround times with the photometer method. Figure 65 shows the turnaround time for each method based on the number of days needed to obtain the final result. Turnaround time for the photometer was less than five days for each campaign, compared to 14 and 22 days for laboratory water analysis. The turnaround time for stream sediment analysis was marginally better, at 17 and 8 days respectively. The photometer thus offers a clear time advantage over a commercial laboratory. This would be a bigger advantage in a larger sampling program, since results could be plotted and interpreted on an ongoing basis thus allowing for more rapid identification and follow up of anomalies.

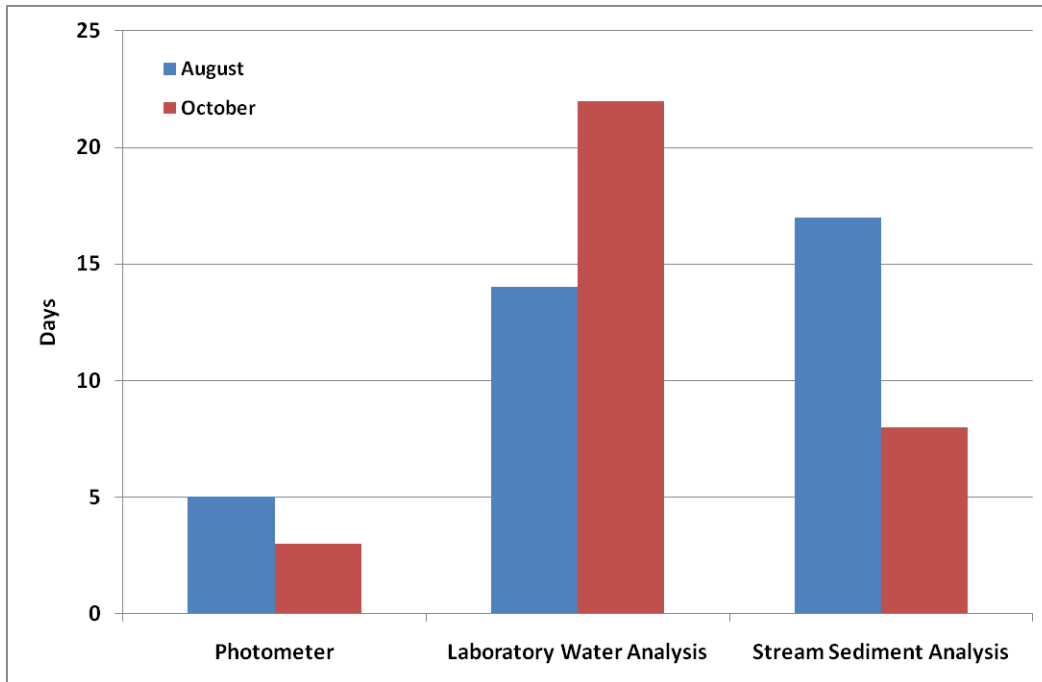


Figure 65. Sample analysis turnaround times. Photometer analysis was performed by single operator in August and two in October

### All in Cost per Analysis

Labour cost for photometer analysis was \$31.25/sample, although this could vary or be considerably lower, depending on size of survey, size of crew etc., type of survey, sample density, ease of access, etc. A breakdown of costs is shown in Table 9.

Table 9. Summary of cost per sample.

Type	Photometer cost per sample	ALS Environmental cost per sample	ALS Minerals cost per sample
Reagents	\$13.14		
Analysis	\$31.25		
Environmental disposal	\$2.08		
Shipping		\$1.89 <sup>1</sup>	\$2.39 <sup>1</sup>
<b>Total</b>	<b>\$46.47</b>	<b>\$196.09</b>	<b>\$28.41</b>

<sup>1</sup>Based on Canada Post Regular Parcel (3 business days) pricing.

## Conclusions

This study shows that a field-portable photometer can be an effective tool for obtaining rapid and low cost measurements of a relatively small selection of cations and anions in surface waters. The tested instrument was found to have acceptable accuracy and precision and results for most analytes compared well with laboratory water analyses. Photometer results compare favourably with stream sediment results from the same localities, but water responses show less downstream dispersion for cations than the stream sediments, particularly in the October results. Results also show that the photometer can provide water analyses at a lower cost and faster turnaround time than a commercial laboratory, albeit with a smaller analyte suite.

## Recommendations

Although this study has successfully addressed many of the questions it set out to investigate, some unanswered points and new questions have been highlighted. The following recommendations are designed to investigate these points:

- Repeat the study in the spring to obtain results from the period of maximum water flow.
- Investigate and test other devices that have come on the market since development of the Palintest 8000. Some new instruments provide a larger range of analytes and have lower detection limits than the Palintest 8000.
- Investigate the benefits of sample preservation and filtering.
- Consider the application of photometer water analysis in a regional exploration context. This could include sampling of NTS map sheet at a similar density to RGS surveys.
- Perform the same type of study around a known mineralization or in a covered environment.
- Test the method on other styles of mineralization (e.g., carbonate hosted Pb-Zn).
- Analysis of partial extraction analysis from stream sediment, soil and crushed rock samples using the photometer.

## Acknowledgments

The authors would like to thank Geoscience BC for funding this study. Special thanks to Peter Bradshaw and Craig Hart for initial concept support. Thanks to Peter Bradshaw, Ray Lett, and Colin Dun for peer review, and Chris Pearson for edits. The lead author would also like to thank Sarah Hashmi for field assistance and advice, and Dean Watts at ALS Environmental for excellent customer support.

## References

- Brown, R. (1995): Poison Mountain porphyry copper-gold-molybdenum deposit, south-central British Columbia; *in* *Porphyry Deposits of the Northwestern Cordillera of North America*, T.G. Schroeter (ed.), Canadian Institute of Mining, Metallurgy and Petroleum, Special Volume 46, pt. B, Paper 20, p. 343–351.
- Hall, G. E.M. (1998): Relative contamination levels observed in different types of bottles used to collect water samples: *Explore*, No. 101, p. 1-7
- Lett, R.E., Sibbick, S. and Runnells, J. (1998): Regional stream water geochemistry of the Adams Lake – North Barriere Lake Area, British Columbia (NTS 82M/4 and 82M/5); BC Ministry of Energy and Mines, BC Geological Survey, Open File 1998-9, 238 p.
- Leybourne, M.I. and Cameron, E.M. (2010): Groundwater in geochemical exploration: *Geochemistry: Exploration, Environment, Analysis*, v. 10, p. 99-118.
- Massey, N.W.D., MacIntyre, D.G., Desjardins, P.J. and Cooney, R.T. (2005): Digital Geology Map of British Columbia: Whole Province; British Columbia Ministry of Energy and Mines, GeoFile 2005-1.
- Raven, W. (1994): Assessment report of diamond drilling and soil geochemistry, Poison Mountain Project, for Bethlehem Resources Corp.; BC Ministry of Energy and Mines, Assessment Report 23243, p. 238, URL <<http://aris.empr.gov.bc.ca/ArisReports/23243.PDF/>> [September 2014].
- Seraphim, R.H. and Rainboth, W. (1976): Poison Mountain; *in* *Porphyry Deposits of the Canadian Cordillera*, A. Sutherland Brown (ed.), Canadian Institute of Mining, Metallurgy and Petroleum, Special Volume 15, pt. B, Paper 22, p. 323–328.
- Taufen, P.M. (1997): Ground waters and surface waters in exploration geochemical surveys; *in* *Proceedings of Exploration 97: Fourth Decennial International Conference on Mineral Exploration*, A. Gubins (ed.), Prospectors and Developers Association of Canada, Toronto, Canada, p. 271–284.
- Yehia, R., Vigouroux, N. and Hickson, C. (2013): Use of a portable photometer for accelerated exploration: testing for geothermal indicators in surface waters; *GRC Transactions*, v. 37, p. 375–381.
- Yehia, R. (2014): Final project report; MYAR Enterprises Inc., unpublished report for Industrial Research Assistance Program, National Research Council, 57 p.
- Zehner, R.E., Coolbaugh, M.F. and Shevenell, L. (2006): Regional ground water geochemical trends in the Great Basin: implications for geothermal exploration; *GRC Transactions*, v. 30, p. 117–124.

Appendix A – Dispersion Analysis Continued

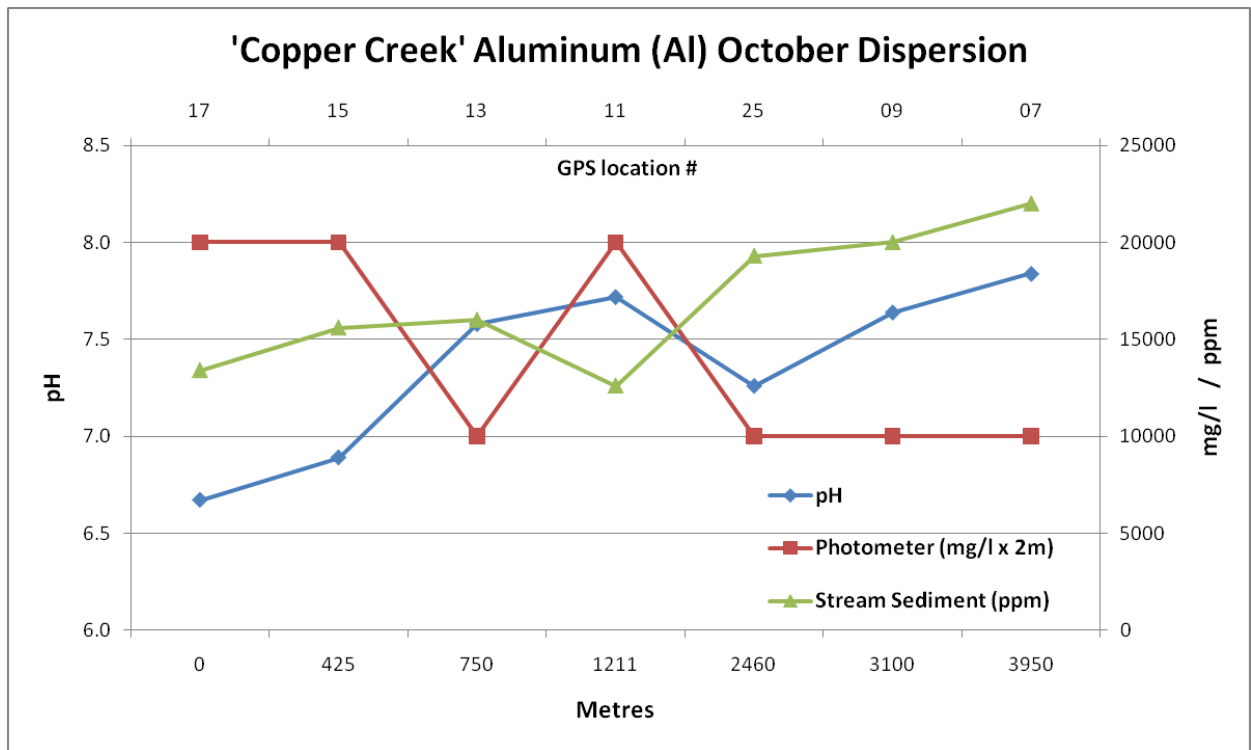
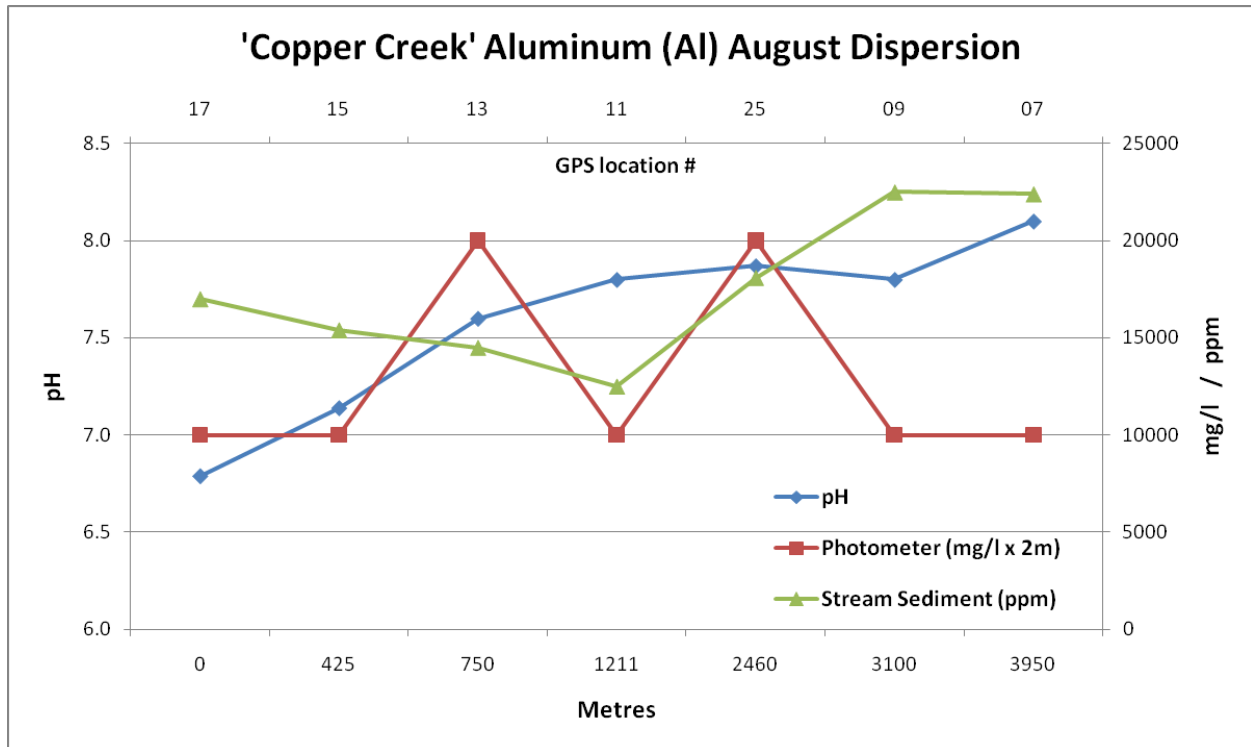


Figure 66. Aluminum 'Copper Creek' dispersion August (top) and October (bottom).

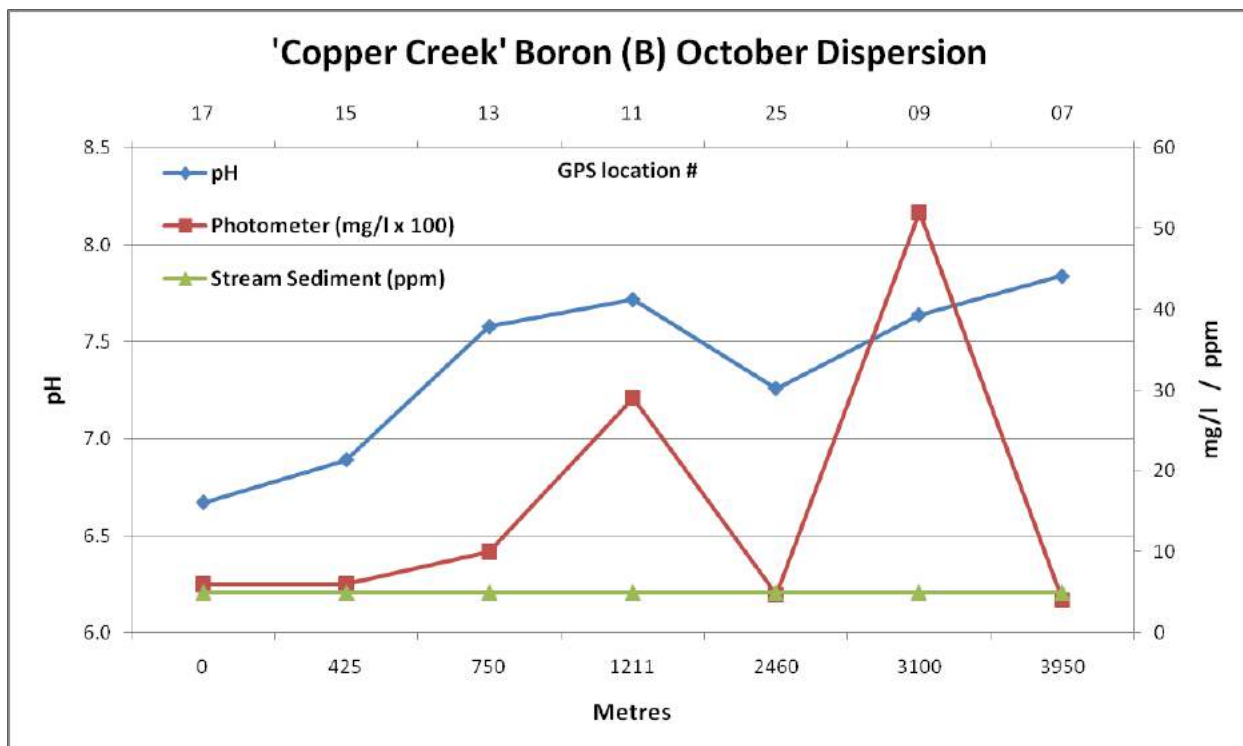
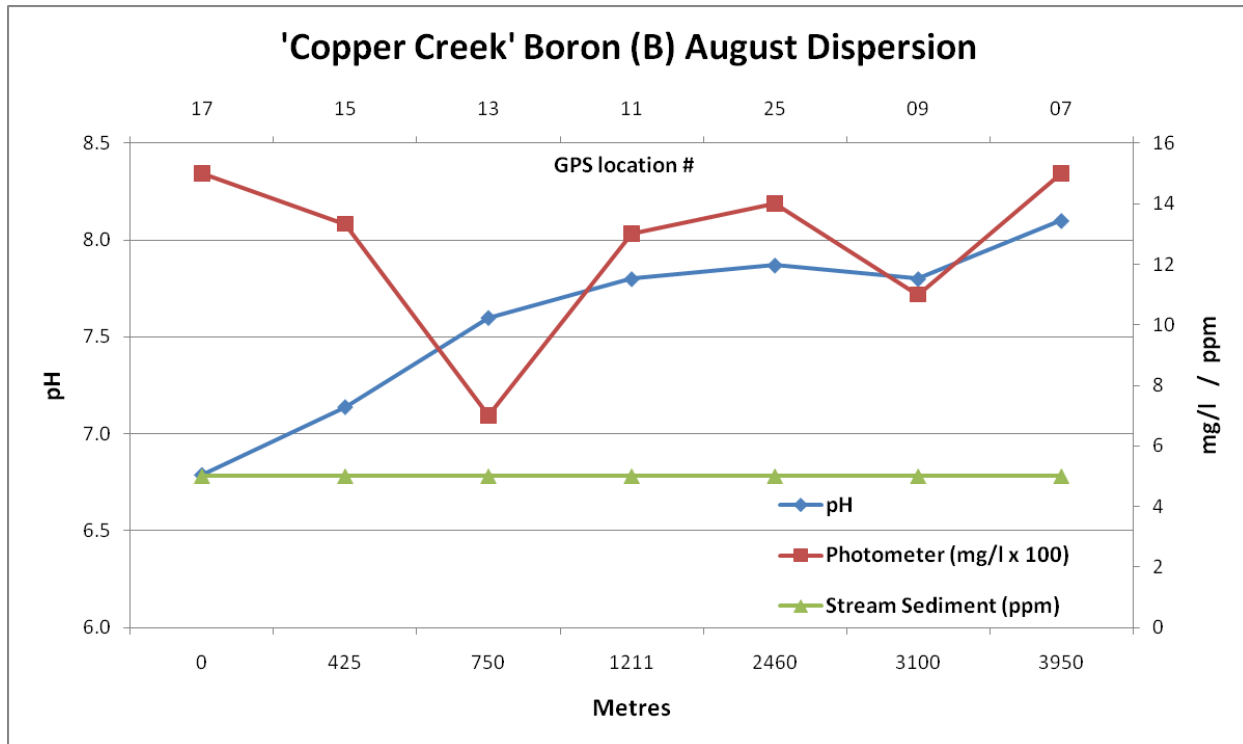


Figure 67. Boron 'Copper Creek' dispersion August (top) and October (bottom).

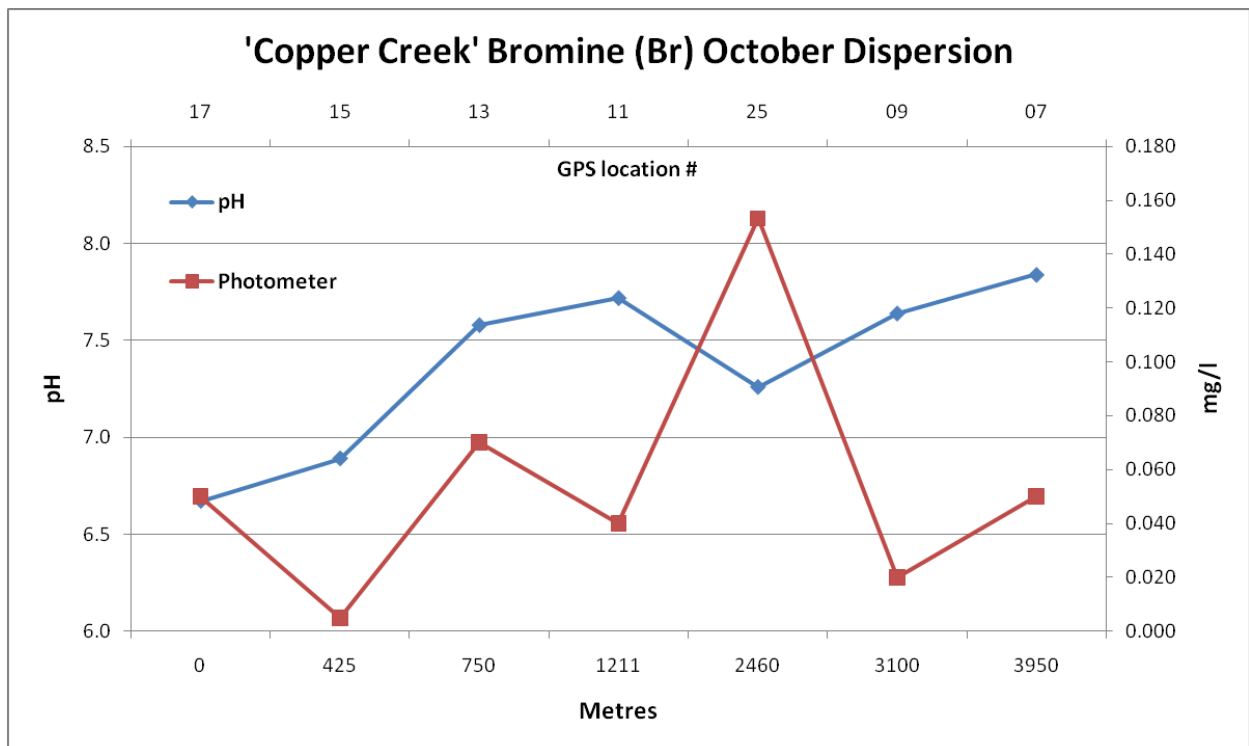
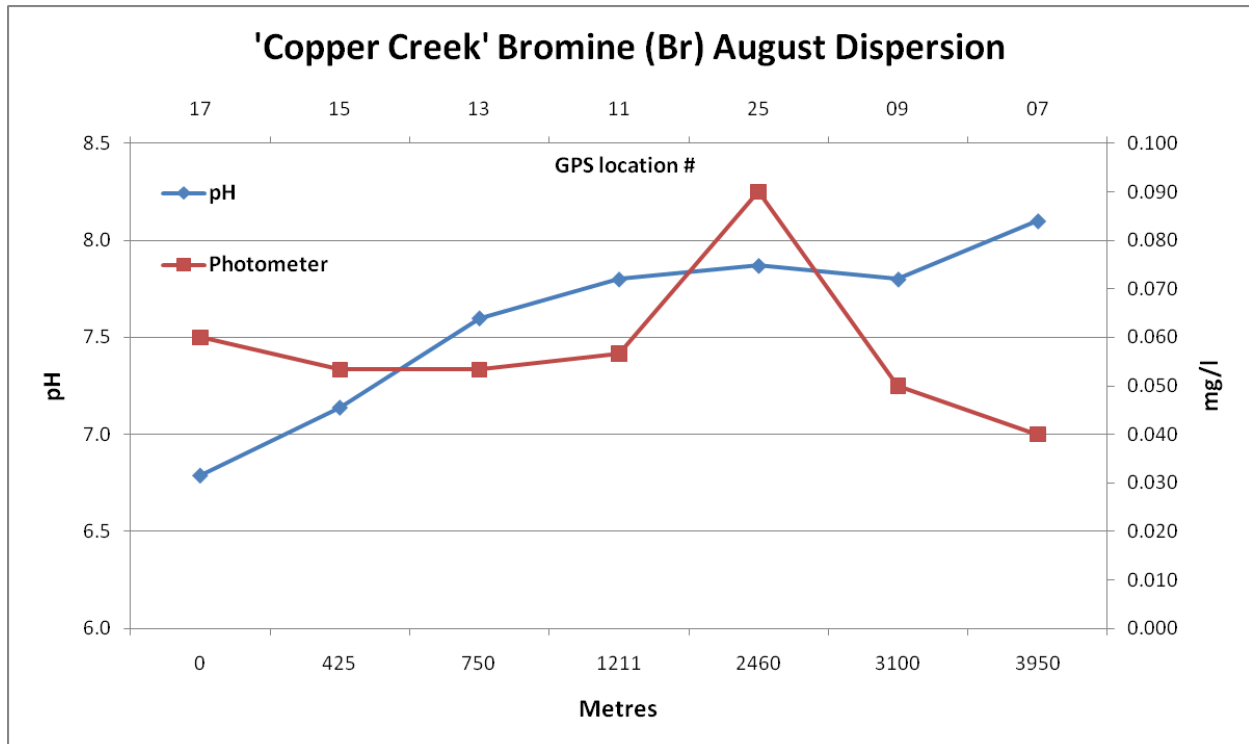


Figure 68. Bromine 'Copper Creek' dispersion August (top) and October (bottom).

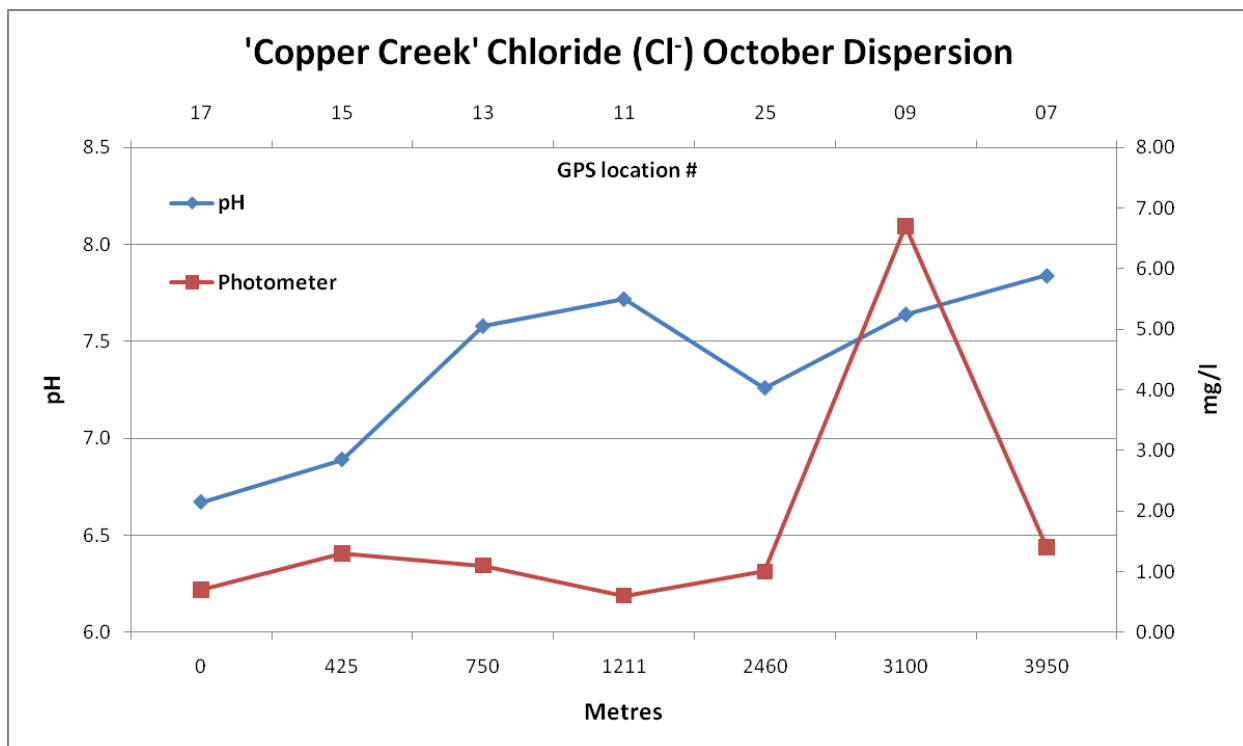
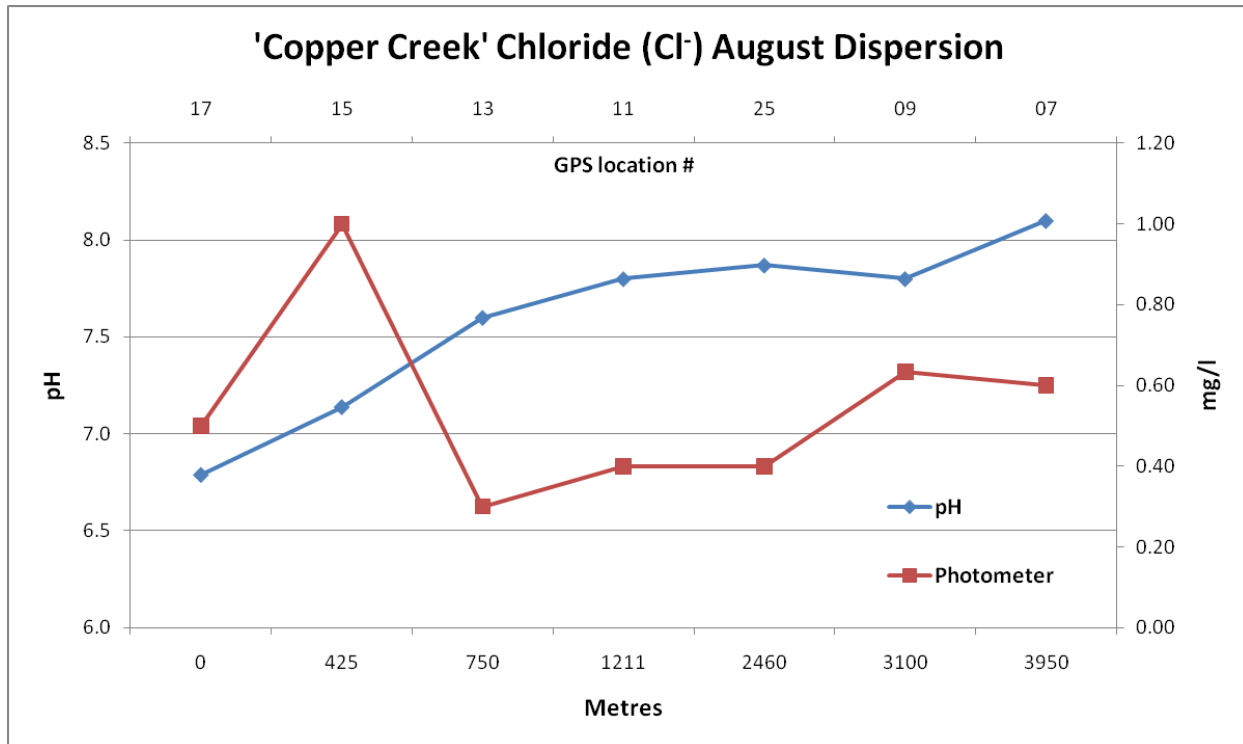


Figure 69. Chloride 'Copper Creek' dispersion August (top) and October (bottom).

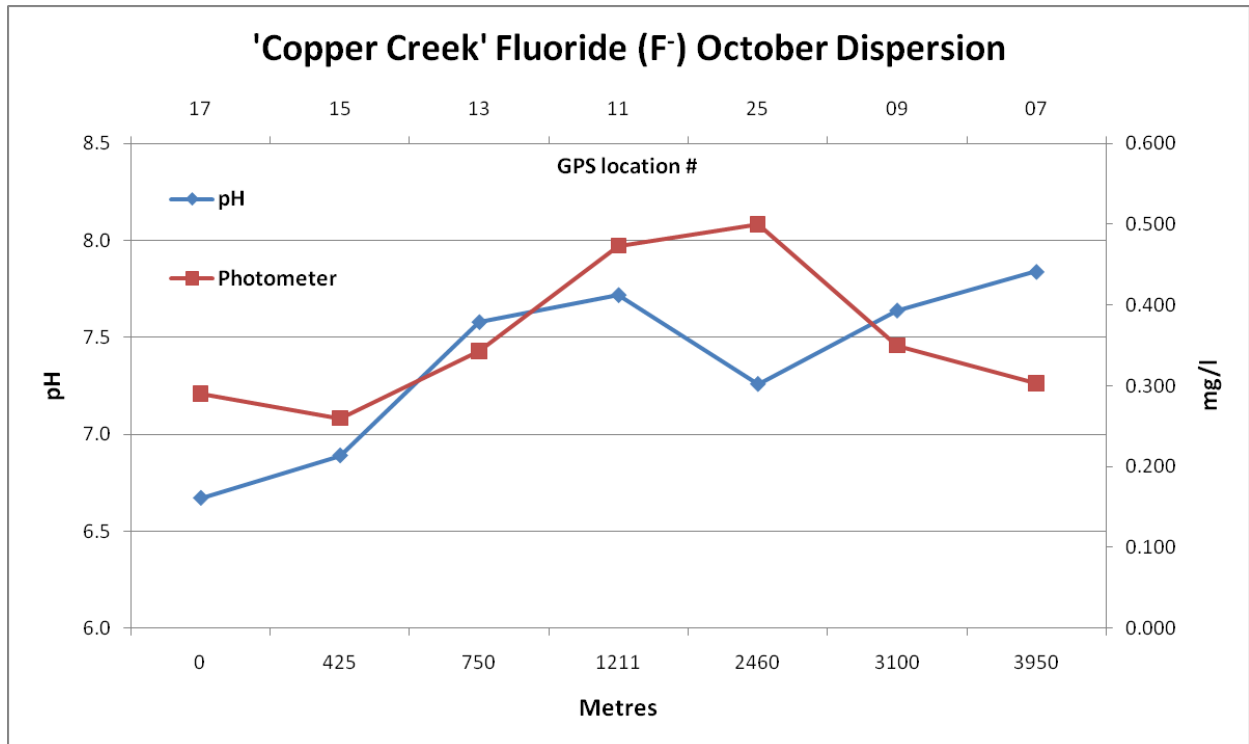
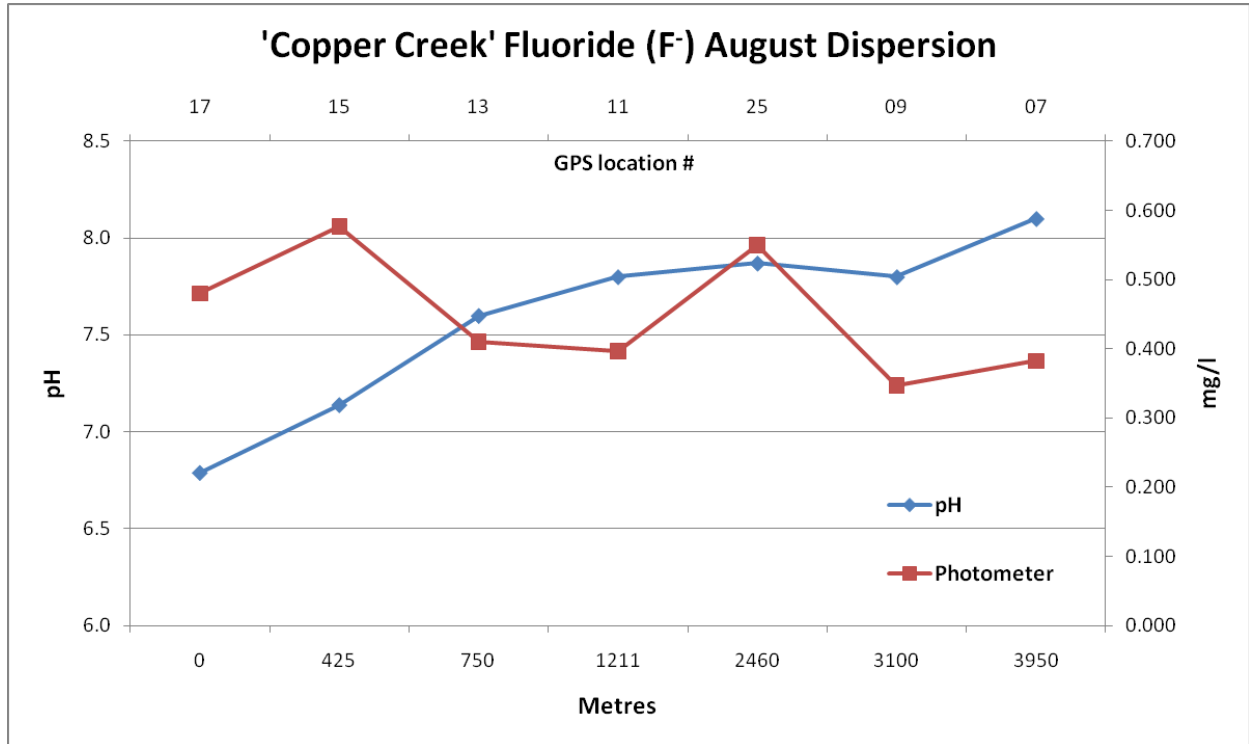


Figure 70. Fluoride 'Copper Creek' dispersion August (top) and October (bottom).

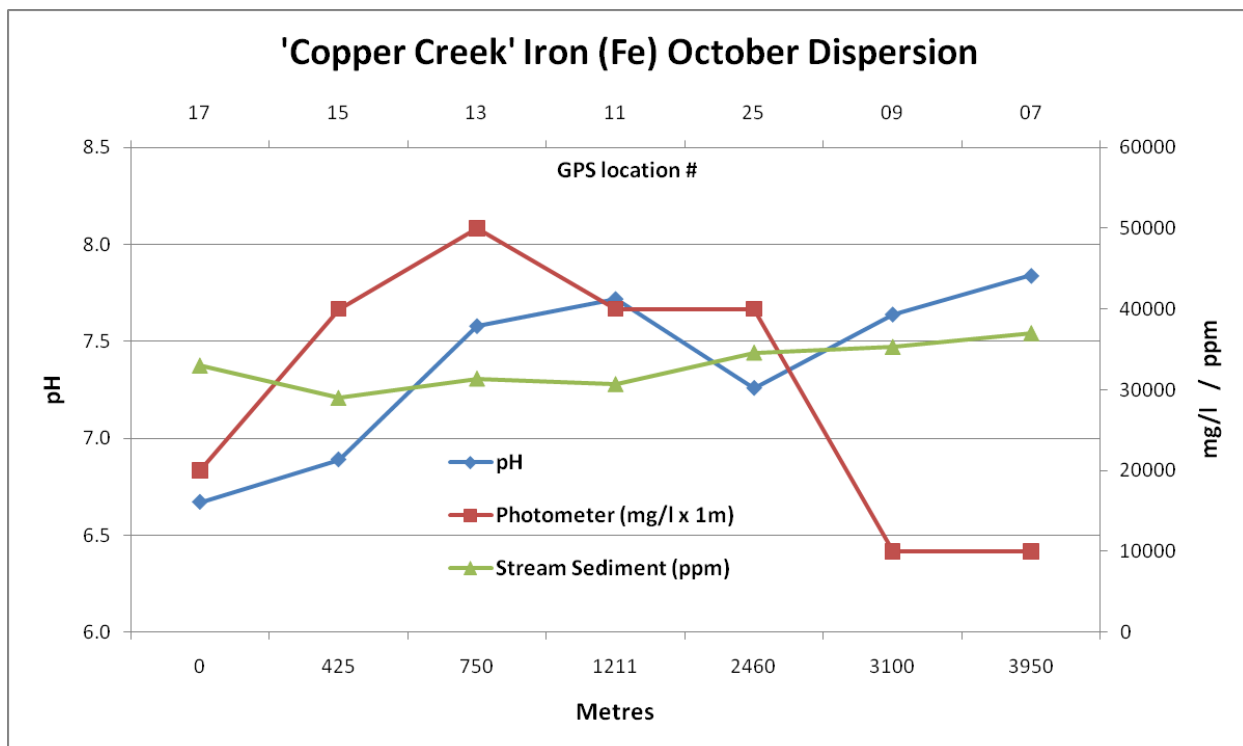
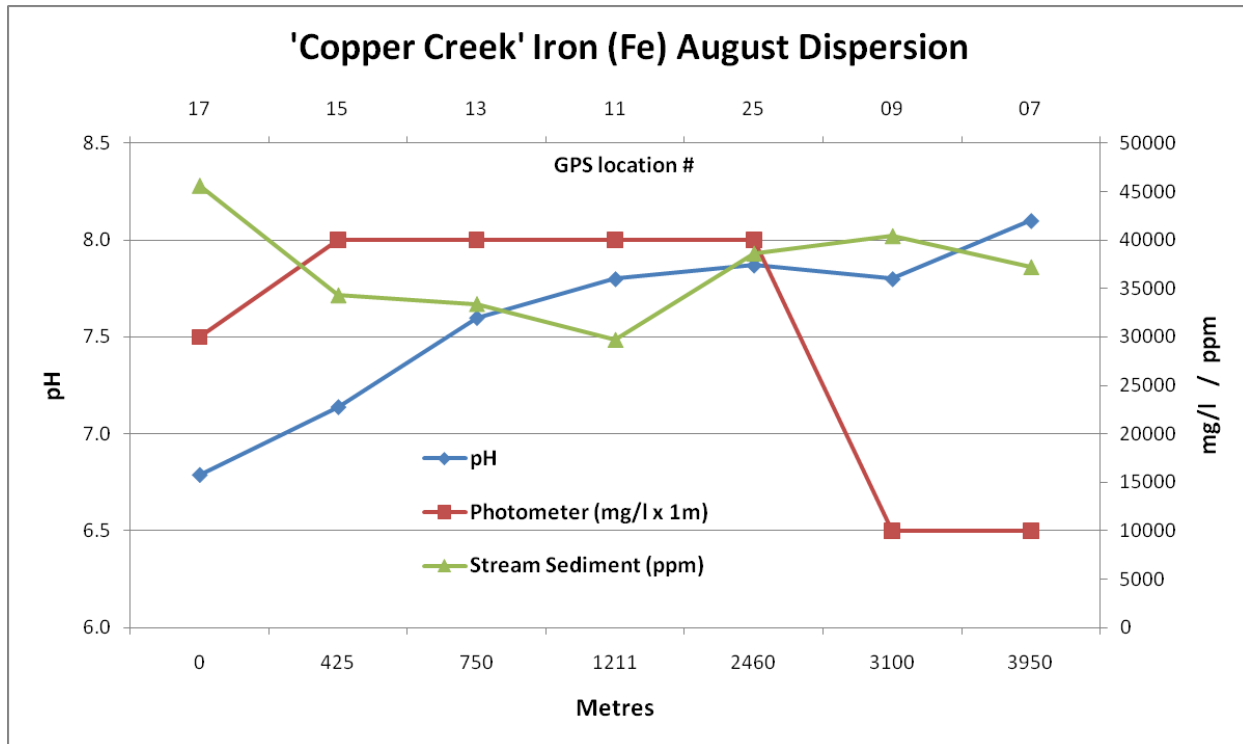


Figure 71. Iron 'Copper Creek' dispersion August (top) and October (bottom).

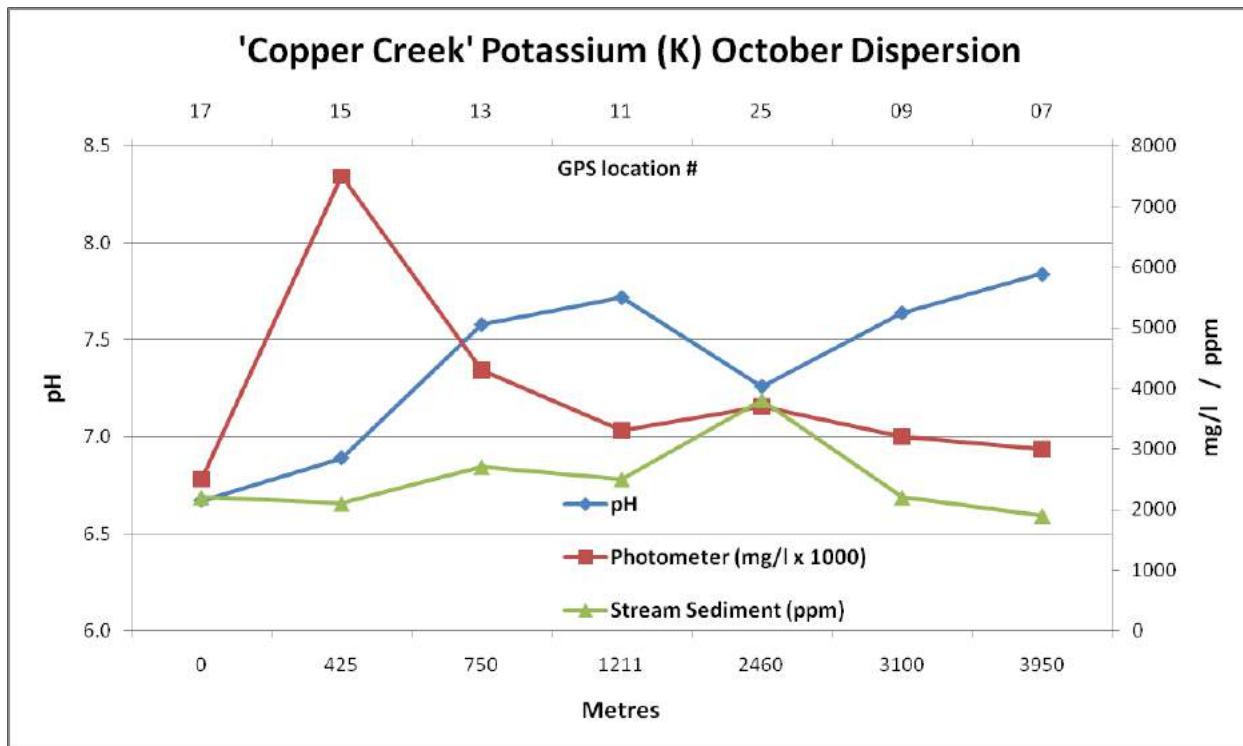
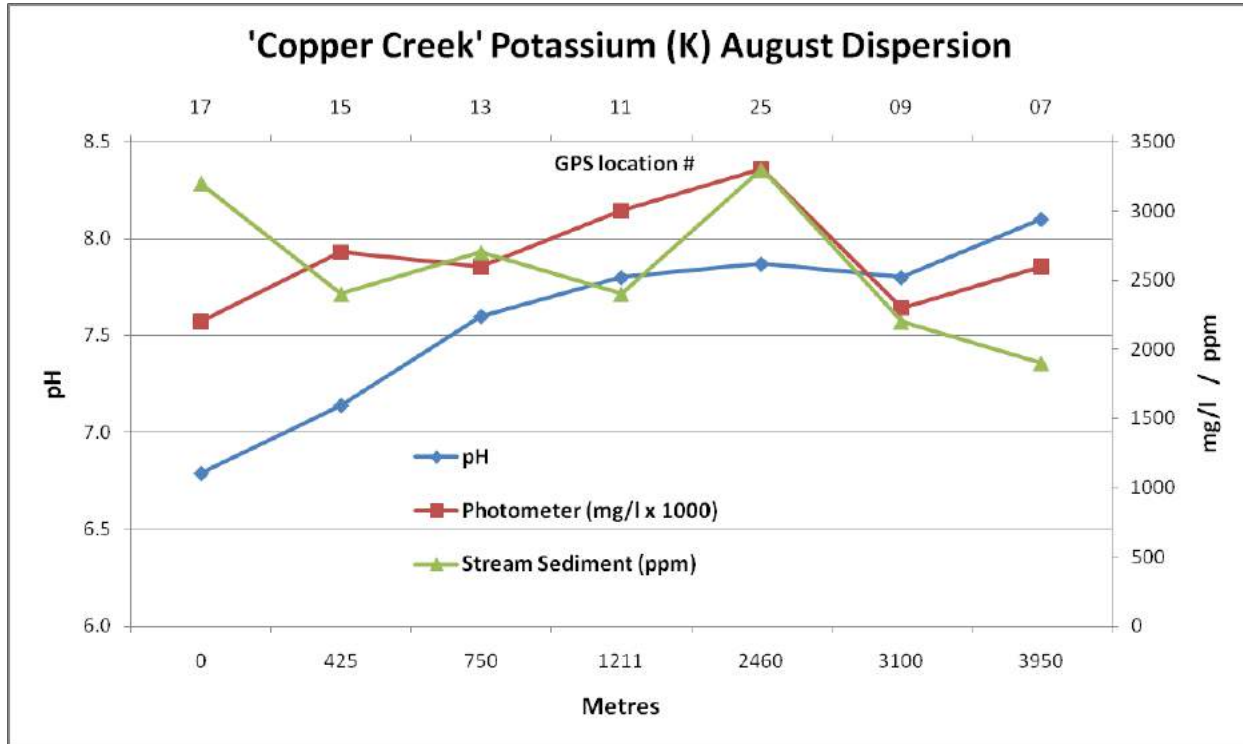


Figure 72. Potassium 'Copper Creek' dispersion August (top) and October (bottom).

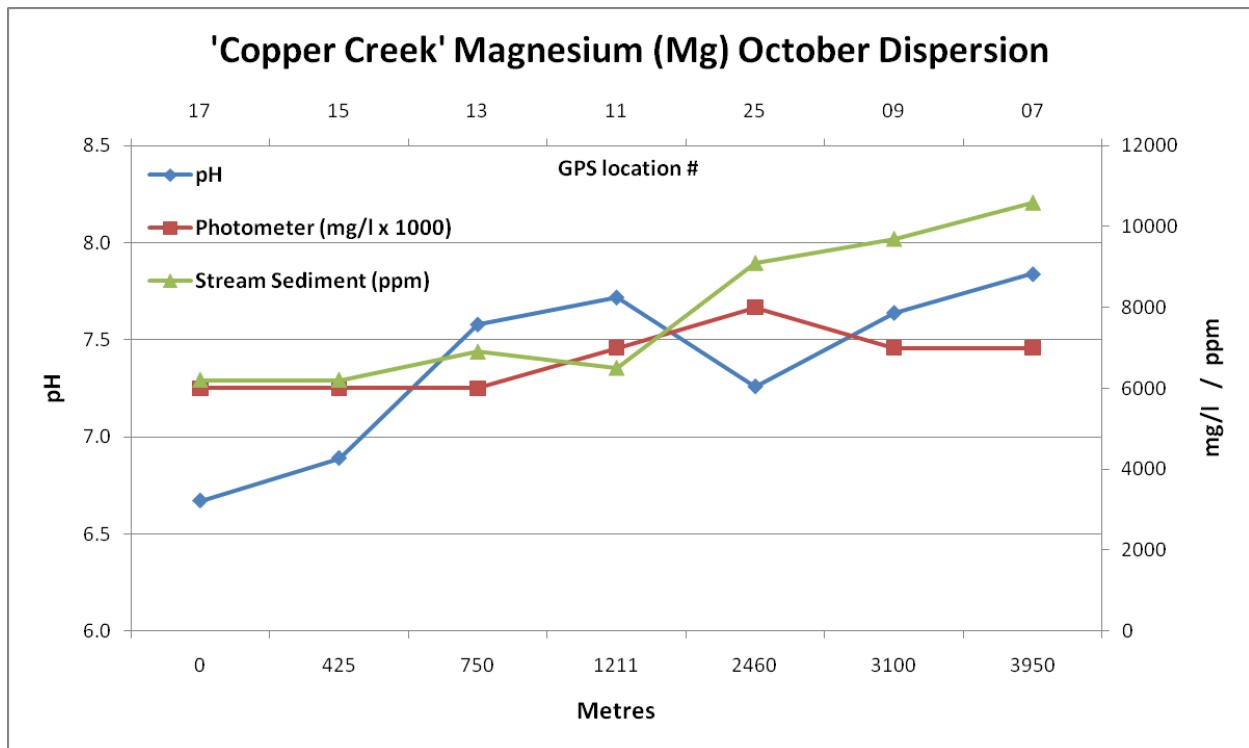
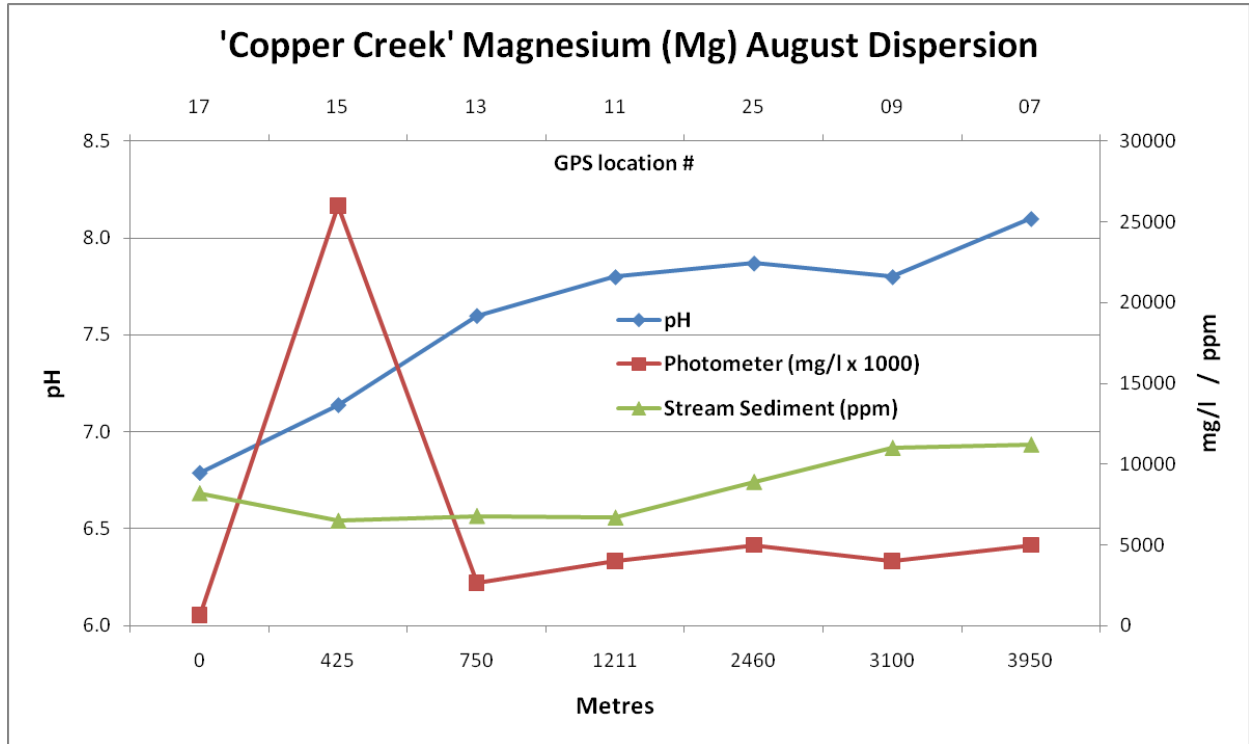


Figure 73. Magnesium 'Copper Creek' dispersion August (top) and October (bottom).

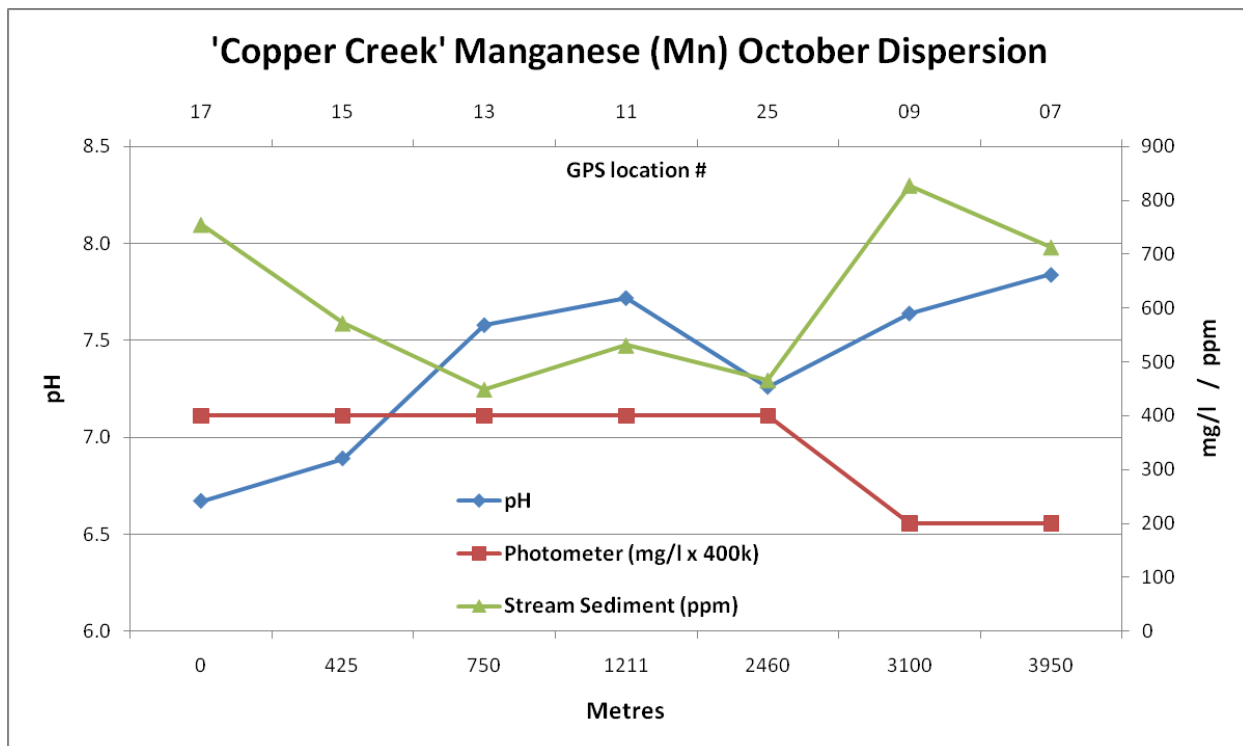
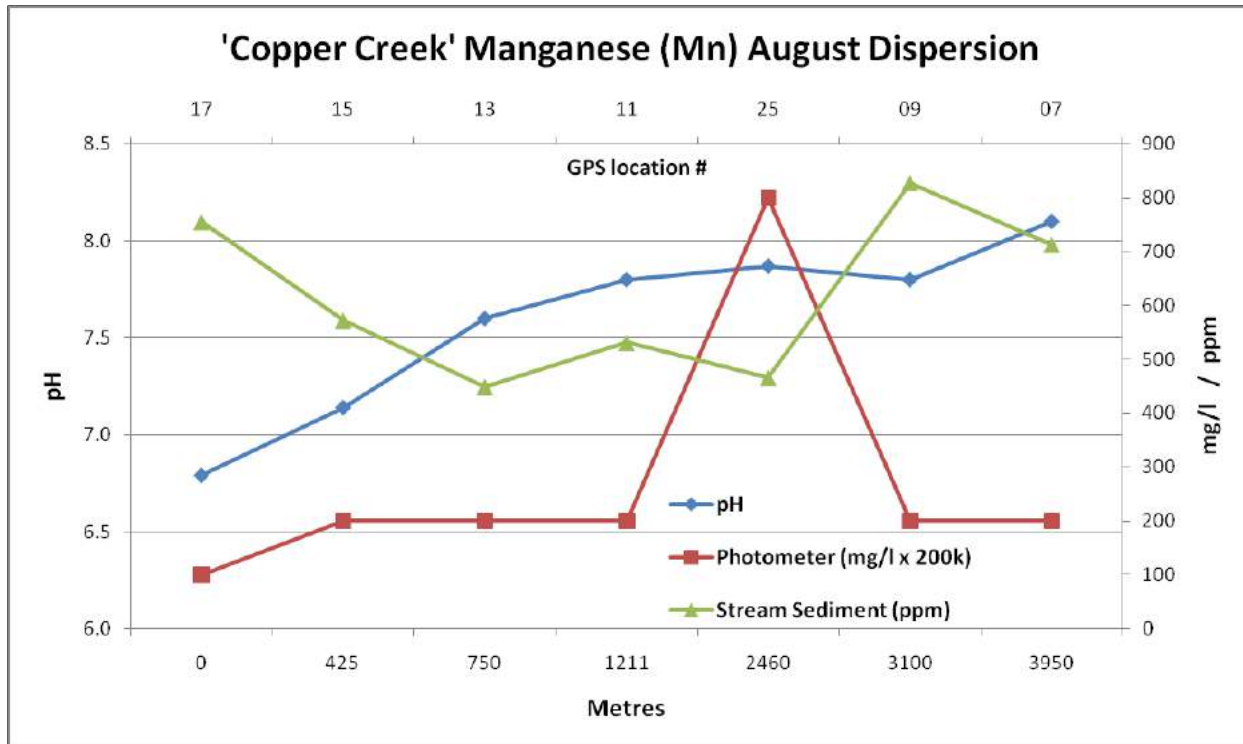


Figure 74. Manganese 'Copper Creek' dispersion August (top) and October (bottom).

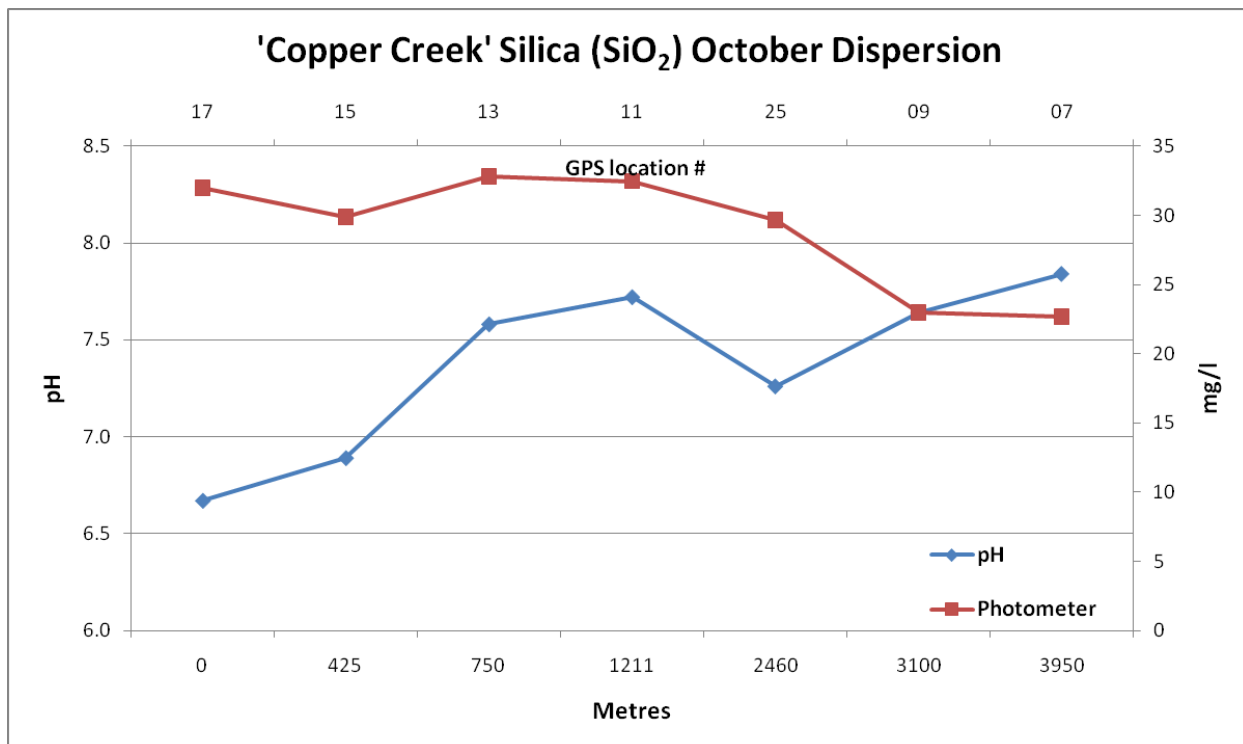
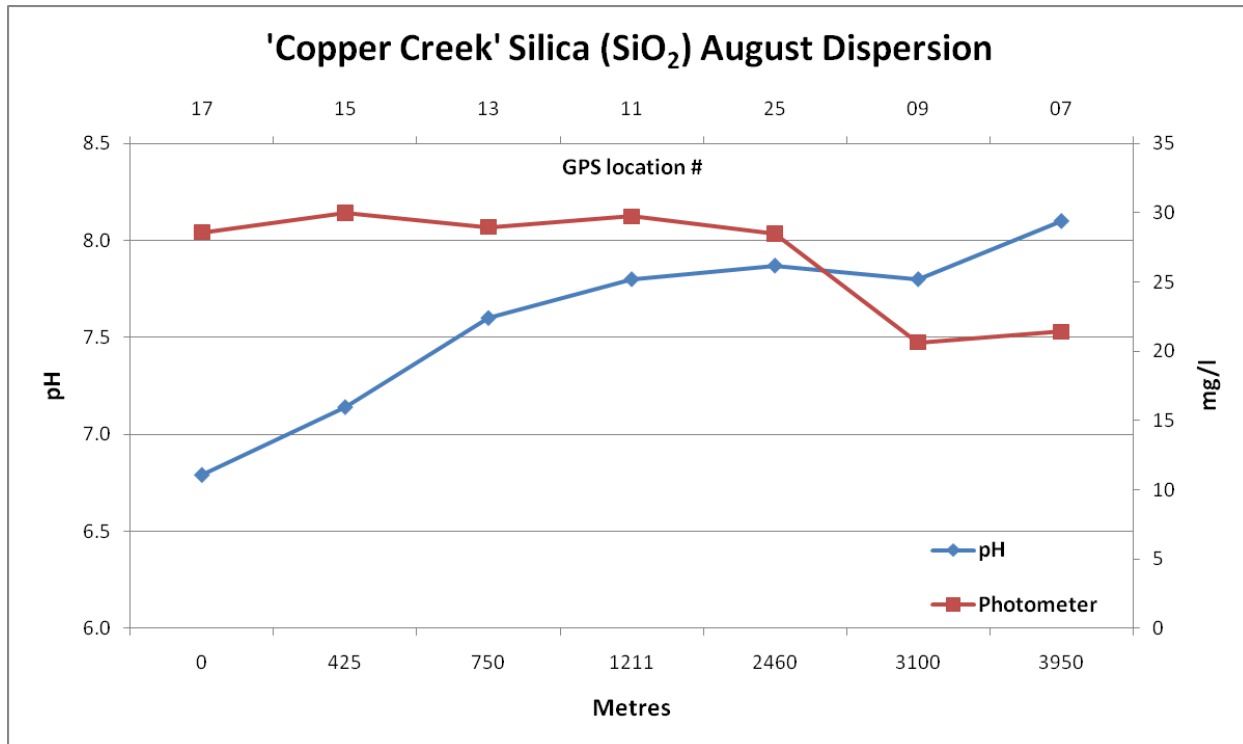


Figure 75. Silica 'Copper Creek' dispersion August (top) and October (bottom).

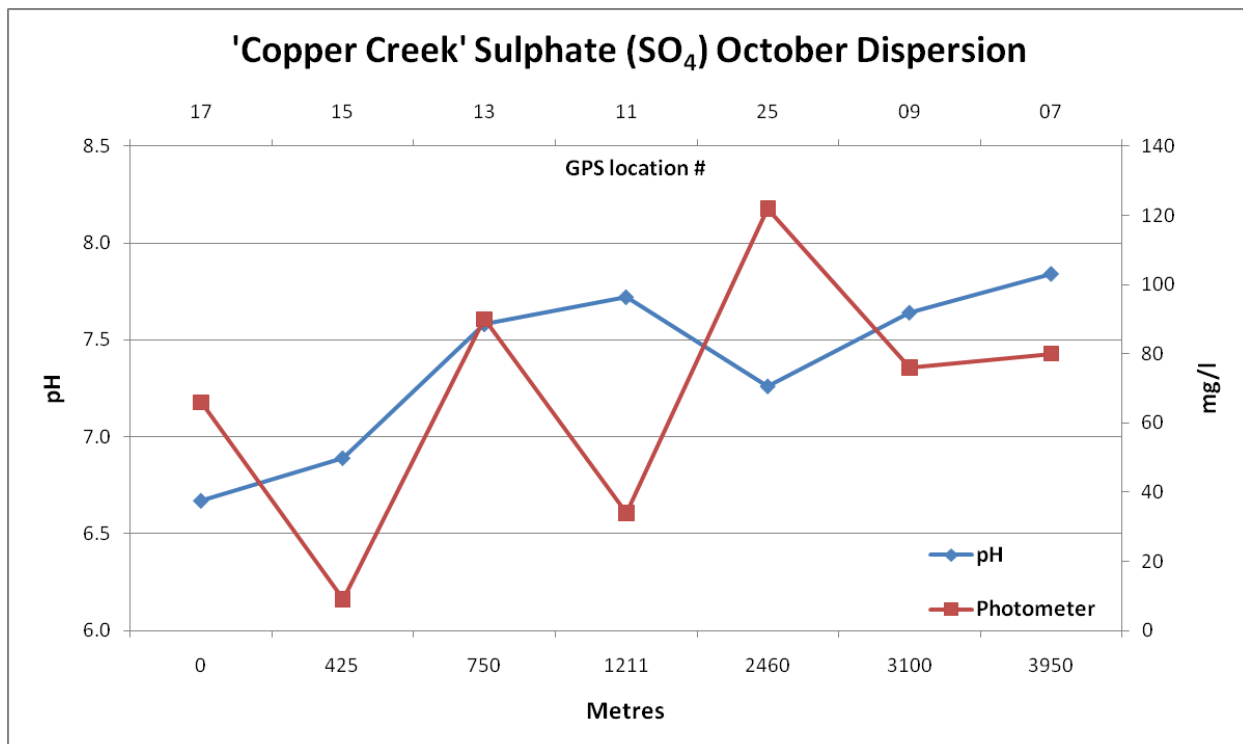
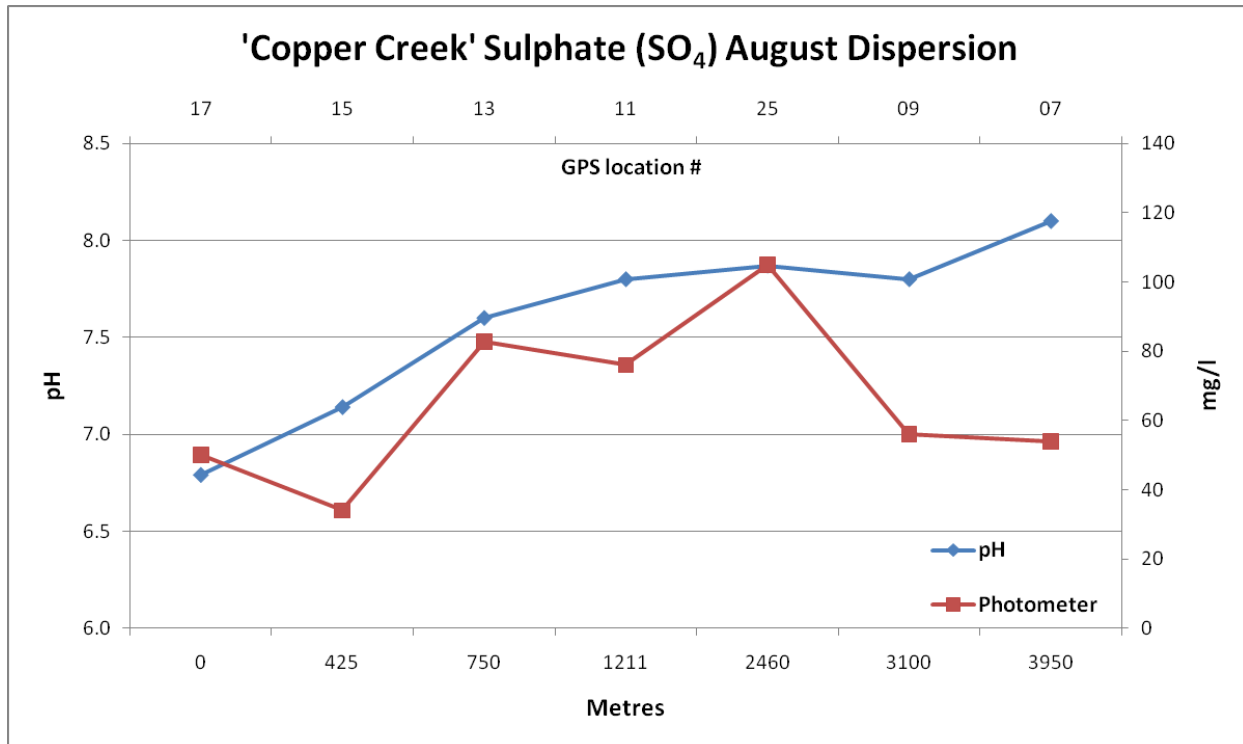


Figure 76. Sulphate 'Copper Creek' dispersion August (top) and October (bottom).

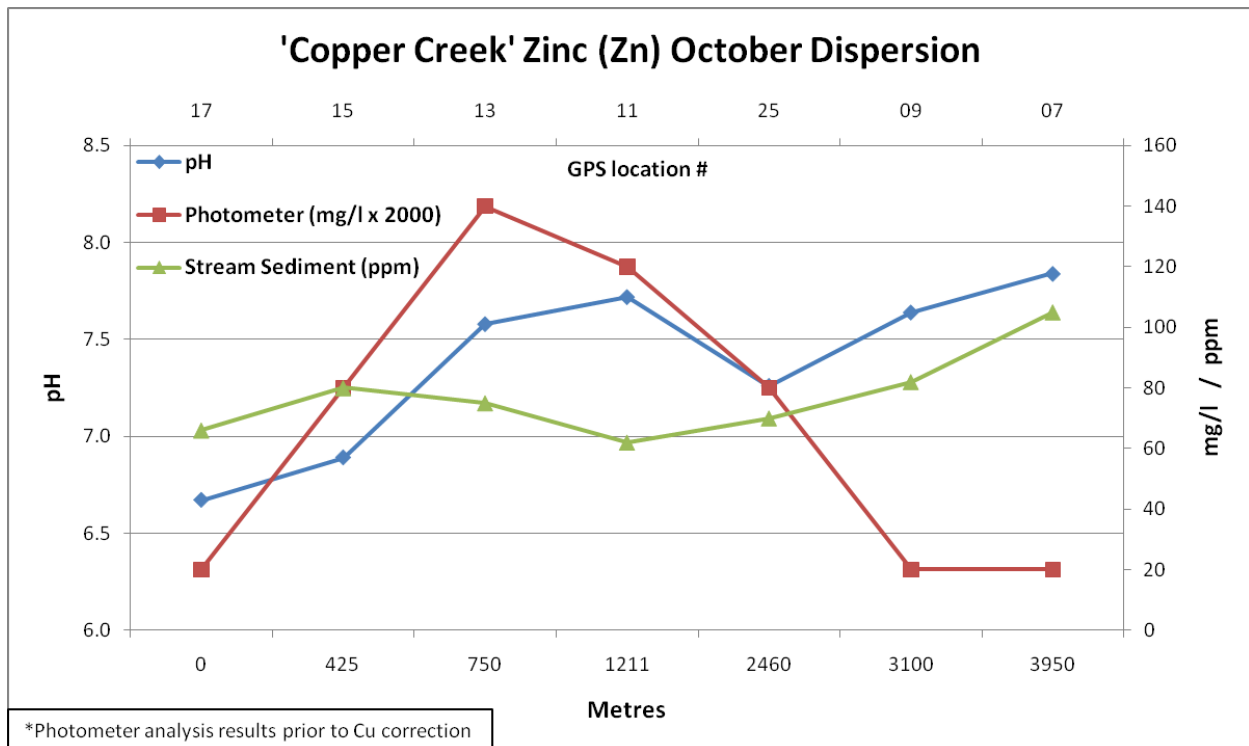
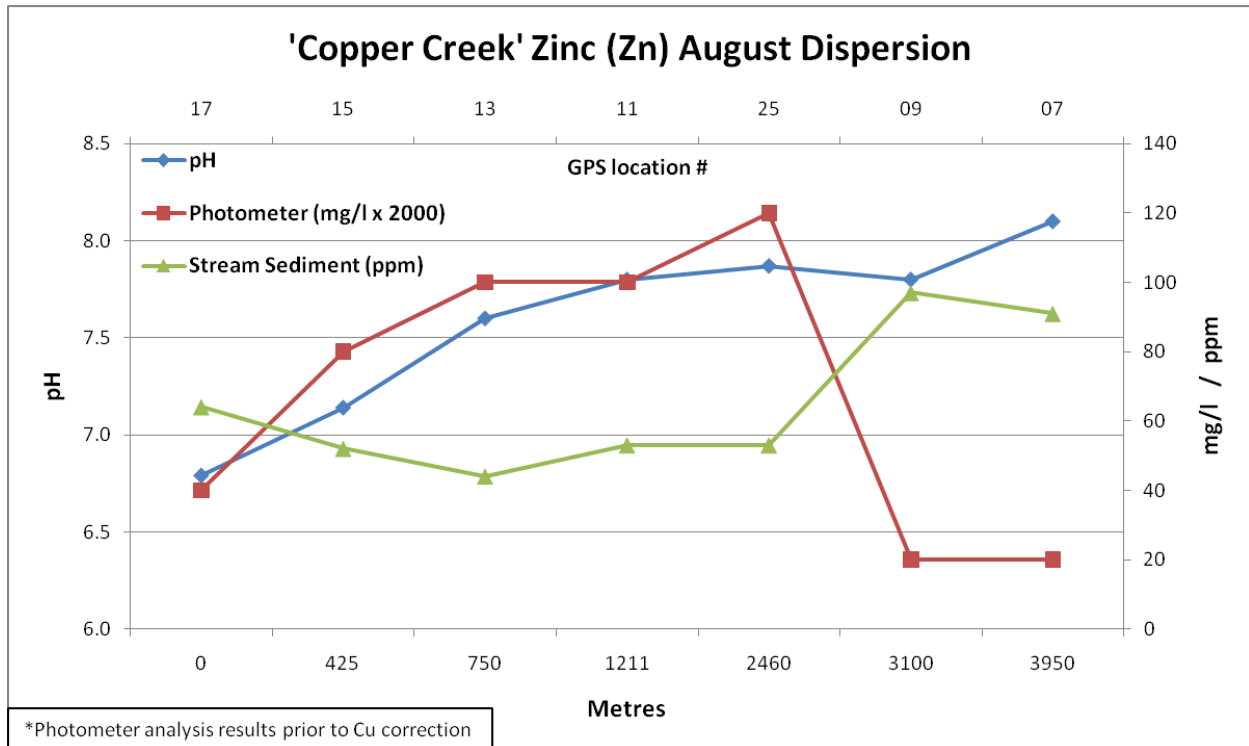


Figure 77. Zinc 'Copper Creek' dispersion August (top) and October (bottom).

## Digital Appendix

Includes the following spreadsheets:

- Field observations
- Analytical data
- ALS Environmental certificate of analysis
- ALS Minerals certificate of analysis